BathySent - An Innovative Method to Retrieve Global Coastal Bathymetry from Sentinel-2.

Work Package 6: BathySent Final Report

Marcello de Michele, Daniel Raucoules, Michalis Foumelis, Farid Smai, Robin Quique, Deborah Idier at BRGM*; Paraskevi Drakopoulou, Vassilis. Kapsimalis, Dimitris Sakellariou, John Morfis, Isidoros Livanos* at HCMR. With the support of *Przemysław Mujta, Maciej Krzyzanowski, Marcin Gil at Clourferro*

Under the supervision of Espen Volden at ESA.

Doc ID number	Creation date	Modification dates	Persons responsible
FR	17/03/2020	15/05/2020	Marcello de Michele

OBJECTIVES of the WP:

To prepare the final documentation and deliverables of the project.

Synopsis:

This document contains the experimental design, the development strategy and the main results and conclusions of the BathySent project (2018-2020), **EO SCIENCE FOR SOCIETY PERMANENTLY OPEN CALL** contract n° 4000124021_IP.

It describes the activities of the project, devided in:

WP1 Title: State-of-the-Art Documentation ;

WP2 Title: Scientific and Technical Development ;

WP3 Title: Algorithm Implementation ;

WP4 Title: Assessment and Validation activities ;

WP5 Title: Wide Area Demonstration ;

Chapter I: State-of-the-Art Documentation

This chapter aims at :

- Presenting a short bibliographic review of SDB (Satellite Derived Bathymetry) with optical imagery
- Presenting innovative aspect and advantages of proposed Sentinel-2 bathymetry retrieval methodology compared to conventional EO-based approaches.
- Presenting implication of utilization of the BathySent approach for different application domains
- Documenting capacity for implementation on cloud infrastructures for global systematic monitoring

Foreword

Given the same satellite scene, the bathysent method can not increase the maximum measured water depth compared to other method as this parameter depends on swell wavelength only. Bathysent advantage with respect to all the other methods, relies on the precise measurement of C (not only lambda) and its spatial evolution within the satellite scene. Therefore, Bathysent results are expected to be more robust, as they rely on the measurements of two physical parameters instead of only one.

I.1. Review of recent scientific literature

In bathymetric retrieval via image analyses, a number of methods exists for ground based instruments or airborne sensors, which parameters are tuned to the users needs and/or ocean waves characteristics. We described them briefly, mainly borrowing concepts from the review made in Yoo (2007), Poupardin et al. (2014, 2016) Danilo and Megani (2016) updating and improving their methodological review. Then, we concentrate on optical Satellite Remote Sensing based methodological review, the so-called 'Satellite Derived Bathymetry' (SDB). We see that constraints on optical satellite data acquisitions, mainly based on the sensor characteristics and acquisition strategy, limit the number of actual algorithm applications, and, as a consequence, how the methodology we propose -based on joint inversion of both celerity and wavelength- is among the most innovative.
An overview of already proposed methodologies for the retrieval of bathymetry based on remote sensing imagery by domain are briefly presented in the following chapter. Given the large number of publications on this topic, this document cannot be completely exhaustive; it has to be intended as a summary.
This text refers to optical domain only. Synthetic Aperture Radar (SAR) methodologies for bathymetry retrieval do exist, but we consider that they exceed the scope of the present document.

Danilo, C., Melgani, F., Wave Period and Coastal Bathymetry Using Wave Propagation on Optical Images, IEEE Transactions on Geoscience and Remote Sensing, **54**, 11, 2016.

Poupardin, A., Idier, D., de Michele, M., Raucoules, D., "Water Depth Inversion From Satellite Dataset", *proceedings of the IEEE Geoscience and Remote Sensing Symposium*, 13-18 July 2014, Quebec City, Canada, DOI 10.1109/IGARSS.2014.6946924.

Poupardin, A., D. Idier, M. de Michele, and D. Raucoules, “Water depth inversion from a single SPOT-5 dataset,” IEEE Trans. Geosci. Remote Sens., vol. 54, no. 4, pp. 2329–2342, Apr. 2016.

Yoo, J. Nonlinear Bathymetry Inversion Based on Wave Property Estimation from Nearshore Video Imagery PhD report of the Georgia Institute of Technology, 2007, 192pp.

I.1.1 Optical Domain – direct and indirect methods

In order to survey nearshore bathymetry remotely, several remote sensing methods have been applied either to measure water depths directly or to estimate water depths indirectly by depth inversion modeling through estimation of water surface movements. The group of direct measurement methods is based on the fact that the light penetrates to different depth levels at various wavelengths in the water column. The group of indirectly estimating bathymetry infers water depths by measuring water surface characteristics. The approach of this group is to model nearshore bathymetry inversely by estimating depth-induced wave properties from remotely captured images, identifying waves, and using water wave dispersion relation. One of the oldest method, belonging to the latter group, have been proposed by William (1947), applied to aerial photos.

I.1.2 Multispectral

These methods use radiance of passive multispectral imagery (e. g. Lyzenga, 1978; Phylpot, 1989; Lafon, 1999, 2002). They are based on the extinction of light with depth. The method provides coastal bathymetry with a high spatial resolution (equal to the resolution of the images), but results depend on water quality, seabed reflection, and atmospheric effects. The accuracy is around 20% from 0 to 6 m (Lafon et al. 2002). As this technique needs *in situ* values for absolute calibration, it is not applicable in non-accessible or turbid water areas.

The techniques in this group depends on optical clarity of sea waters, and usually requires empirical algorithms for retrieving water depths from optical complexities caused by scattering and attenuation of incident light in the water column, and bottom reflection as well. For the direct extraction of the coastal bathymetry, spectral satellite/airborne technology (Adler-Golden et al., 2005; Benny and Dawson, 1983; Bierwirth et al., 1993; Lee et al., 2001; Sandidge and Holyer, 1998), and light detection and ranging (LIDAR) technology (Irish and Lillycrop, 1999) have been suggested.

Benny and Dawson (1983) and Bierwirth et al. (1993) demonstrated retrieval of water depths with Landsat multi-spectral scanner (MSS) and Landsat Thematic Mapper (TM). Benny and Dawson (1983) could detect and contour shallow water area and shoals less than 18 m depths in a region at the northern end of the Red Sea using the Landsat MSS system. Bierwirth et al. (1993) applied the Landsat TM system to survey Shark Bay in Western Australia and their method overestimated water depths by several meters. Sandidge and Holyer (1999) used hyperspectral image data from the Airborne Visible/Infrared Imaging Spectrometer (AVIRIS) to derive nearshore bathymetry in Tampa Bay in Florida and in the Florida areas over a depth range of 0 to 6 m. The root mean square (rms) errors when compared to ground truth data in the two areas were 0.84 m and 0.39 m respectively. Lee at el. (2001) also applied an AVIRIS technique to survey water subsurface properties in Tampa Bay using a model-driven optimization algorithm without prior knowledge of the water optical properties. The derived depths ranged from 0.3 to 4.6 m. Adler-Golden et al. (2005) applied a physics-based algorithm which uses minimal ground truth input to hyperspectral (AVIRIS; LASH - Littoral Airborne Sensor Hyperspectral) and multispectral (Quickbird) imagery to retrieve depths and seafloor topography in Tampa Bay in Florida and in Kaneohe Bay in Hawaii. The accuracy of the computed depth was within 2~3 meters over a depth range of 0 to 10 m. The LIDAR-based method, named SHOALS, of Irish and Lillycrop (1999) showed greater bathymetry estimation performance than the spectral methods mentioned above, having maximum measurable water depths of up to 60 m and a vertical accuracy of about 15 cm. The direct bathymetry survey methods are highly dependent on water clarity and require prior knowledge of the relation between the optical water properties and water depths.

Adler-Golden, S.M., P.K. Acharya, A. Berk, M.W. Matthew and D. Gorodetzky. 2005. Remote Bathymetry of the Littoral Zone from AVIRIS, LASH, and QuickBird Imagery, IEEE Trans. on Geos. and Rem. Sens., 43 (2), 337-347.

Benny, A. H., and G. J. Dawson. 1983. Satellite imagery as an aid to bathymetric charting in the Red Sea, Cartogr. J., 20, 5–16.

Bierwirth, P. N., T. J. Lee, and R. V. Burne. 1993. Shallow sea-floor reflectance and water depth derived by unmixing multispectral imagery, Photogramm. Eng. Remote Sens., 59(3), 331– 338.

Irish, J.L., and W.J. Lillycrop. 1999. Scanning laser mapping of the coastal zone: The SHOALS system, ISPRS J. Photogramm. Remote Sens., 54, 123–129.

Lafon V. (1999). Méthodes de bathymétrie satellitale appliqués à l'environnementcôtier : exemple des Passes d'Arcachon. Thèse de Doctorat, Université Bordeaux 1,Talence, 240 pages.

Lafon V., Froidefond J.M., Lahet F. et Castaing P. (2002). SPOT shallow water bathymetry of a moderately turbid tidal inlet based on field measurements. Remote Sensing of Environment 81, 136 – 148.

Lee, Z., K.L. Carder, R.F. Chen, T.G. Peacock. 2001. Properties of the water column and bottom derived from Airborne Visible Infrared Imaging Spectrometer (AVIRIS) data, J. Geophys. Res., 106, 11639-11651.

Lyzenga D.R. (1978). Passive remote sensing techniques for mapping water depth and bottom features. Applied Optics 17 : 379 – 383.

Philpot, W. D., "Bathymetric mapping with passive multispectral imagery," Appl. Opt., vol. 28, no. 8, pp. 1569–1578, Apr. 1989.

Sandidge, J. C., and R. J. Holyer. 1998. Coastal bathymetry from hyperspectral observations of water radiance, Remote Sens. Environ., 65, 341–352.

I.1.3 Inverse methods. Introduction : the dispersion relation.

The depth inversion methods based on FFT methods and timestack methods, compute water depths by relating wave parameters such as wave period (T) and wavelength (L) and current velocity to the general form of the Airy surface gravity wave dispersion relation,

$$\omega = \sqrt{gk \times tanh\,(kh)} + \vec{U} \cdot \vec{k}$$

(Eq. 1)

where ω= 2π/T is the angular frequency, g is the gravitational acceleration, h is the local depth, U is the water mean velocity vector (generally, the stream we neglect in the further equations), and *k* = (kx,ky) is the wave vector of magnitude (wave number) k which is defined as 2π/L. Since water waves become less dispersive and wave phase speed (or celerity) becomes more strongly dependent on water depth rather than on the wave parameters as they propagate toward shallower water, the phase speed has been more practically used for depth determination by substituting for either one of the frequency and the wave number as shown as the follows:

$$c = \frac{\omega}{k} = \sqrt{\left(\frac{g}{k}\right) tanh\,(kh)}$$

(Eq. 2)

with the assumption of U · k = 0. In deep water (kh > 0.5), Eq. 2 simplifies to

$$c_o = \sqrt{\frac{g}{k}} = \frac{g}{\omega} = \frac{gT}{2\pi} = \frac{L_o}{T}$$

(Eq. 3)

where the subscript o denotes deep water conditions and Lo is the deep water wavelength obtained from Eq. 1 with no currents and deep water assumptions as

$$L_o = \frac{gT^2}{2\pi}$$

(Eq. 4)

From Eqs. 2 and 3, the celerity of a wave propagating from deep water toward shallower water can be expressed as

$$c = c_o\sqrt{tanh\,(kh)}$$

(Eq. 5)

In shallow water and/or long wavelengths (kh < 0.05), the approximation of Eq. 2 becomes

$$c = \sqrt{gh}$$

(Eq. 6)

which is a function of water depth only, being independent of wave number. However, a number of previous researches have shown that the shallow water linear dispersion relation underestimates the wave speed within the surf zone close to shoreline because of the finite amplitude effects.

There are several different ways to classify depth inversion methods: frequency domain inversions or time domain inversions; a priori or full approaches; depth-induced spatial water surface variation based inversions, depth-induced wave property based inversions or wave breaking generated dissipation pattern-based inversions; field-data- based or synthetic-data-based inversions.

A variety of depth inversion methods have been developed along with the advance of various remote sensing techniques. Each of those remote sensing platforms has its own limitations as well as advantages over others in terms of image resolution, spatial image coverage, and temporal image collections, etc. For this reason, several different approaches for remotely estimating littoral seafloor topography can be considered depending on input image data types.

The airborne optical platforms allows much more orthogonal measurements over the sea surface than shore-mounted platforms, and continuous sampling wave imagery at high frequencies over a target area on the scale of an hour to a day, flying around the area of the interest.

In contrast to locally operated platforms, satellites orbit around the Earth and acquire only one snapshot image or can sample wave images over a target area for a few seconds. For cases where the surface information is collected sparsely in time, Dalrymple et al. (1998) developed two depth inversion methods using the Hilbert transform and lag-correlation methods from two sequential images. In fact, Dalrymple et al. (1998) numerically generated the two sequential surface elevation maps with a reasonably short time interval, instead of using actual images.

Current operating satellites (2018) acquire images in a sparse time-lapsed fashion (for the exception of skysat, which records videos of the Earth Surface, but its data are not available for the public). This category is the one we are interested in, particularily.

I.1.4 Satellites methods based on Lambda and waves surface parameters (inverse methods)

The exploitation of wave propagation. This technique does not require temporally dense image sequences, and utilizes one or two sequential images of wave phase or surface elevation maps over a reasonably short time interval less than wave period. Leu et al. (1999), and Leu and Chang (2005) deduced water depths less than about 12 m from two SPOT satellite images taken in deep and shallow water regions. Assuming waves are propagating from deep water to shallow water, first, dominant deep water wavenumber and wave frequency are estimated from 2-D wave phase information of the deep water image. Thereafter, 2-D wavenumber spectrum of the shallow water image is analyzed, thereby deriving the water depth using the linear dispersion relation. The physical distance of sampling window was 200 m (32 pixels), which is not adequate for the nearshore region close to the shore. The effect of the nonlinear wave amplitude dispersion contributes significantly to the errors of depth inversion in the nearshore area via the linear dispersion relation.

When the water depth is less than half the dominant wavelength, the latter decreases toward the coast due to the decrease in water depth. It is then possible to estimate the water depth knowing the dominant wavelength and the wave period by using linear wave theory. This method has been explored since at least the Second World War (Wilson, 1942). However, the spatial resolution is often reduced by the calculation of the wavelength. Its application to satellite images in the optical domain is rarely reported in the scientific literature (Wu and Juang, 1997; Leu et al., 1999)]. In Leu et al. (1999), an average error of 17.5% of the ground-truth bathymetry is found between 0 and 15 m for a spatial resolution of 400 m. For this method, the determination of the wave period is crucial and may be obtained with ancillary data or through *a priori* knowledge of water depth.

Recently, Danilo and Melgani (2016) developed a method based on Landsat 8 images to extract bathymetry. They propose a method based on combining wave tracing and linear wave theory for the estimation of wave period and bathymetry in coastal areas. The method is developed for landsat but can work on different types of satellite optical images. Their experimental results are conducted on several sites located around the Hawaiian island of Oahu, they used 13 Landsat-8 images. Results show that wave period estimations are compatible with the wave buoy measurements in all cases. In addition, bathymetry estimations show a standard deviation of less than 15% of the observed depth out of the surf zone until 20 m, for sites with a direct exposure to the swell and with an absence of clouds. The proposed method does not rely on ancillary data; it works using satellite images in which waves are present. We recall here (2018) that this method is implemented in the ESA coastal TEP (Thematic Exploitation Platform) using Sentinel 2 data.

I.1.5 Methods based on joint use of Celerity-Lambda couples: Innovative aspects of Bathysent project

The use of two consecutive images with a time delay of a few seconds (Abileah, 2006; Mancini et al., 2012; de Michele et al., 2012; Danilo and Binet, 2013; Poupardin et al., 2014, 2016). This method also relies on linear wave theory. As it uses two images with a short time delay to measure C. Furthermore, more than one swell wavelength contributes to bathymetry estimation. This allows for the increase in the final resolution compared with the previous solutions. Using this method, Mancini *et al.* in (2012) estimated the relative errors to be less than 20% of the water depth for a spatial resolution of 125 m and a water depth between 4 and 16 m. This method can be also used for sea surface current estimation. Its main drawback is the small number of images available with the required time delay.

With the measurement of C in addition to the estimate of the wavelength, the problem of wave period is instantly resolved. Abileah (2006) using Ikonos stereo pairs have introduced the measurement of C from optical satellite data. de Michele et al. (2012), improved the method by using the small time lag between two bands of Spot5 dataset. Danilo and Binet (2013) have detailed the concept and limiting factors. As other methods, these methods exploit the dispersion relation in Eq. 2. Nevertheless, they are more robust, in principle, as they make the joint use of independently measurements of C (celerities) and L (wavelengths). This is the BathySent based algorithm, which, to our knowledge, based on automatic measurements of C and L, has been successfully applied to satellite datasets by two teams only: Abileah (2006, 2012, 2013; Mancini 2012) and ours (de Michele et al., 2012; Poupardin et al., 2014, 2016). de Michele et al. (2012) showed that C could be measured by a cross correlation algorithms by exploiting the time lag between two spectral bands - quasi simultaneous- acquisitions from a single passage of a satellite platform. They applied it to SPOT 5 in the published study, but virtually the algorithm applies to all the push broom sensors that present CCDs (Charged Couple Device) offsets on the focal plane of the instrument. On this basis, Poupardin et al., (2014, 2016) proposed a local spectral decomposition prior to the celerities estimates in order to produce local C, L pairs to derive depth based on the dispersion relation. In this methodology, for every L the backward Wavelet transform is calculated so that the estimation of C can be performed by local correlation in the real domain. This procedure has one disadvantage : the computing cost. In the BathySent concept, we make a step forward. We calculate C as the phase shift of the Fourier transforms between N Sentinel 2 bands, reducing the computing cost. Let's see some crucial step in the algorithm.

The BathySent concept starts from the method developed in de Michele et al. (2012) and Poupardin et al (2016). The basis of the Bathysent concept also rely on the fact that Sentinel 2 is able to correctly image the swell and that the swell spectrum can be computed correctly and fruitfully as recently shown in (Kudryavtsev et al., 2017). The BathySent algorithm uses multiples bands from Sentinel 2, each of which is acquired with a characteristic time delay ranging from 0,5 s to 2 sec. The bands are resampled to the highest resolution available (10 m). The Fourier spectrum is calculated. The algorithm scans the spectrum and search for instantaneous frequencies related to the most energetic wavelengths. Then, the phase differences for each selected frequency is calculated among all Sentinel 2 bands. Phase differences are converted to swell phase velocities, yielding a set of couples C-L. C-L couples are then used in the dispersion relation to retrieve H. The Sentinel dataset is scanned on the base of a moving window, yielding H at each step of the grid. This grid defines the final spatial resolution of the bathymetric map. The resolution in H is imposed by the physics of the phenomenon (i.e. the dispersion relation). It ranges typically from L/2 and L/20. Therefore, in the Mediterranean sea -where swells have typically less than 40 to 60 meters wavelengths- one can expect between 20 and 30 meters maximum H measurements with BathySent. In oceanic basins, a priori, H can be measured deeper than in sea basins because the swell could potentially reach larger wavelengths.

Abileah, R. "Mapping shallow water depth from satellite," in Proc. ASPRS Annu. Conf., May 2006, pp. 1–7.

C. Danilo, R. Binet, "Bathymetry estimation from wave motion with optical imagery: Influence of acquisition parameters", *OCEANS - Bergen 2013 MTS/IEEE*, pp. 1-5, 2013.

Danilo, C., Melgani, F., Wave Period and Coastal Bathymetry Using Wave Propagation on Optical Images, IEEE Transactions on Geoscience and Remote Sensing, **54**, 11, 2016.

de Michele, M., S. Leprince, J. Thiebot, D. Raucoules, and R. Binet (2012), Direct measurement of ocean waves velocity field from a single SPOT-5 dataset, Remote Sens. Environ., 119, 266–271.

Kudryavtsev, V., M. Yurovskaya, B. Chapron, F. Collard, and C. Donlon (2017), Sun glitter imagery of ocean surface waves. Part 1: Directional spectrum retrieval and validation, J. Geophys. Res. Oceans, 122, 1369–1383, doi:10.1002/2016JC012425.

Leu, L. G., Y.-Y. Kuo, and C.-T. Liu, “Coastal bathymetry from the wave spectrum of spot images,” Coastal Eng. J., vol. 41, no. 01, pp. 21–41, Mar. 1999.

Mancini, S., R. C. Olsen, R. Abileah, and K. R. Lee, “Automating nearshore bathymetry extraction from wave motion in satellite optical imagery,” in Proc. SPIE Algorithms Technol. Multispectral, Hyperspectral Ultraspectral Imagery XVIII, 2012, pp. 1–12.

Poupardin, A., D. Idier, M. de Michele, and D. Raucoules, “Water depth inversion from a single SPOT-5 dataset,” IEEE Trans. Geosci. Remote Sens., vol. 54, no. 4, pp. 2329–2342, Apr. 2016.

Wu, J. and J. T. Juang, “Application of satellite images to the detection of coastal topography,” Coastal Eng. Proc., vol. 1, no. 25, pp. 3762–3769, 1997.

I.1.5.1 Limitations of the methodology based on Lambda-C couples

The first limitation is this method relies on the fact that the swell needs to be imaged by the sensor. This is a physical limitation, in the sense that quite a few characteristics need to be fulfilled. They are:

1) absence of clouds
2) turbid water; if the sea is transparent the swell might not be visible in the satellite dataset
3) the relative geometry between the Sun, the sensor and the waves front needs to be favourable (see Danilo and Binet, 2013); need to have swells with different periods or wavelengths (Mediterranean VS open oceans)
4) The pixel size (either in terms of image resolution –we need at least two pixels to oceans measure the smallest wavelengths).
5) The final grid of the bathymetry map is coarser than the one retrieved by the multispectral method. This is because of the window size of the 2D correlation.
6) The cost of the data could be a limiting factor if one has to use a certain number of data to improve precision/accuracy.

These are crucial issues as, if the data acquisitions are not frequent, the chances to acquire an “exploitable” dataset are reduced. As a first approximation, based on our experience, one dataset over 20 acquisitions is exploitable.

I.1.5.2 How Sentinel 2 data can fulfil the needs for improving our methodology

The first advantage of Sentinel 2 is the frequent data acquisition. This factor statistically improves the number of exploitable data either in terms of 'cloud free data, either in terms of favourable relative geometry, or in terms of imaging the swell having multiple periods (different days, different waves conditions). Moreover, Sentinel 2 data are free of charge, which is a practical advantage.
The second advantage is that the focal plane geometry of Sentinel 2 is undisclosed. Therefore, we know exactly what is the time lags between multiple bands. The third advantage is that Sentinel 2 offer the possibility to jointly use multiple bands (with multiple time lags) within a single run or our processor. This yields different measurements of C and L, which we use to improve the accuracy of the results. The pixel size of Sentinel 2 (10 meters) is a limiting factor for very shallow bathymetry retrieval (between 0 and 10 meters). Nevertheless, the ability of our correlator to measure sub-pixel offsets could partially fill this

gap. On the other hand, third party missions with very high resolution sensors might be employed jointly.

I.2. Importance towards open scientific issues

Nowadays, knowledge of near-shore bathymetry is essential for multiple applications both scientific, such as for the study of submarine morphodynamics, coastal erosion, tsunami propagation towards the coast and climate change initiatives as well as operationally, by local authorities and decision makers. This information is vital for planning sustainable coastal development, coastal risks assessments (including tsunamis) and conservation of submarines ecosystems. Moreover, coastal bathymetry represents a crucial input for near-shore navigation and submarine resources exploration. Follows few examples of French or international projects (ongoing) that would benefit from coastal bathymetric mapping from space.

INseaPSION (INtegrating SEA-level Projections in climate services for coastal adaptation). Brgm is the project coordinator. http://www.inseaption.eu/

The objective of INSeaPTION is to co-produce three sets of coastal climate services with three distinct groups of users:
-Global to regional coastal climate services, addressing the needs of:
(1) major companies such as port authorities and coastal engineering companies for sea-level information for strategic long term locational and planning decision making; and
(2) international organizations, governments and donor organizations to have globally consistent information for climate policy making finance for climate adaption, disaster risk reduction and loss & damages. These services will include regional projections of mean and extreme sea-level, their flooding and erosion impacts and adaptation pathways together with related uncertainties covering the world’s coastline, from now to 2100 with extensions up to 2300.
- Regional to local coastal climate services addressing the needs of planers and policy makers for *local tailored sea-level projections*, impact and adaptation information useful for long-term development, infrastructure and land-use planning for two high impact territories: the Maldives and French Polynesia.
Detailed local sea-level rise impact analysis is required, because the resilience of each coast will be different depending on the exposure to waves and currents and geomorphological characteristics (e.g., bathymetry). Here, INSeaPTION will benefit from field work and remote sensing observations that will allow to draw vulnerability profiles for different types of coasts in the Maldives and French Polynesia.

ECLISEA : European advances on Climate Services for Coasts and SEAs. BRGM is partner of this EU funded project. http://www.ecliseaproject.eu/

ECLISEA is a project that aims to advance coastal and marine climate science and associated services through developing innovative research of sea surface dynamics. The project is built upon the premise that the outcomes should be applicable throughout Europe. ECLISEA proposes an integral research plan that starts with assessing the needs of specific stakeholders; includes groundbreaking investigation related to mean sea level rise, storm surge, waves, total water level and coastal flooding and erosion methodologies, and ends up with the development of an on-line open prototype of a coastal climate service in Europe. Relevant issues for climate sensitive sectors in coastal areas such as the characterization and change of extreme met-ocean conditions or the assessment of uncertainties of regional historical and future mean sea level rise are considered, as well as relatively unexplored research on wind-waves and storm surge climate predictability from seasonal to decadal time scales.

Storisk: Small islands addressing climate change: towards storylines of risk and adaptation. Brgm is partner of this ANR (Agence Nationale pour la Recherche) funded project.

The 48-month project aims to develop a transdisciplinary methodological protocol to improve knowledge and understanding of the vulnerability and adaptability of tropical island societies to extreme events of climatic origin (tropical cyclones, distant swells, ENSO phenomenon) and gradual changes due to global warming (rising sea levels and increasing ocean temperatures) and ocean acidification.

West African Coast Areas WACA program. Brgm is contributing via a National Research grant.

The aim of WACA program is to develop resilience of West African coastal zones by implementing natural risk management taking into account technological risks induced towards coastal populations.

MAREA : Modélisation et Aide à la décision face aux Risques côtiers en Euskal Atlantique https://www.marea-paysbasque.fr. BRGM is a partner in this EU funded project.

MAREA for "Modeling and Decision Support for Coastal Risks in the Atlantic Euskal", is a cross-border research project, aimed at better understanding the episodes of storms on the Basque coast to predict the risks of marine submersion and coastal erosion thanks to the setting up of innovative warning tools. Thus, MAREA's partners wish to develop high-resolution numerical and statistical modeling tools capable of locally predicting the energy and water levels reached by extreme waves, as well as the volumes of sediments displaced by storms. BRGM works within the on-going MAREA project, and on-going post-doc and PhD student working on shoreline modeling (Robinet et al., 2018) accounting for in situ measured bathymetries.

Robinet A., Idier D., Castelle B., Marieu V. (2018) A reduced-complexity shoreline change model combining longshore and cross-shore processes: The LX-Shore model, Environmental Modelling & Software, 109, 1-16.

Sent2Coral project (https://sen2coral.argans.co.uk/)

The objective of ESA’s SEOM Programme Sen2Coral (2016-2018) is the preparation of the exploitation of the Sentinel-2 mission for coral reefs by developing and validating appropriate, open source algorithm available for the community. The project objectives are the scientific exploitation and validation of the Sentinel-2 Multispectral Instrument (MSI) for mapping (habitat, bathymetry, and water quality) and detection change for coral reef health assessment and monitoring, and algorithm development dedicated to Sentinel-2 capabilities to satisfying these objectives.

I.3. Applications domains that would benefit from the utilization of the proposed technology

Coastal bathymetry is essential to characterize seabeds, monitor their evolution, or model currents, waves, water level, submersion or sediment transport. Among the applications, we can highlight:

• optimization of dredging operations (eg migration of sandbanks hindering navigation)

-coastal bathymetry is a dynamic environment. Civilian and military Eco-sounder cannot yet designed do routine monitoring of shallow bathymetry. Often, this equipment is heavy enough not to allow the ship to approach shallow bathymetry area (0 – 30 meters).

• hazard study or submersion risk

-given the name, hazards may occur in remote area that are not accessible for men. Nevertheless, the study of shallow depth coastal hazard in remote areas could be key in understanding geophysical phenomena. Also, tsunami risk depends on submarine morphology. Therefore, bathymetry is essential to understand and model tsunami propagation.

• aquaculture and fisheries

-repeat pass, shallow bathymetry maps may reveal evolving ecosystems.

• condition of accessibility / disembarkation in remote areas.

-for military/humanitarian operations, it is important to have a knowledge of shallow bathymetry in remote areas.

• submarine archaeology

-precise, low cost, shallow bathymetric maps may help submarine archaeologist to plan a diving mission.

Potential scientific applications are foreseen in Storisk and INSeaPTION project, some of them are described in Collin et al., 2018, “Understanding Interactions between Shoreline Changes and Reef Outer Slope Morphometry on Takapoto Atoll (French Polynesia)”, Journal of Coastal Research,85,496-500, doi = 10.2112/SI85-100.1,

Finally, nearshore bathymetric data are a need well expressed in this white paper from ISSI (International Space Science Institute, Bern), to which BRGM contributed (Goneri Le Cozannet) http://www.issibern.ch/forum/costzoneevo/wp-content/uploads/2016/11/ISSI-forum_Coastal_White paper_18nov2016_Final.pdf and in the following article:

Cazenave, A., Le Cozannet, G., Benveniste, J., Woodworth, P.L. and Champollion, N., 2017. Monitoring coastal zone changes from space. *Eos*, *98*.

I.4. Potential implementation to existing national and international initiatives (ESA Thematic Exploitation Platforms, DIAS etc.)

Potential integration to ESA Thematic Exploitation platforms:

ESA has started in 2014 the EO Exploitation Platforms (EPs) initiative, a set of R&D activities that in the first phase (up to 2017) aims to create an ecosystem of interconnected Thematic Exploitation Platforms (TEPs) on European footing, addressing, Coastal, Forestry, Hydrology, Geohazards, Polar, Urban themes, Food Security.

In short, an EO exploitation platform is a collaborative, virtual work environment providing access to EO data and the tools, processors, and Information and Communication Technology resources required to work with them, through one coherent interface. As such, the EP may be seen as a new ground segments operations approach, complementary to the traditional operations concept. BathySent is meant to join this philosophy. In our idea, near shore bathymetry is an important issue for:

Coastal TEP (all issues concerning mapping)

Polar TEP (how deep is the water where ice melts?)

Food Security TEP (FS-TEP) –exploratory- Do shallow bathymetry maps help planning fisheries and aquaculture development ?

BathySent could then contribute to the aforementioned TEPs.

I.5. Potential integration to cloud processing platforms (Copernicus Data and Information Access Services (DIAS) platforms).

Given the processing requirements for robust satellite-based bathymetry retrievals, in addition to the large spatial coverage and high temporal repeatability of the Copernicus Sentinel-2 mission, the conceptual design of the BathySent algorithm was initially foreseen as a cloud-friendly implementation. This will allow proper exploitation of the entire Sentinel-2 archive and the future globalization of bathymetric measurements by the proposed methodology.

Excellent candidates for such implementation are the ESA Thematic Exploitation Platforms (TEPs) as well as the upcoming Copernicus Data and Information Access Services (DIAS) platforms. Back in 2014, ESA has started the TEPs initiative, a set of R&D activities aiming in creating an ecosystem of interconnected platforms addressing processing needs of various EO thematic domains (e.g. the Coastal TEP). The emergence of DIAS platforms, facilitating access to Copernicus data alongside with processing resources, tools and other relevant data, is expected to boost further EO data user uptake and pave the ground for the generation of innovative and global scale products and services.

Currently available cloud processing services are limited to some commercial initiatives, such as the CloudFerro computing cloud and servers, which is utilized within the frame of the project for demonstrating the capability of the proposed methodology. The involvement of the IT project partner in one the DIAS consortia serves as a catalyst in tackling challenges related to the cloud implementation of the algorithm and the potential impact of the activity for the EO society.

I.6. Potential integration in national + international initiatives: EMODnet http://www.emodnet-bathymetry.eu

The EMODNet Bathymetry portal was launched in 2009. It is an European initiative aiming at collecting and distributing bathymetric maps to the end-users, from a variety of campaigns

and field data. In May 2010, the first release took place of the digital bathymetry for the North Sea, Celtic Seas, Channel, Western and Central Mediterranean Seas. Services are mainly based on survey. Further upgrading of the EMODnet DTM is ongoing in 2018 and includes incorporating more surveys and further improvement of the digital bathymetry. In addition, Satellite Derived Bathymetry (SDB) data will be included for covering gaps in survey coverage. Moreover, developments are underway for increasing the overall resolution from 1/8 to 1/16 arc minute and to expand the coverage of the DTM to include also the European coastal zones as well as the European arctic region and Barentz sea. Furthermore, higher resolution DTMs will be developed and made available where data are available and released for publication by its owners. Bathysent could play a role here, as a tool for high resolution shallow-water bathymetry.
The **EMODnet** Bathymetry portal is operated and further developed by a European partnership. This comprises members of the SeaDataNet consortium together with organizations from marine science, the hydrographic survey community, and industry.

SeaDataNet is a leading infrastructure in Europe for marine & ocean data management, initiated and managed by the National Oceanographic Data Centres (NODC's). It is actively operating and further developing a Pan-European infrastructure for managing, indexing and providing access to ocean and marine data sets and data products, acquired via research cruises and other in-situ observational activities. The basis of SeaDataNet is interconnecting Data Centres into a distributed network of data resources with common standards for metadata, vocabularies, data transport formats, quality control methods and flags, and access. SeaDataNet is aiming for an extensive coverage of available data sets for the various marine environmental disciplines, such as physical oceanography, marine chemistry, biology, biodiversity, geology, geophysics and bathymetry. This is implemented by seeking active cooperation at a national scale with institutes and at a European scale with communities, that are engaged in data management for these disciplines, and by seeking opportunities for including their data centres and data collections in the SeaDataNet metadata and data provision.

In the field of bathymetry, a number of Data Centres in SeaDataNet manage bathymetric data sets, such as multibeam surveys from scientific cruises. However, there are several other parties engaged in the provision of bathymetric data. These comprise:

Hydrographic Offices, that are responsible for surveying the navigation routes, fairways and harbour approach channels and producing from these the nautical charts on paper and as Electronic Nautical Charts (ENC), that are used for navigation. The HO's are members of the International Hydrographic Organization (IHO) that has its data policy, which supports restrictions in the delivery of high resolution data sets, mostly for safety and security reasons. Moreover, nautical charts have a legal status. Every ship captain must use certified nautical charts and the production and publication of these is an activity that must follow stringent international procedures. The latter results in a condition that HO's are careful in delivering and distributing bathymetric survey data sets.
Authorities, responsible for management and maintenance of harbours, coastal defenses, shipping channels and waterways. These authorities operate or contract regular bathymetric monitoring surveys to assure that an agreed nautical depth is maintained or to secure the state of the coastal defenses.
Research institutes that collect multibeam surveys as part of their scientific cruises.

Industry, especially the energy industry that contracts multibeam surveys for pipeline and cable routes (in case of windfarms) and the telecommunication industry for phone and internet cable routes.

Chapter II: Scientific and Technical Development

This chapter aims at:

- Outlining proposed innovative method for bathymetry retrieval using Copernicus Sentinel-2 data
- Outlining scientific and technical development for Sentinel-2 bathymetry retrieval
- Defining optimum retrieval parameters for various environmental conditions
- Highlighting some potential utilization of processing by-products (cloud masking, average wind direction, etc.) in different EO-based application
- Detailing technical characteristics of corresponding downstream products (definitions, specifications, assumptions and limitations).

II.1 *OBJECTIVE OF SCIENTIFIC AND TECHNICAL DEVELOPMENT OF BATHYSENT:*

The proposed method is an adaptation of the method detailed in Poupardin et al. 2016 (CWB, i.e. Correlation Wavelets Bathymetry) to sentinel-2 data. As explained in the TN1 document, the concept is to produce celerities/wavelengths pairs that can be associated to a water depth values through the linear dispersion relation.

In some ways, the CWB method can be seen as a demonstrator (applied to SPOT 5 data) of bathymetry derivation from wave characteristics obtained using inter-band image correlation and not an operational method. If theoretically CWB can be applied at any push-broom sensor, in fact the algorithm resulted excessively slow for processing in a reasonable computing time extended areas as required for the BathySent project. The reasons rest on the fact that CWB (for each local depth estimation):

- is based on repeated wavelet decomposition for estimating the dominating wavelengths and orientation. The choice of using wavelet decomposition instead of Fourier Transforms in CWB was due to a potential source of increase of precision.
- applies spatial correlation on the computed wavelets in order to associate celerity to the detected dominating waves.

Noteworthy is the fact that if CWB resulted precise, the procedure does not take advantage of the possibility of computing both wavelength and celerity in the spatial frequency domain. We therefore propose to design a faster method to process Sentinel-2 data in order to be able to process large images. For this purpose, we investigate FFT (Fast Fourier Transform) based methods for producing in a simple step the local waves spectrum and its associated celerities. The basic idea will be to use the combination of local Fourier spectra of the different bands - that contains both spatial frequency and phase - that can be combined in order to derive the significant celerities/wavelengths pairs. The combined local spectra contain all the information to locally characterize the waves.

Two additional activities will be necessary for further platform operational implementation:

- Adaptation of the produced algorithm as a Python code for easier implementation in a platform
- Identification of additional functionalities required for an easy use. In particular the ability of selecting co-registered images with reduce cloud cover, visible wave fields, with diverse wavelengths and directions
-

For the adaptation of a CWB-like method for Sentinel-2, the Sentinel 2 sensors characteristics and their differences respect SPOT 5 (sensor for which CWB was designed) must be analyzed:

- Resolution (10m vs 2.5 in PAN and 10m in MS for Spot 5). The resolution is a limitation for image correlation precision: typically, the precision we can expect could be between 1/2 to

1/10 pixels. In addition, theoretical wavelength that can be detected is limited by the Shannon theorem to twice the pixel size.

- The Repeat cycle of 5 days of Sentinel 2 is of major interest:

  - That allows increasing of precision by cumulating wave states of different dates: i.e. using waves with different directions and wavelengths
  - To produce larger archive for selecting images with reduced cloud cover and significant waves that can be detected.
  -

- Another parameter influencing the result to be analyzed is the time span between the sensors' bands. For Sentinel 2 it is about 0.6 s (between B2 and B4) vs 2 s for SPOT 5 (between Panchromatic and multi-spectral). The resulting celerity estimation will be less precise. However – as we will show further – the spectrum combination method offers the possibility of using 3 bands (e.g. R, B, NIR) or even more to increase precision. In fact, the NIR band is less resolute but can be used as complement.

- For recording an image line, the Sentinel-2 uses a set of 14 CCD modules instead of a single line CCD (as SPOT 5). For technical reasons, two adjacent modules are inverted: i.e. if the first records band 2 before band 4, the second will record band 4 before band 2. That results in a time inversion if we consider band 2 as the reference. However, the sign of celerity has no impact in the dispersion relation (that uses the absolute value of the displacement). Nevertheless, at the border between 2 modules local correlation can fail resulting in narrow (about half the size of the correlation window) bands where information is lost. Such areas can be easily interpolated (figure 1).

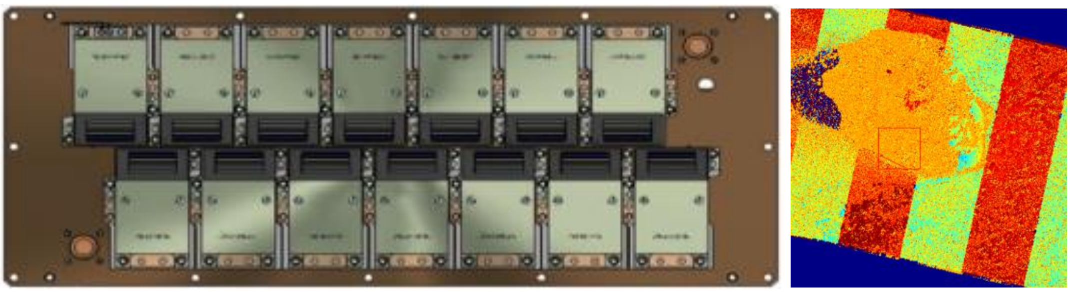

Figure 2.1. Left: Sentinel 2 focal planes modules (FPM, source ESA). Right: inter-band image correlation of S2 data on a dataset acquired over La reunion Island (France, Indian Ocean). The 180 degrees rotation of each FPM becomes signs opposition of pixels offsets due to waves celerity.

- The swath of Sentinel 2 images is close to 250 km swath allowing covering large coasts. Therefore, it requires performant algorithm to process large images in acceptable duration.

II.2 *SCIENTIFIC AND TECHNICAL DEVELOPMENT FOR SENTINEL-2 BATHYMETRY RETRIEVAL*

Based on the objectives detailed in Section 1, the required developments for an operational application of the method for deriving bathymetry based on wave characteristics to Sentinel 2 data are:

- To adapt the CWB method on a “single FFT” processing method in order to have an efficient (sufficiently fast method for processing extended areas.)
- To be able to propose multi-band (more than 2) and multi-date processing to take advantage of Sentinel-2 sensor (repeat cycle, number of bands)

Additional developments of tools for helping users for selecting suitable images could be valuable, as this issue - although not critical – has been identified as needing potential improvement.

II.2.1 *IDENTIFICATION OF STATE-OF-THE-ART PROCESSING TECHNIQUES AND ALGORITHMS FOR THE VARIOUS PROCESSING STEPS INVOLVED*

The following section describes the theoretical aspects of the improvements we propose in the framework of the BathySent method.

A. *Local spectra*

In order to adapt the concepts from Poupardin et al. 2016 to a faster algorithm, we propose to use a method based of local FFT. For simplifying, let us consider 2 bands (A and B) as in figure 2. On a small window (e.g. 64 pixels) located where we want to extract the depth, we compute the Fourier Transforms (by FFT) of each band (F_A and F_B^*). Then we compute a function R defined as:

$R = F_A F_B^* = Ae^{i\theta}$ [1]

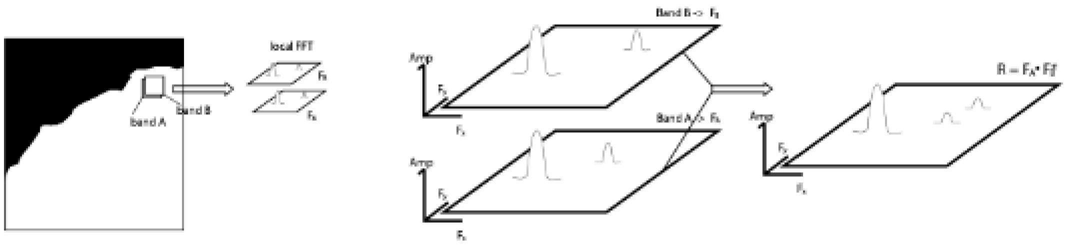

Figure 2: sketch of computation and combination of the local spectra from two bands.

The basic idea of the algorithm is to estimate in one-step both the wavelengths and the celerities. The offset in the motion’s direction (δr) between the two bands can be related the phase of R by $\delta r = \frac{\lambda\theta}{2\pi}$. When the offset is not wavelength dependent that allows the well-known phase correlation algorithm (e.g. Leprince et al. 2007). That not applies here where the observed motion is the combination of displacements at different wavelengths. However we just need to produce (λ, θ) pairs that can be converted knowing δt to (λ, c). The amplitude (A) on the spectrum R can be seen as a criterion for selecting the most significant waves.

The algorithm will consist in scanning the image using small windows (less than 1 km, size compatible with maximum expected wavelengths and the pixel size).The idea previously described can be generalized as:

$$R_{i,j} = F_i \ F_j^* = A_{ij}e^{i\theta_{i,j}} \ [2]$$

Once $\theta_{i,j}$ rescaled by the $\delta t_{i,j}$ (time span between band i and band j) the $R_{i,j}$ can be combined in a single complex spectrum R. Time rescaling of $\theta_{i,j}$ rescaling can be carried out by just dividing $\theta_{i,j}$ by the corresponding $\delta t_{i,j}$: in this case the corresponding velocity will be $c_{i,j} = \frac{\lambda \, \theta_{i,j-\mathrm{rescaled}}}{2\pi}$

$$R = \sum_{j>i} R_{i,j} = Ae^{i\theta}[3]$$

This procedure allows multiband combination (e.g. 3 bands resampled at the same sampling step) but also multi-date (allowing for a give location the use of different wave regimes) provided the imaged are correctly co-registered.

B. *Extracting(c, λ) pairs.*

For this, we define small intervals (delimited by two circles in the Fourier domain) of wavelengths. Above a given threshold value on spectrum value, we estimate the weighted average of the phase. We therefore obtain phases values associated to wavelengths and characterization of their significance through the amplitude value.

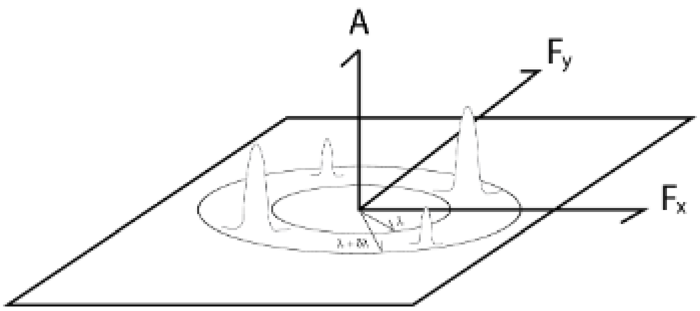

Figure 3: definition of the sector of the spectrum containing the wavelengths in $[\lambda, \delta\lambda]$. On the figure 2 waves regimes (illustrated by "peaks") associated to the same wavelength but with different directions are represented in this illustration of a R function. As we assume a nearly

constant depth in the FFT window, their celerities (and thus their phase – the wavelength been the same) should be the same. We have to "average" the phases of all the significant values of R included in $[\lambda, \delta\lambda]$ to deduce an estimate of a pair $(c, \lambda + \frac{\delta\lambda}{2})$. $\delta\lambda$ should not exceed the size of few image pixels in order to be sufficiently discriminant.

We can therefore estimate for each (c, λ) a value of h and a significance value based on the corresponding A. A weighted average of all the produced h will therefore produce a depth value.

II.2.2 *QUALITATIVE ANALYSIS FOR DEFINITION OF OPTIMUM RETRIEVAL PARAMETERS FOR VARIOUS ENVIRONMENTAL CONDITIONS*

We identified the following list of parameters that will potentially affect the BathySent result.

Parameter	Consequence on EO data and/or BathySent product	Optimum
Swell wavelength	-Actual resolution of the final product of the order of the wavelength. -Minimum theoretical detectable wavelength: twice the pixel size (i.e. 20 m for Sentinel 2) -shorter wavelengths are less sensitive to deeper bathymetry than larger	Contradictory requirements respect to resolution and depth. We need to be able to analyze simultaneously different wavelengths (short and large) to address both issues.
wave directions	Need to be adapted to the coast geometry	Ideally perpendicular to coast. In case of complex geometry of the coast several wave regimes with different direction could be useful for addressing the presence of obstacles to waves.
wave visibility	Must be clearly identifiable on the image	Waves pattern that a user can be clearly identify on a Sentinel 2

		image. An a priori automatic detection process could be valuable for image selection.
Water	In the BathySent method, the visibility of water is a limitation if the bottom is observed: stable features in the image can affect the celerity estimation. In the other hand, surface turbidity can result in patterns with a motion different from the waves also resulting in errors in the celerities estimates.	Not clear water where wave visibility surpass other features (bottom and surface turbidity issues)
cloud masking	Clouds, event partially transparent affect the celerity estimation due to their own motion.	No cloud on the studied area

Concerning the waves' characteristics, two ways to address the issue can be considered: 1°) use the knowledge of the physical forcing (weather, wind, sun, direction, rough bathymetry) to derive approximate characteristics of the wave images for the acquisition day. 2°) scan (automatically or visually) in order to detect images with suitable swell characteristics. The first approach aims at describing the optimal conditions for the application of the method, the second approach aims at selecting in an existing archive a suitable data subset.
For this reason we think the 2°) is more adapted than 1°) for large sentinel-2 archives if a fast automatable identification of images with low cloud cover is available and if we are able to estimate a spectrum giving significant wavelengths in the interval [30m-250m] and waves directions during the image selection step.
That suggests the importance of proposing an image selection tool based on those characteristics prior to the BathySent processing.

II.2.3 *PROPOSED PROCESSING CHAIN*

The different steps to carry out the processing of the Sentinel 2 are:

Inputs: Sentinel 2 image, area of interest limits, time spans between bands

- Generation of a land/sea mask based on the NIR band
- Extraction of band 2, band 4 and - in option - band 8
- Resizing band 8 to the bands 2/4 resolution
- Extraction of excerpts of each band and mask on area of interest

- Scanning the area of interest using a moving window (size between 250m to 1km depending on wave characteristics). The scanning step is user defined (typically half window size)

  - estimating the local spectrum (by FFT) for each band and rescaling the spectra phases
  - Combination of spectra
  - generation of (c, λ) pairs using the method proposed in 2.2 (each pair is estimated in an area between 2 circles in the Fourier Domain)
  - estimation of depth (h) for each(c, λ) by using the linear dispersion relation.
  - average of the obtained h weighted (c, λ): this value will be the depth associated to the center of the moving window.

  Output: raster (geotiff) of the obtained water depths.

  The algorithm and pseudo code will be detailed in TN3 and TN4 reports.

II. 3 *DEFINE LEVEL OF AUTOMATION IN TERMS OF REQUIRED USER INTERACTION*

1) Pre-processing: Selection of images

The image selection is a step where automation can help the user. In fact, the selection of the required images can be complicated on the ESA EO Hub as the Sentinel 2 previews do not have in most cases a sufficient resolution to show the waves. As consequence, the user must select all the images on his area of interest, open them and decide which image can be processed (i.e., if he can visually detect waves on the image). That is a potential source of excessive duration for the processing.

We can therefore imagine an automatic procedure that associates (ideally in the EO Hub) on the area of interest, few parameters: the most significant wavelength in the range 30m-250m, a signal to noise ratio associated to this parameter and the most significant wave direction.

These indicators could be obtained by computing few image spectra by FFT in different sectors of the area of interest and selecting significant peaks by thresholding the amplitude of the spectra. Position of the peak will provide wavelengths and direction.

2) BathySent processing

In terms of processing, the intervention of the user should be ideally limited to introduce the limits of the area of interest (e.g. 4 corners), the images' selection to be used (helped by the indicators of 5.1 if provided and the cloud cover indicator) and the bands to be processed (by default: 2,4,8). This is the level of automation we have to target.

II.3.1 *DOCUMENT POTENTIAL UTILIZATION OF PROCESSING BY-PRODUCTS (CLOUD MASKING, AVERAGE WIND DIRECTION, ETC.) IN DIFFERENT EO-BASED APPLICATION*

The inter-band offset tracking by local correlation can provide information on the cloud motion. As the cloud moves as a block and without dispersion (its speed is the same for all the local wavelengths, and generally faster than expected for ocean's waves), it can be easily discriminated from waves' motion.
Such characteristics can be used for detecting and mapping clouds on Sentinel 2 images.
In addition, the speed of the cloud can be representative of the wind speed at altitude. For instance, these two observations have been used for analyzing volcanic clouds in de Michele (2016).

Noteworthy is the fact that such altitude wind estimations apply to different kind of images than BathySent as the presence of clouds on the image is a major limitation for the bathymetry derivation from spaceborne data.

II.3.2 *TECHNICAL DOCUMENTATION OF THE PROPOSED METHODOLOGY AND CORRESPONDING DOWNSTREAM PRODUCTS (DEFINITIONS, SPECIFICATIONS, ASSUMPTIONS AND LIMITATIONS)*

1) *Input images data types:*

   The processing chain must be adapted the standard Sentinel 2 product: Jpeg2 raster image, 16 bits integer. The processing level envisaged for BathySent is: level 1B (ortho TOA). Other input formats could be possible –geotiffs, raw matrixes, other formats- if we need to implement the use of third party missions data. The processing can be done on the entire S2 frame or on a “user selected” box (this option should be recommended for processing time issues), within the S2 frame. By default the S2 bands to be used are: B2, B4 and B8.

   The user should select a dataset without clouds over the area of interest. Also, the swell should be visible on the dataset in order for the algorithm to work. For this specific task, there are two solutions. The first consists of a dedicated tool which task is searching the S2 archive automatically for “no clouds” datasets and – with the help of a FFT based tool – search for images where the swell is visible. The second consists of user visual inspection over the S2 archive. These two point have to be discussed (and maybe built) with ESA.

2) *Output:*

   The output is a floating-point matrix (in Geotiff format), where each element represents the water column depth with respect to a relative nearshore value (the tides are not automatically take into account in this version). Each matrix element has an associated geographic information. The size of the matrix is the same size of the input data divided by the sampling step. The sampling step could be user defined according to the maximum lambda observable in the AOI. This require the user to be an expert already. Else, by default, we propose a step of 300 meters. This represents the final grid resolution equal to maximum common lambda based on experience. The correlation window could be adaptive or fixed. Ideally, the correlation window should reduce in size as it approaches the coastline. At this step of development, we propose a fixed correlation window. Its size (we propose 600 m) corresponds to 2 to 3 times the longer waves we can expect in rather normal conditions.

   The acquisition frequency is every 5 days. The more the acquisitions are included in the bathymetry computation, the better the final precision of the bathymetric map.

3) *Limitations:*

   The limitations of the processing are mainly related to clouds free data and the presence of the swell in the image. These parameters depends on the nature of the test site, its geography its climate and its location. Frequent data acquisition improves the chances of imaging a test site presenting favorable conditions. Other two limitations are related to swell wavelength and the image pixel size. Swell wavelength controls the final bathymetry maximum measurable depth. S2 pixel resolution controls the minimum visible lambda, nearshore, and the measure of the celerity.

Second, the satellite specific parameters should enable description of the waves, i.e., not too large DX_{max} (to enable proper detection of the wavelengths in the wavelet analysis), not too large DT (to avoid ambiguity in the wave-displacement estimate), and not too small DT with respect to DX_{min} (to enable detection of displacement in the cross-correlation step). Given DXmax = the lowest resolution allowed pixel size, DXmin = the highest resolution allowed pixel size, DT = the time lag between two bands acquisitions, physically, for the procedure presented here, the image/sensor characteristics should be such that:

$$[\, DX_{max} < \lambda/2 \quad ; \quad DX_{min} < 2\, c\, DT \quad ; \; DT < \lambda/2c \;] \qquad [4]$$

The first inequality defines the minimum wavelength that can be reliably estimated given the sensor characteristics; the two others define the acceptable celerity range. These inequalities (from Poupardin et al., 2016) provides the critical limit of application of the CWB method. For instance, as DX_{max} becomes small, the results will be reliable, but for $DX_{max} \geq \lambda/2$, the wavelength λ will not be detected at all. Therefore, if those conditions are not satisfied, the proposed method cannot be used.

II.4 References

de Michele, Raucoules D., Idier D., Smai F., Foumelis M.. Shallow bathymetry from Sentinel 2, by joint estimation of swell celerity-wavelengths. Remote Sensing of Environment, in review, 2020.

de Michele M., Raucoules D., Arason Þ, 2016, Volcanic Plume Elevation Model and its Velocity Derived From Landsat 8, *Remote Sensing Of Environment,* vol. 176, 219-224

Leprince, S., Barbot, S., Ayoub , F. , & Avouac, J.-P. , 2007, Automatic and precise orthorectification, coregistration, and subpixel correlation of satellite images, application to ground deformation measurements , *IEEE Transactions on Geoscience and Remote Sensing*, 45,1529-1558

Poupardin A., Idier D., de Michele M., Raucoules D., 2016, Water depth inversion from a single SPOT-5 dataset, *IEEE trans. In Geosci and Rem. Sensing*, vol. 54, 2329-2342

Chapter III: Algorithm Implementation

This chapter aims at:

- Outlining the path to code implementation and Consolidation of the Python code using Sentinel-2 data
- Outlining the initial performance assessment of bathymetry retrieval approach
- Reporting on the scouting the CREODIAS platform
- Outlining processing requirements and hints to optimization for cloud processing

III.1 Algorithmic implementation of Sentinel-2 bathymetry retrieval approach

For research use and debugging purposes, from the algorithm (TN2) we firstly wrote a code in IDL (Interactive Data Language). IDL is vectorized, numerical, and interactive, and is commonly used for interactive processing of large amounts of data (including image processing). The syntax includes many constructs from Fortran and some from C. We commonly use it in BRGM.

Once we found the IDL code sufficiently robust, we converted the IDL code into a Python script. Python is an interpreted, object-oriented, high-level programming language with dynamic semantics. Its high-level built in data structures, combined with dynamic typing and dynamic binding, make it very suitable for rapid application development, as well as for use as a scripting. It is easily portable, no license is required, and it allow an easy transfer from IDL codes. These are some of the reasons why we chose Python for this stage of BathySent project. The pseudo code is described in details in TN4.

III.2 Assessment of algorithm computational performance

We performed several tests using Sentinel 2 archives on coastal areas in the Mediterranean basin (Lyon Gulf, image here below) and on the Atlantic coast (Ile d'Yeu). The input is one S2 dataset, at one given date, as found in the ESA S2 archives. The size of the test area is 34x34 km; Sentinel 2 data resolution is 10 meters per pixel. Over the test area, for one given date, the code runs in 4 minutes on a Processor Intel(R) Core(TM) i5-7300HQ CPU @ 2.50GHz, 2501 MHz, 4 cores, 4 logic processors. Memory cost: 800 Mb RAM (i. e. 3 times one image size, once loaded).

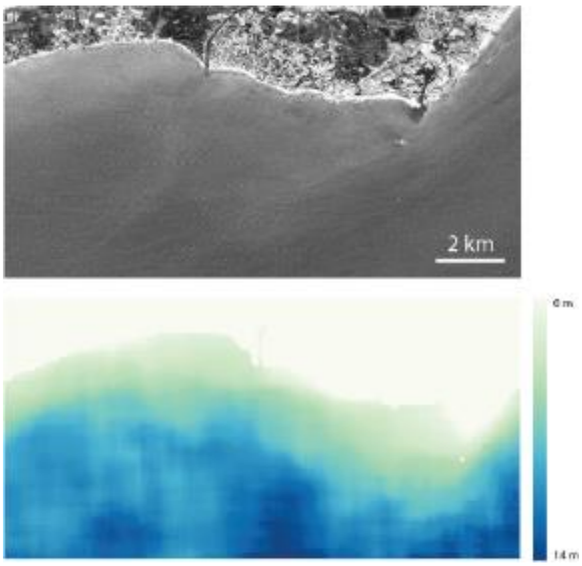

Figure 3.1: BathySent processing results on a test site in France, Gulf of Lyon. Above, S2 image. Below, bathymetry. The area is 18x10 km.

III.3 Define the level of complexity for implementation on cloud infrastructures: scouting CREODIAS platform

We open an account on CREODIAS platform www.creodias.eu, we could find the whole offer for Computing&Cloud (which is similar to EOCloud environment) and EO collection database.

We could see on CREODIAS website that they provide cloud computing (baremetals, virtual machines, operating systems – if applicable, etc.) and storage (standard HDD and fast – SSD) services. They provide in addition a wide range of network services.

The access to all Earth Observation (EO) data catalogues which are listed at https://discovery.creodias.eu/dataset. The user can use them for free. CREODIAS is able to provide EMS data collection on demand according to Copernicus policy. The user can use tools for EO data search and discovery access over API and download free of charges – an example: EO Finder https://finder.creodias.eu/www/ and EO Browser https://browser.creodias.eu/.

Access to EO data and to above EO tools are for free.

In order to test CREODIAS offer, at the beginning the user should register at https://portal.creodias.eu/register.php and ask for 150 EUR free credit.

Brgm Order Number is 3244006747. Domain (openstack): cloud_03422. We asked to try to run the code for BATHYSENT project on the cloud. First Payment Amount is 0,00 EUR. Recurring Amount: 0,00 EUR Billing Cycle: Free Account

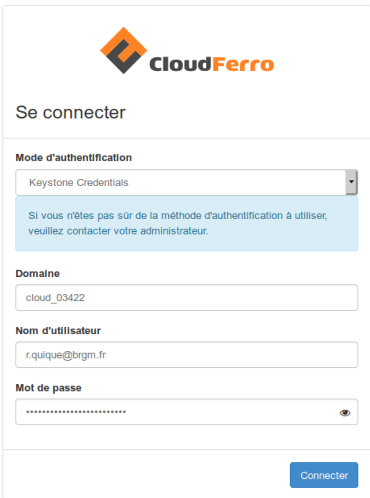

Then the user have to choose the cloud « project_with_eo » in order to be able to access, later, the EO data.

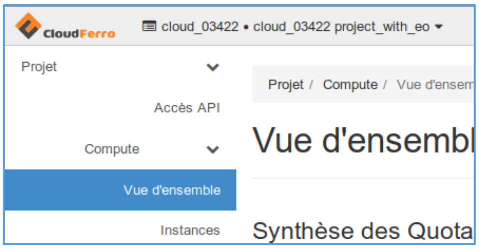

Then the user create a pair of SSH keys: https://cf2.cloudferro.com/project/key_pairs/

The create an instance, virtual machine (VM) from an image disk:

https://cf2.cloudferro.com/project/images

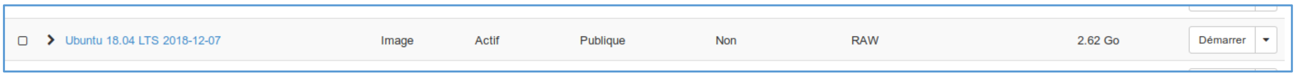

Then one choose the type on instance, then click on START. The user need to give a name at the given instance:

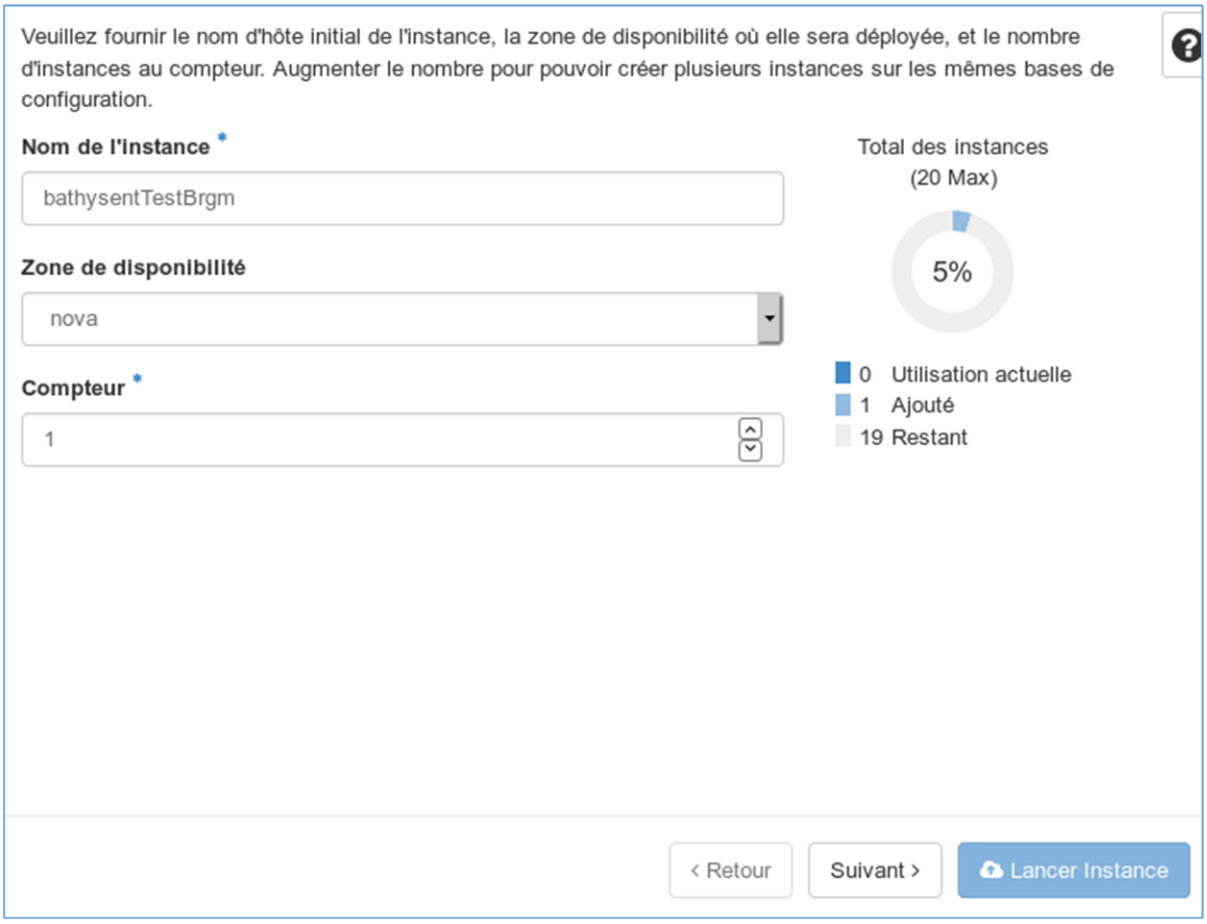

On the "Source" side: we keep the default values, we chose the framework « EO [size of our instance] », then select the top arrow to select a template.

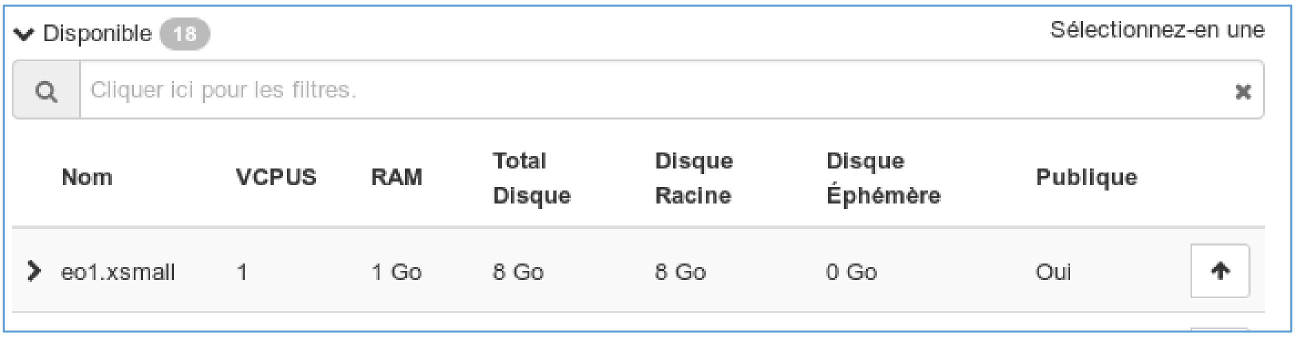

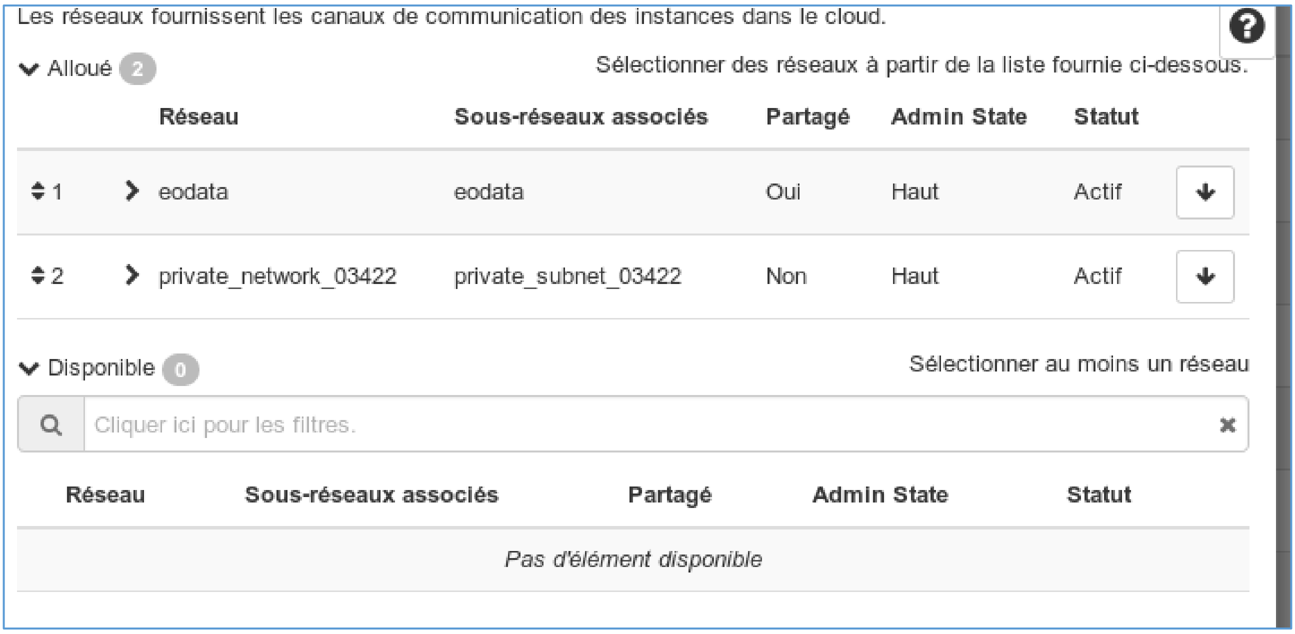

The user has to choose a private network and the EO network.

« Security group »: should be set to "allow_ping_ssh_rdp":

https://eocloud.cloudferro.com/knowledgebase.php?action=displayarticle&id=64

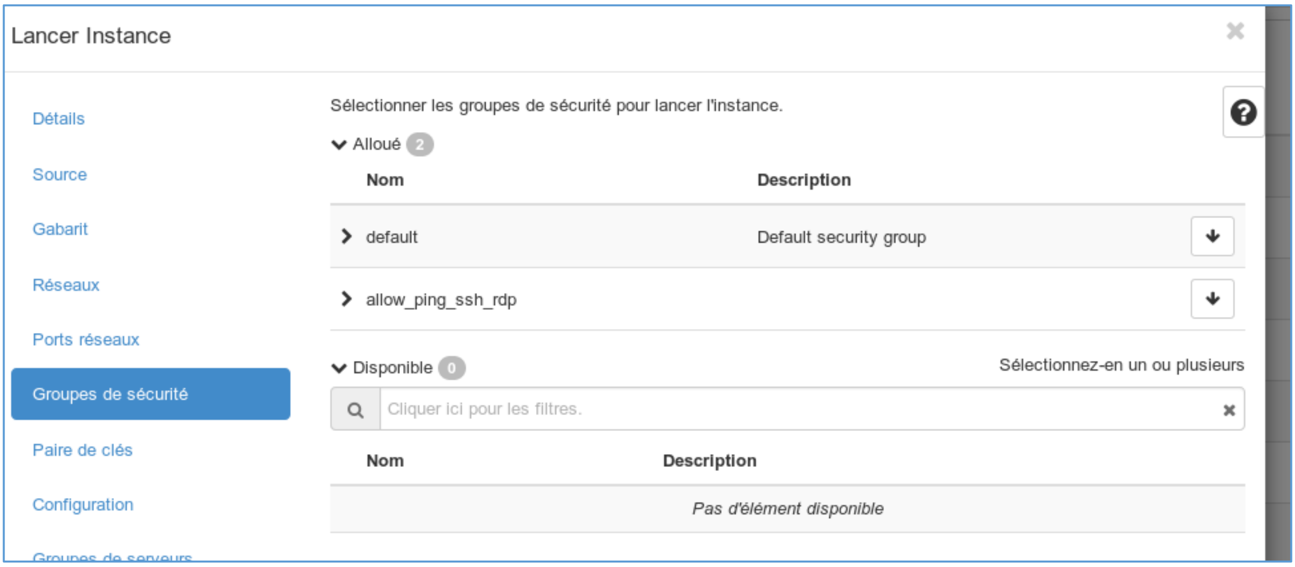

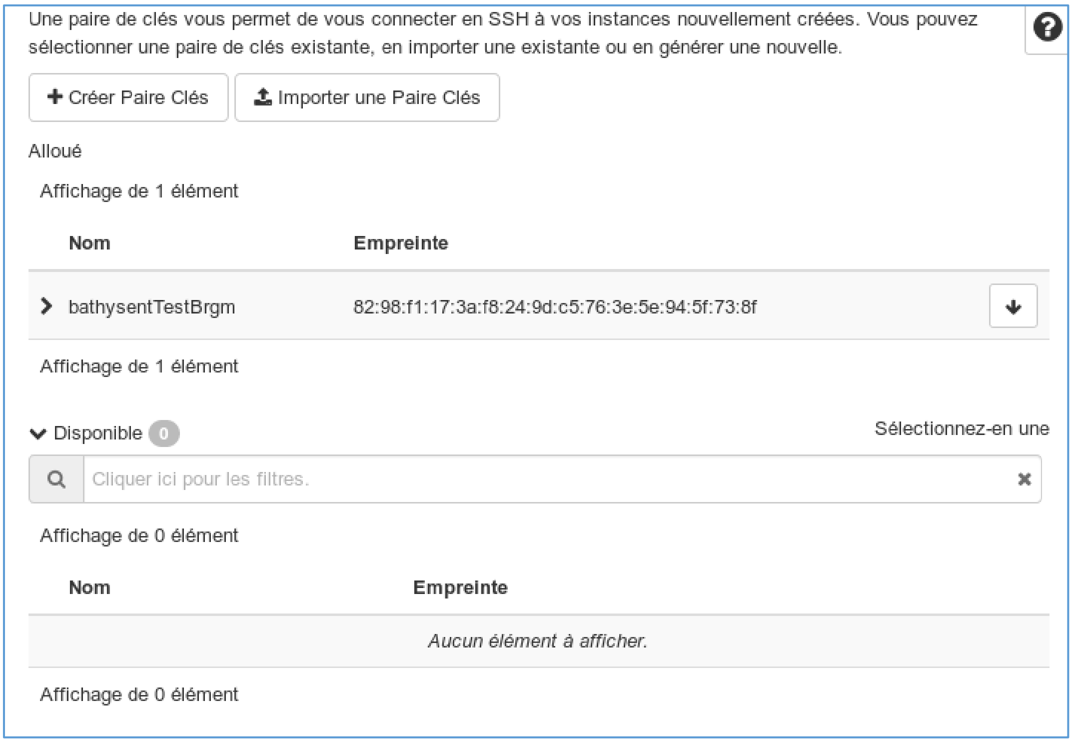

The user need to add a Key to the KeyPairs

Now the configuration is achieved, the user can launch the instance. When the instance is launched, it is visualized here: https://cf2.cloudferro.com/project/instances/. If the user would like to connect remotely, one needs to add a floating IP. This option is foreseen in CREODIAS:

https://eocloud.cloudferro.com/knowledgebase.php?action=displayarticle&id=195

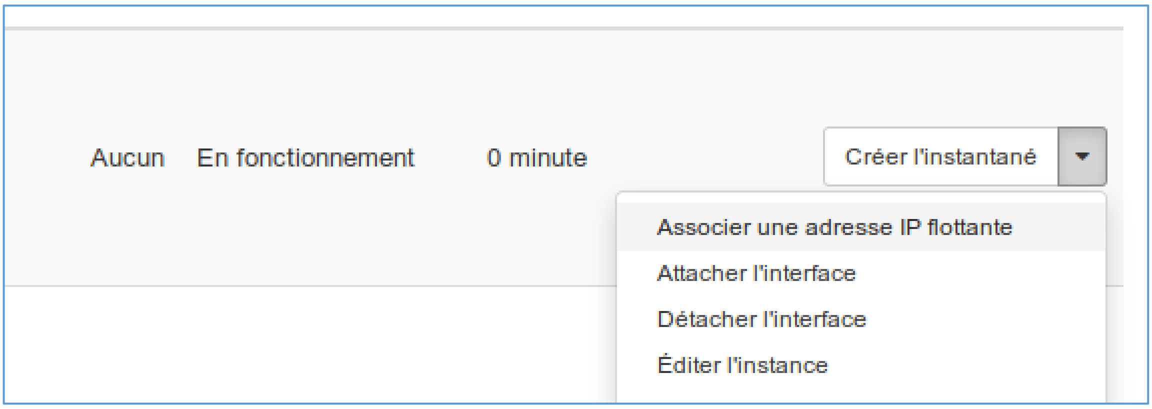

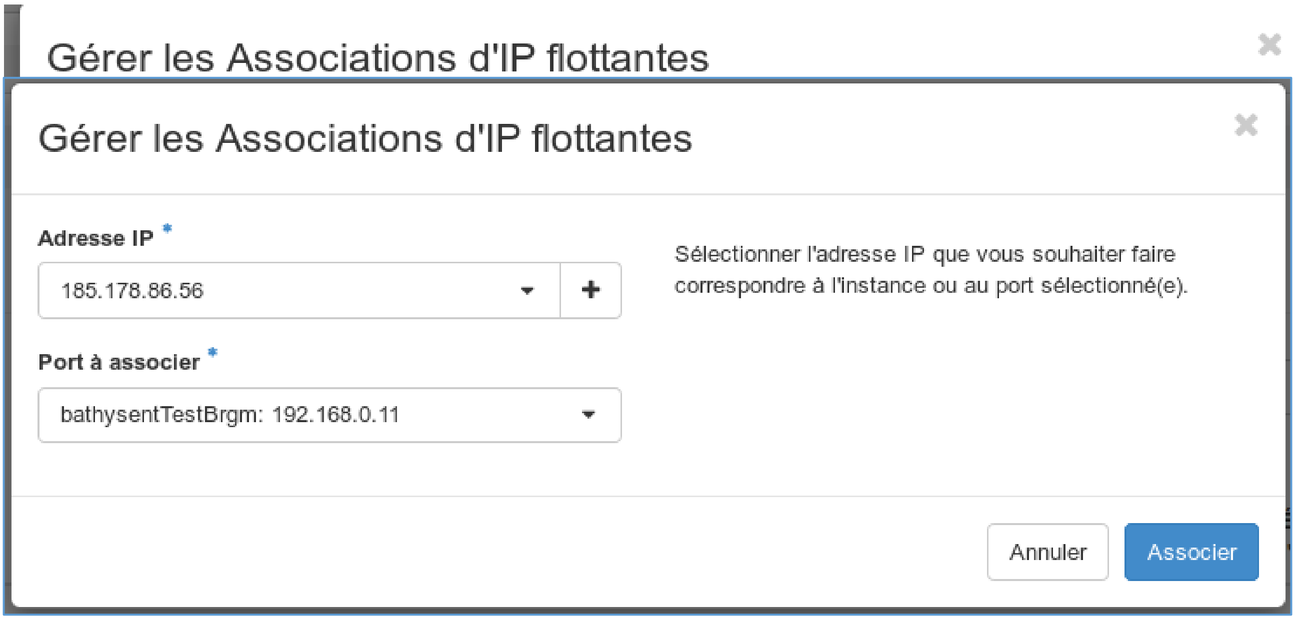

By clicking on « + » one choses the associated Port to the network 192,...

Affichage de 1 élément

	Nom de l'instance	Nom de l'image	Adresse IP	Gabarit	Paire de clés	Statut		Zone de disponibilité
☐	bathysentTestBrgm	-	eodata 10.111.0.217 private_network_03422 192.168.0.11 IP flottantes : 185.178.86.56	eo1.xsmall	bathysentTestBrgm	Active		nova

Affichage de 1 élément

On this instance, we get an external IP address (i.e. 185.178.86.56). The user need check that the ping command [ip instance], is working fine, for example:

ping 185.178.86.56

PING 185.178.86.56 (185.178.86.56) 56(84) bytes of data.

64 bytes from 185.178.86.56: icmp_seq=1 ttl=49 time=48.0 ms

64 bytes from 185.178.86.56: icmp_seq=2 ttl=49 time=47.5 ms

64 bytes from 185.178.86.56: icmp_seq=3 ttl=49 time=46.9 ms

^C

--- 185.178.86.56 ping statistics ---

3 packets transmitted, 3 received, 0% packet loss, time 2002ms

rtt min/avg/max/mdev = 46.974/47.517/48.066/0.445 ms

Else, if no packages are received, the procedure need to be re-checked, as underlined in the documentation https://eocloud.cloudferro.com/knowledgebase.php?action=displayarticle&id=29

Our query resulted in the opening of an IP on port 22 from a BRGM terminal: from IP 185.178.86.56 to our RSSI BRGM. https://eocloud.cloudferro.com/knowledgebase.php?action=displayarticle&id=68

To connect with SSH, the user is:

“eouser

chmod 600 private_cloudferro.ppk

ssh -i private_cloudferro.ppk eouser@185.178.86.56

"

Then we verify that eodata are in the directory :

"cd /eodata

ls -U | head -4

eouser@bathysenttestbrgm:/eodata$ ls -U | head -4

CAMS

CEMS

CLMS

CMEMS

"

The code could be run at this stage. Once the processing is done, the user is supposed delete the instance and to disconnect –else the payment does not stop.

The typology of our described network is here:

https://cf2.cloudferro.com/project/network_topology/#/close

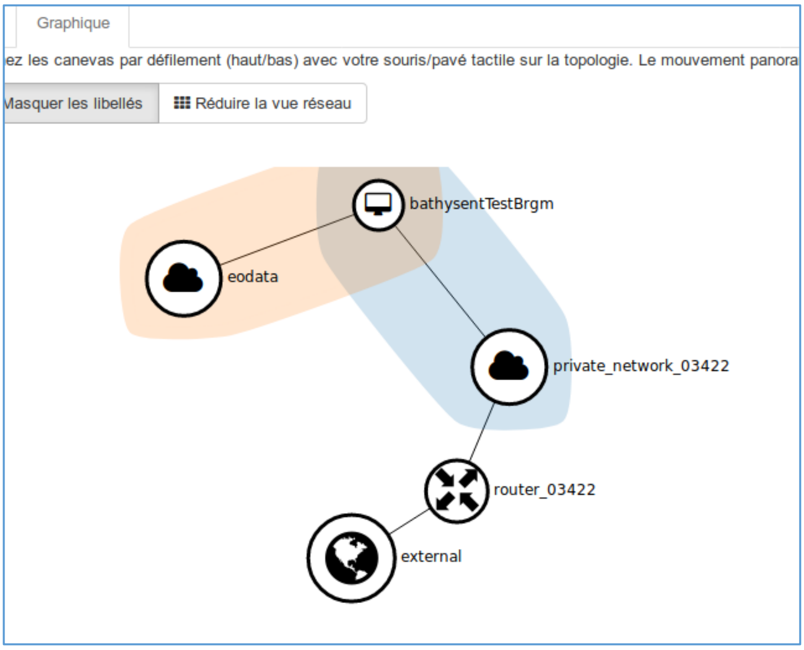

Our configuration is similar to the one described in the following page:

https://eocloud.cloudferro.com/knowledgebase.php?action=displayarticle&id=78

In terms of costs, this is the amount we spend for a given processing:

https://portal.creodias.eu/clientarea.php?action=products

https://portal.creodias.eu/reports.php

And these are the overall costs :

https://eocloud.cloudferro.com/dl.php?type=d&id=19

https://creodias.eu/price-list

As an example:

- Data access fee to products in "Big Data" storage

54,68 months

Per VM for access to whole EO data repository per all VMs in an environment with EO data access

- Internet transmission ("in" direction): 0,0064 par Giga

- Internet transmission ("out" direction): 0,0064 par Giga

- CPU - in batch processing mode, with access to EO data: 0,0444 per VCPU core per hour

Research API for eodata:

https://eocloud.cloudferro.com/knowledgebase.php?action=displayarticle&id=66

https://finder.eocloud.eu/resto/api/collections/Sentinel2/search.json?_pretty=true&q=Poland

Follows an example of instance that we created as a test:

"

8h48 :
Instances actives : 1
RAM active : 1Go
VCPU-Heures de cette période : 3,50
Go-Heures de cette période : 27,97
RAM-Heures de cette période : 3579,81

9h17

Instances actives : 1
RAM active : 1Go
VCPU-Heures de cette période : 3,98
Go-Heures de cette période : 31,84
RAM-Heures de cette période : 4075,36

13h06: suspend

„

III.3 Quantitative definition of optimum processing parameters

Two main parameters need to be defined. The first, is the window size for the cross spectrum analysis. The second, is the spatial sampling rate, which define the size of the final grid.

The window size is set to be 64 pixels = 640 meters. This is decided in order to be able to measure both short and long wavelengths in a given area of interest. We recall that long wavelength – although the final resolution of the obtained bathymetry is coarser that with short wavelengths - allow the potential measurements of deeper water columns. The sampling step is defined as a percentage of the correlation window. In this preliminary implementation, we chose 75% (one measure every 16 pixels = 16 meters) in order to obtain smoother results. This parameter can be easily modified; in a future implementation, as a perspective, the user should be able to change this parameter (as well as the window size) as an advanced option.

III.4 Processing of Sentinel-2 data over selected pilot sites

In terms of the validation and intercomparison area, which concerns the field work, HCMR have proposed a pilot site in the northern coasts of Kos Island in the "BathySentProposal".
This site, where the new coastal multibeam bathymetric survey has been proposed to take place, is exposed to wave activity (also swell) and the isobaths of 20 and 50m are placed at about 1.6 and 4.5 km respectively, far from the coastline. It is an extended shallow area, where a coverage of approximately 20km2 multibeam bathymetric survey can be achieved during the five days of the field work that have been foreseen in the proposal.
If this site reveals not to be suitable concerning the S2 geometrical characteristics, we propose two alternative sites, (a.) Kasos & Armathia Islands Strait - South West Karpathos and (b.) the strait between Paros and Naxos Islands.

S2 available track/frame on KOS Island in 2018, potentially suitable for BathySent processing:

S2A_MSIL2A_20180806T085601_N0208_R007_T35SNA_20180806T123203.SAFE

S2A_MSIL2A_20180816T085551_N0208_R007_T35SNA_20180816T160658.SAFE

S2A_MSIL2A_20181025T090031_N0209_R007_T35SNA_20181025T124151.SAFE

S2B_MSIL2A_20180801T090019_N0208_R007_T35SNA_20180801T153100.SAFE

S2B_MSIL2A_20180811T085549_N0208_R007_T35SNA_20180811T134626.SAFE

S2B_MSIL2A_20180821T085549_N0208_R007_T35SNA_20180821T152859.SAFE

S2B_MSIL2A_20180831T085549_N0208_R007_T35SNA_20180831T145951.SAFE

S2B_MSIL2A_20180910T085549_N0208_R007_T35SNA_20180910T153413.SAFE

S2B_MSIL2A_20180920T085619_N0208_R007_T35SNA_20180920T112248.SAFE

S2B_MSIL2A_20181010T090019_N0209_R007_T35SNA_20181010T135737.SAFE

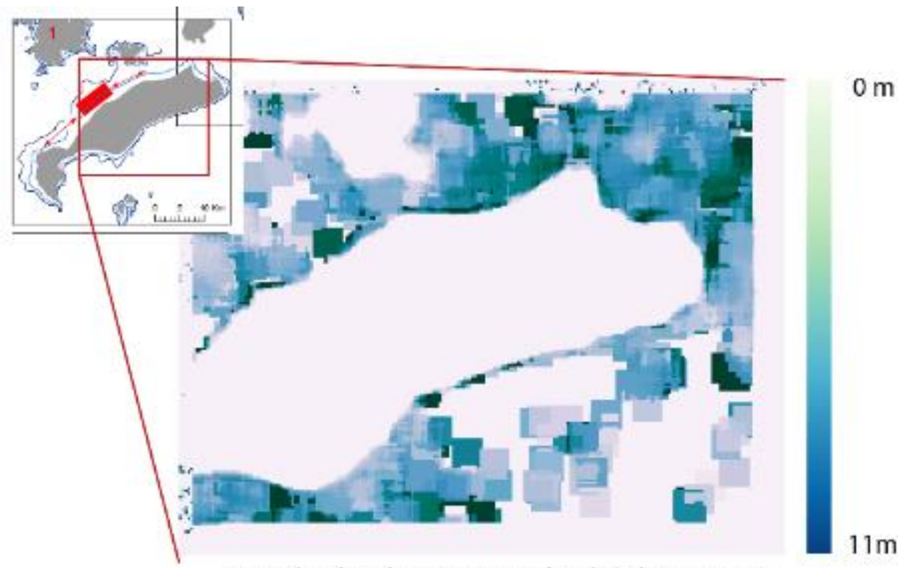

Kos Island Bathysent water depth (white is NaN)

III.5 Potential optimization for cloud processing. Perspectives

Minimum processing requirements are set by the tests on a local PC described in the computational performances paragraph, above. On a cloud, there are no a priori “upper” limits (so the requirements should be less restrictive than on local PC).
There are rooms for code optimization for cloud processing. Some ideas are provided in this paragraph.

Firstly, the user do not need to load the entire S2 frame, we could proceed by cutting the S2 frames according to the AOI. This will reduce the memory allocation, but would add CPU-time. Secondly, code parallelization (image by image) would allow multiple processing on the same S2 frames at different dates, and/or in different geographic areas. Thirdly, automatisation: in the CREODIAS cloud, we could work on the automatic creation and suppression of instances/volumes, via the use of API OpenStack.

Progress can be done in terms of algorithm optimization (loops reductions, mathematical simplifications) but also in terms of optimization in terms of results quality. For instance, multi temporal image stacking. The multidate processing idea goes beyond simple redundancy; if the depth is assumed identical per AOI per dates, the waves regimes (i.e. wavelengths and direction) are different from one date to another. In other words, beyond improving the precision, this method would aim at completing the missing information.
There is also the possibility of estimating the depth by eliminating the difference between the phase of the spectrum and the theoretical phase that depth should produce. For that, we could "invert" the dispersion relation. Instead of having the celerity in function of lambda and depth, it would be theta according to lambda and depth. The good depth H, would be the one that maximizes sigma. Such as:

(A(ij) cos(theta_mesured(ij)) - theta (h, lambda(ij))

with A being the amplitude of the spectrum.

Chapter IV: BathySent Assessment & Validation

this chapter aims at:

- Undertake a dedicated multi-beam bathymetry campaign over a selected site in Greece
- Assessment and validation of BathySent performance in terms of retrieval of coastal bathymetry using in-situ bathymetry measurements
- Comparison between conventional EO-based bathymetry retrieval approaches and proposed innovative solution using Sentinel-2 data over pilot sites.

IV.1. INTRODUCTION

The main objective of the WP4 is to specify the uncertainty of the derived coastal bathymetry results as extracted by the proposed novel approach using the Sentinel-2 mission. To validate the Sentinel-2 bathymetry retrieval results, it is necessary to compare them to reference bathymetry. The accuracy assessment will be performed using statistical indices such as RMSE and mean absolute error (MAE) and plots which will be computed between the algorithm results and reference depths.

To this end, three Data Packages (DP) for three different pilot sites in the South Aegean and Cretan Seas (figure 1), were delivered by BGRM team in order to be compared with bathymetric ground truth data.

To this end, three Data Packages (DP) for three different pilot sites in the South Aegean and Cretan Seas (figure 1), were delivered by BGRM team, in order to be compared with bathymetric ground truth data. The reference bathymetry used for the validation and assessment activities were a. the EMODnet DTM-2018 (DP1, DP2), b. from HCMR-IO's national high bathymetry database (DP2), and c. new reference bathymetry from the carried bathymetric campaign, which took place within the framework of the BathySent - WP4 (DP3).

Furthermore, for Kos island coastal area, the northern coasts, the Stumph- Linear Ratio Model (Stumpf et al, 2003) was applied on a Sentinel-2 imagery in order to derive bathymetry to be compared with the BathySent results. In the next paragraphs the above activities are described in details. The dedicated multi-beam bathymetry campaign to the north coasts of Kos island, will be described first, then the evaluation of the three data packages and finally the comparison between conventional EO-based bathymetry retrieval approaches and proposed innovative solution using Sentinel-2 data over pilot sites according to the WP4 objectives.

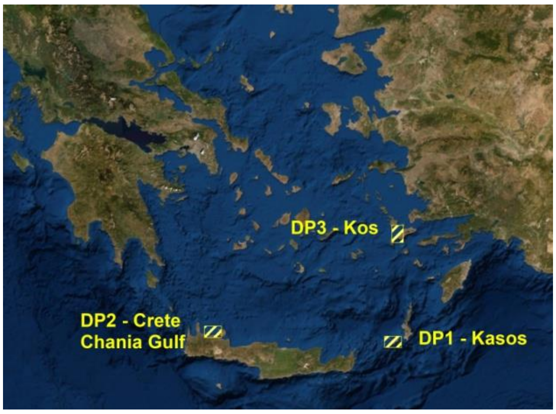

Figure 4.1. Pilot sites location.

IV 2. DEDICATED MULTI-BEAM BATHYMETRY CAMPAIGN OVER THE NORTHERN COASTS OF KOS ISLAND

Ultra-resolution swath bathymetry data were acquired onboard R/V Alcyon (HCMR) (Figure 2) during a 4-day cruise realized from 8th to 12th of October 2019. A surface area of ~25 km^2 ranged at water depths from 4 to 40 m was mapped by the use of a Teledyne Reson SeaBat 7125 dual head (200 and 400 kHz). During the cruise, data were recorded in real time by a RTK GPS system achieving horizontal and vertical accuracy of less than 10 cm with respect to the local reference GPS station. The collected data were post-processed by the Teledyne Reson PDS-2000 software package including removal of spurious soundings, noise filtering, and tide and sound velocity profile corrections. A digital terrain model (DTM) was produced by a

Geographic Information System Software Suite (ERSI ArcGIS®) gridded into the resolution of 2-m cell size (Figure 4.2).

In addition, bathymetric data were collected at very shallow waters (1-10 m) by the use of a single beam echo sounder (Humminbird HELIX 9 CHIRP SI GPS G2N). The device's transducer was mounted on the side of the inflatable boat "Kirki", which was moving at an average speed of 5 nautical miles. The 200-kHz frequency was selected in order to succeed the optimum resolution. Depths were acquired with a step of 1 sounding per second along 50-nm tracks (~25000 soundings). The coordinate system was the WGS84, while the GPS/WAAS receiver provided a horizontal accuracy within 2.5 meters.

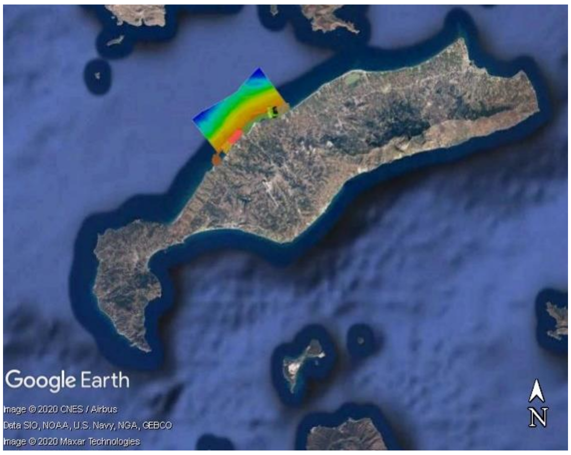

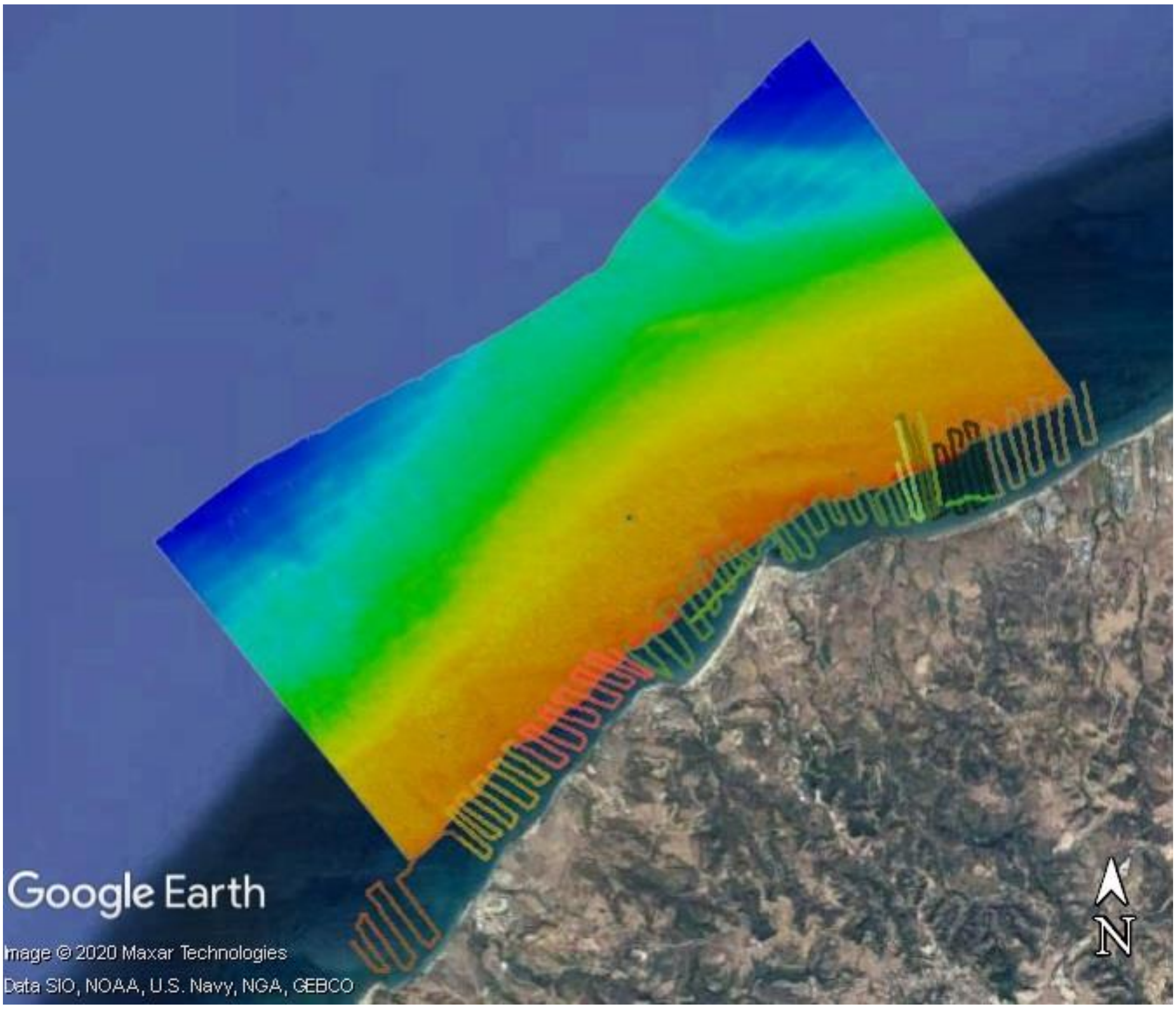

Figure 4.2. Top left: HCMR's R/V ALCYON (LOA : 13.40 m, Width : 3.7m). Top right: the area covered covered by multi and single beam echo-sounder during the during a 4-day cruise realized in of October 2019 (in zoom the bottom image).

IV.3. ASSESSMENT & VALIDATION OF BATHYSENT PERFORMANCE OVER PILOT SITES

C. 4.3.1 Assessment of DP1 - Kasos using EMODnet 2018 bathymetry.

The DP (DP1) on Kasos island was the first "test" for the comparison of the Sentinet-2 bathymetry retrieval results with a reference bathymetry. The dataset was delivered in ENVI format georeferenced (UTM 35N), positive values towards deeper bathymetry and of 160m resolution (Figure 3). The DP-1 was transformed in a ESRI raster geodatabase format so that all the analysis to be taken place through the ArcGIS suite. The BathySent result image was then studied/analyzed regarding the depth values. The retrieved depths was up to 20m with the covered area to extend much more deeper. Figure 4.4 shows the distribution of the retrieved depths.

Figure 4.3. Sentinel - 2 results (as delivered)

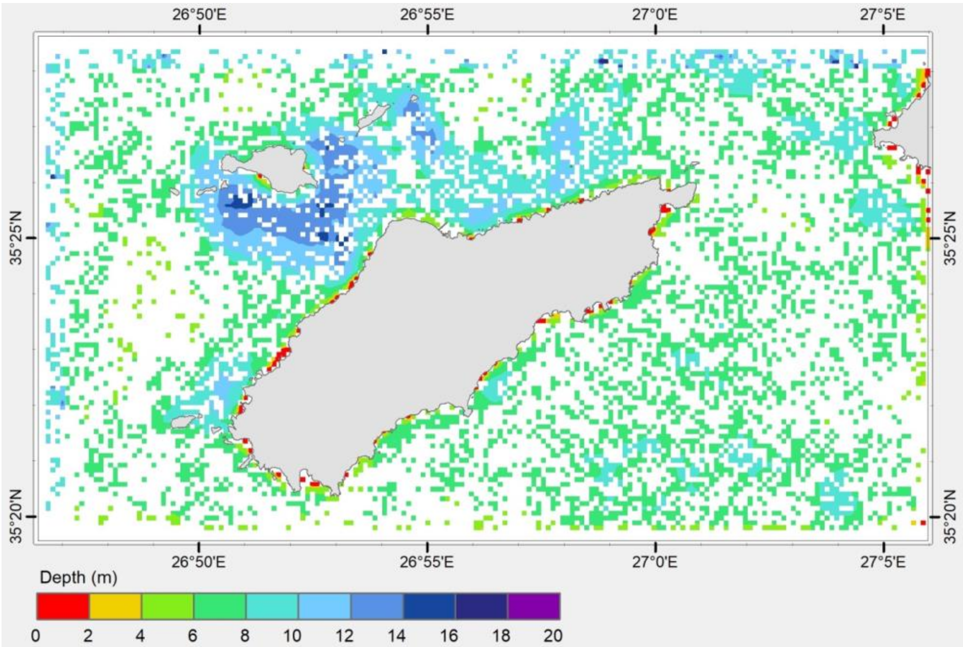

Figure 4.4. Sentinel - 2 retrieved depth distribution

The available reference bathymetry for Kasos coasts, was from EMODNET High Resolution Seabed Mapping Lot, in 1/16 arc minute (~ 120 m) resolution. The relevant DTM for Kasos area downloaded from the EMODnet bathymetry portal (https://portal.emodnet-bathymetry.eu/). A subset of the DTM, the depth zone of 0–55m was extracted (Figure 5). The data sources of the extracted EMODnet DTM are: a. GEBCO, for the 17-50m depth area and b. Satellite derived bathymetry, for the area of 0-17m depth (Figure 5).

The resolution of GEBCO data is low (30 arc-second upsampled to 3.75 arc-second, https://www.gebco.net/data_and_products/gebco_digital_atlas/) and regarding the satellite derived data the general description of the vertical accuracies is given based on worldwide validation with acoustic and Lidar data and comparisons with nautical charts. For this area an on side validation was not possible because of the absence of modern surveyed data using acoustic or lidar technology (https://www.emodnet-bathymetry.eu/metadata-amp-data/composite-dtms-catalogue-service#/metadata/SDN_CPRD_4667_greece1007).

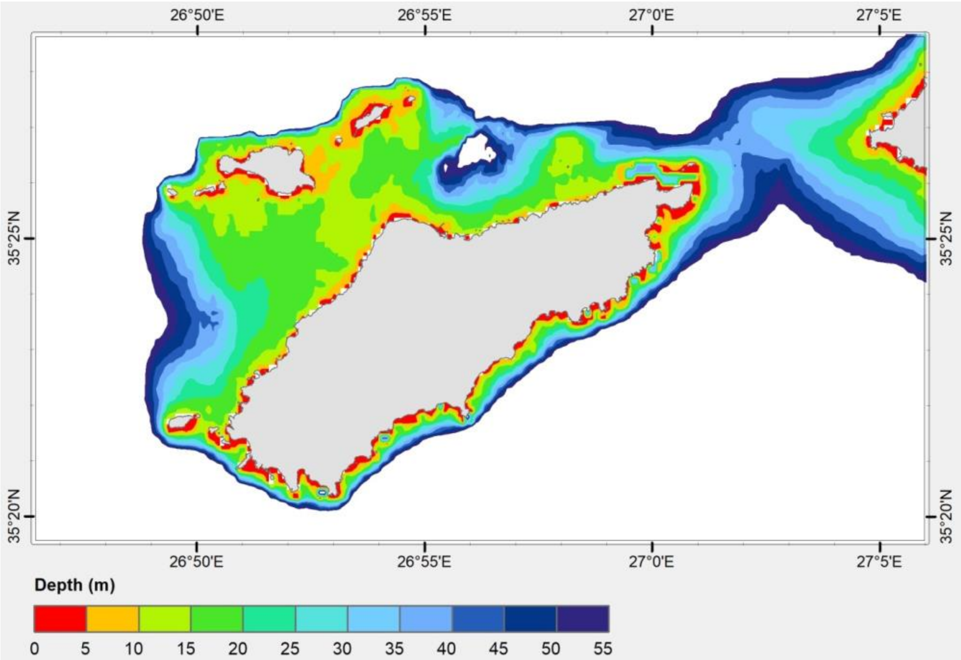

Figure 4.5. EMODnet Bathymetry (~120m res)

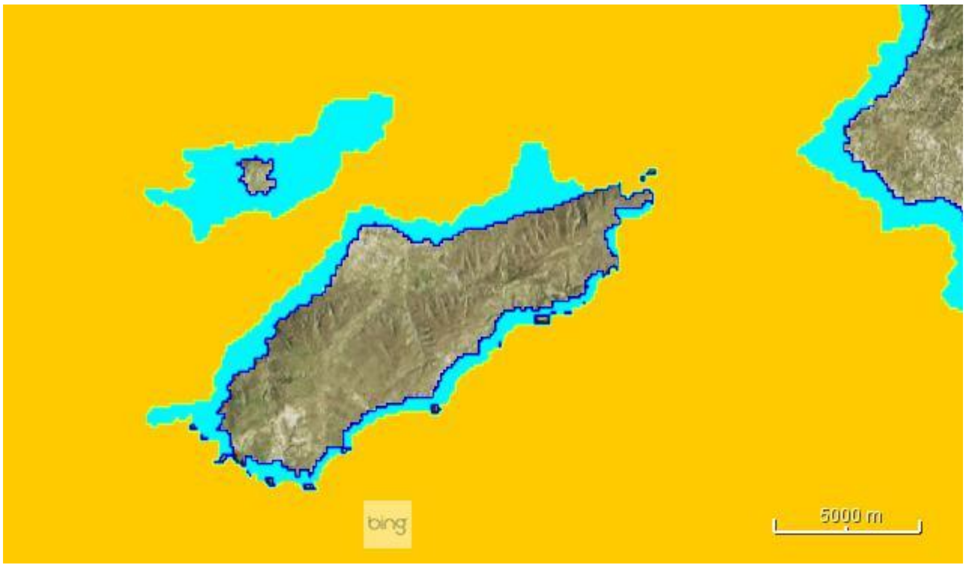

Figure 4.6. EMODnet data sources (orange: GEBCO, cyan: satellite derived bathymetry)

Subsequently, the reference DTM was resampled in order to match the spatial resolution and the extent of the Sentinel 2 result raster. The second, was then converted to point feature (vector layer) and the depth values were included in its attribute table. After that, a subset of the points that lies within 0-55m depth (based on EMODnet depths) was selected (Figure 7). Finally, the depth values from EMODnet grid were extracted (for the points subset) and the differences between the values of Sentinel 2 results and EMODnet depths were calculated (Figure 8) in order to be performed the results' statistical evaluation.

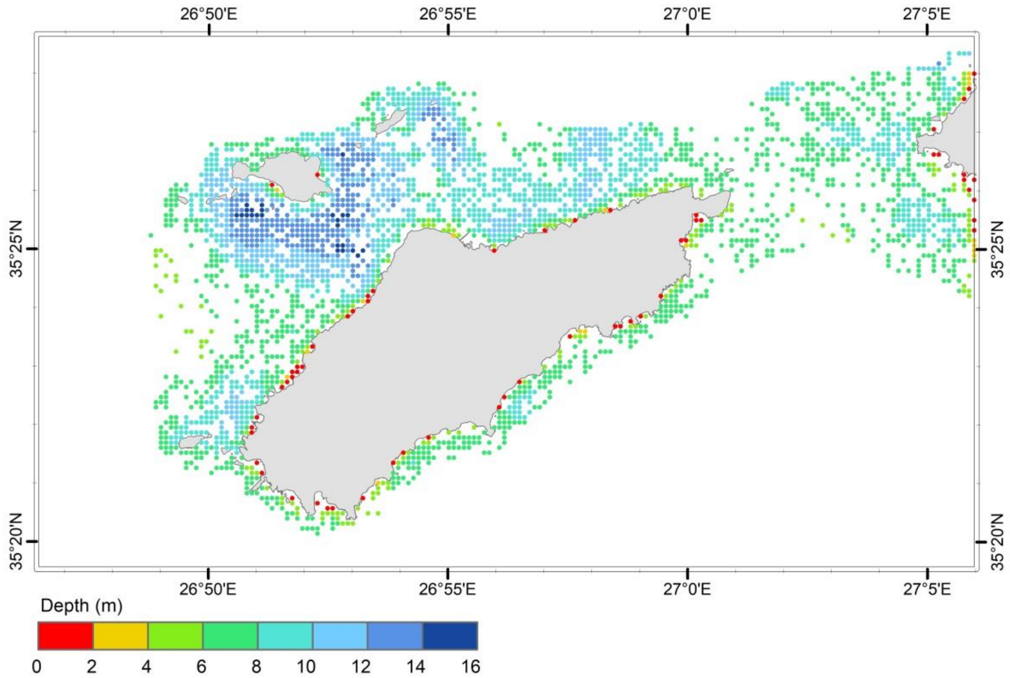

Figure 4.7. Sentinel 2 results used for the assessment

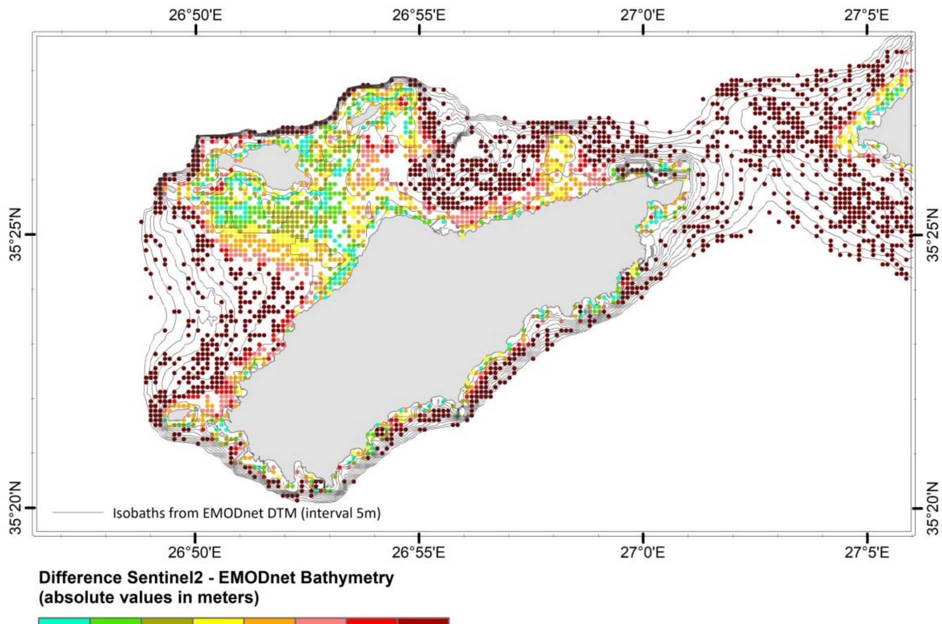

Figure 4.8. Absolute Differences (m) between Sentinel 2 results and EMODnet Bathymetry

The histogram of the frequencies of the absolute differences between the Sentinel 2 results and the EMODnet bathymetry depths and the Bland-Altman plot, shows the difference between the depths retrieved from BathySent algorithm and EMODnet depths vs EMODnet depths and the 95% confidence interval limits [mean±(1.96*st.dev)] a. for the depth zone 0-60 m and b. for the depth zone 0-17 m, are shown in Figures 9 and 10 respectively.

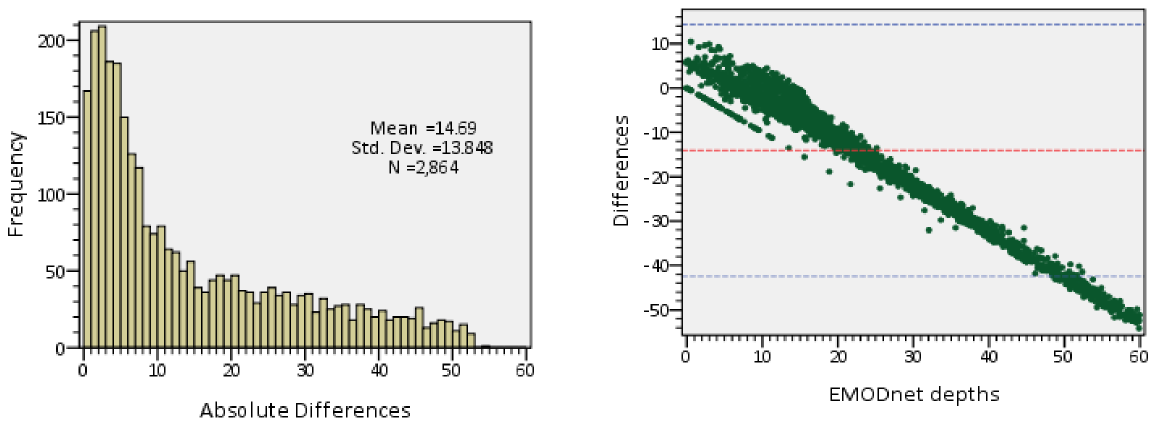

*Figure 4.9. Left- Histogram of the frequencies of the absolute differences between the Sentinel 2 results and the EMODnet bathymetry depths. Right - Bland-Altman plot, shows the difference between the depths retrieved from BathySent algorithm and EMODnet depths vs EMODnet depths and the 95% confidence interval limits [mean±(1.96*st.dev)]. Both applied for the depth zone 0-60 m.*

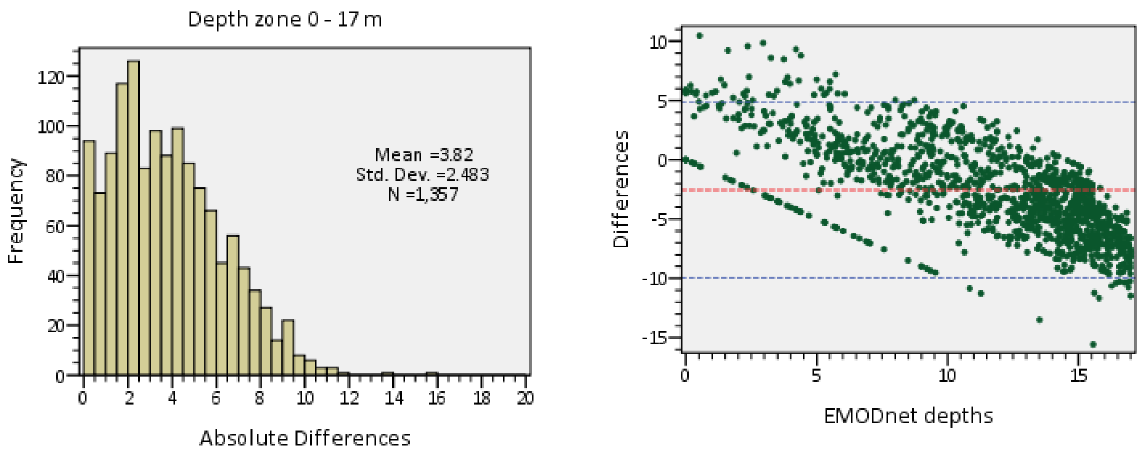

*Figure 4.10. Left- Histogram of the frequencies of the absolute differences between the Sentinel 2 results and the EMODnet bathymetry depths. Right - Bland-Altman plot, shows the difference between the depths retrieved from BathySent algorithm and EMODnet depths vs EMODnet depths and the 95% confidence interval limits [mean±(1.96*st.dev)]. Both applied for the depth zone 0-17 m.*

The statistical analysis performed, also the map of the absolute differences (MAE) between the BathySent derived bathymetry and the EMODnet DEM, are shown that in the zone of depths up to 20m the difference is around 3.5 m. More specific, and as shown in the histogram, for the absolute differences in the zone of 0-17m depth, the 25% corresponds to differences lower than 1.8 m, for the 50% of the assessed points the differences are lower than 3.5 m , while for the 75% of them the differences range up to 5.4m. Finally, RMSE for both zones of depth, 0-17 & 0-55 m, is 4.56 m and 20.19 respectively and also the MAE for each zone 3.82 m and 14.69 m same order.

D. IV.3.2. Assessment of DP2 - Crete using EMODnet 2018 & HCMR bathymetry.

The second Data Package (DP2) provided by BGRM was for the N-NW coasts of Crete -the Gulf of Chania. According the BGRM data description the processed S2 data were from 2018 and 2019; not all the data were suitable for BathySent approach but were finally found 3 acquisitions where the algorithm performs the best. The dataset was also provided in ENVI format georeferenced (UTM 34N), double precision coding, positive values towards deeper bathymetry and of 80m resolution (Figure 11).

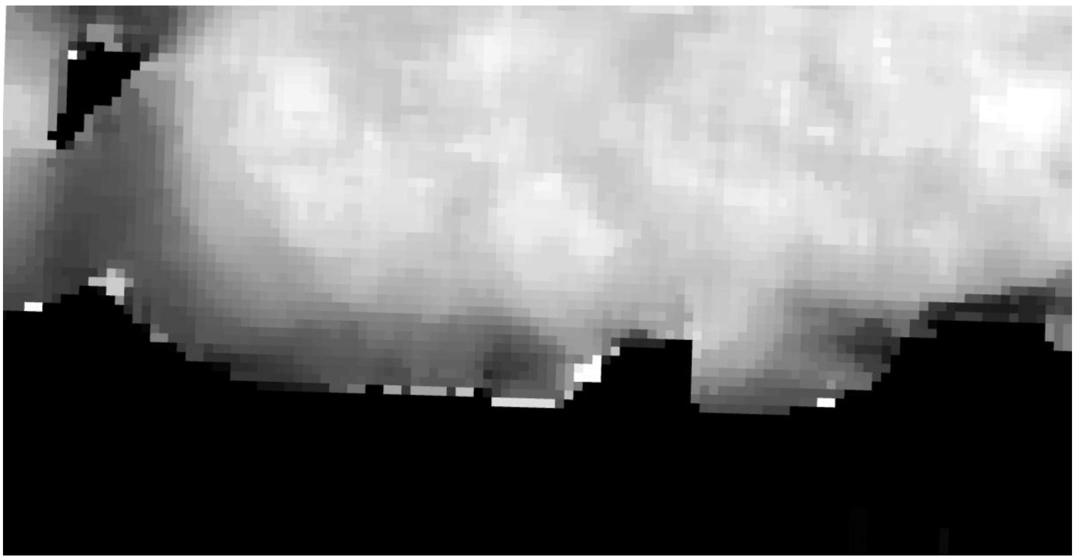

Figure 4.11. Sentinel - 2 results (as delivered)

The DP-2 was transformed in a ESRI raster geodatabase format like DP-1. The "pre-processing" steps (all process needed to result the geo dataset with the required info to perform the assessment) were mostly the same as the steps followed for the DP1. However, few differences took place during the preprocessing. Thus, the steps followed, is presented in bullets and also their image-results. Detailed description when the process was different from the one of DP1.

Pre-processing steps:

1. Sentinel 2 result image was studied/analyzed regarding the depth values. In addition, histogram of the retrieved depths' distribution was included (Figure 12).
2. Bathymetry for Crete area was downloaded from the EMODnet bathymetry portal (EMDnet DTM2018). The depth distribution from EMODnet DTM covering the same area as Sentinel2-result image is presented In Figure 13.

3. In Figure 14 is presented the depth distribution from EMODnet DTM covering the same depth zone (0-22m) with the Sentinel2-result image.

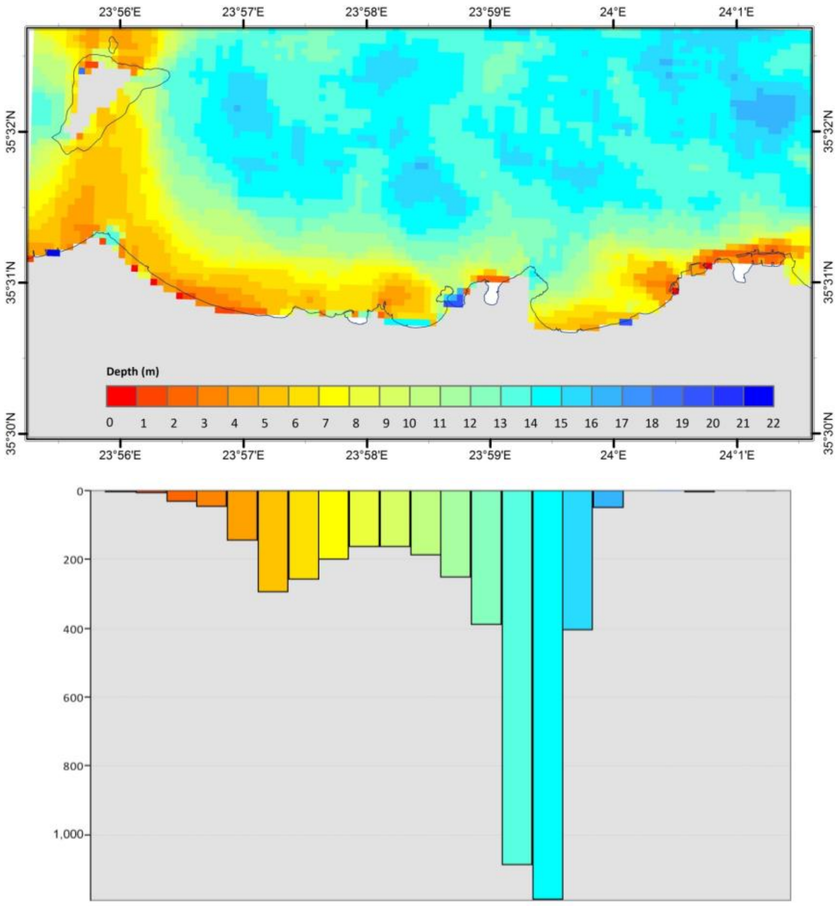

Figure 4.12. Sentinel - 2 results - Retrieved Depths distribution

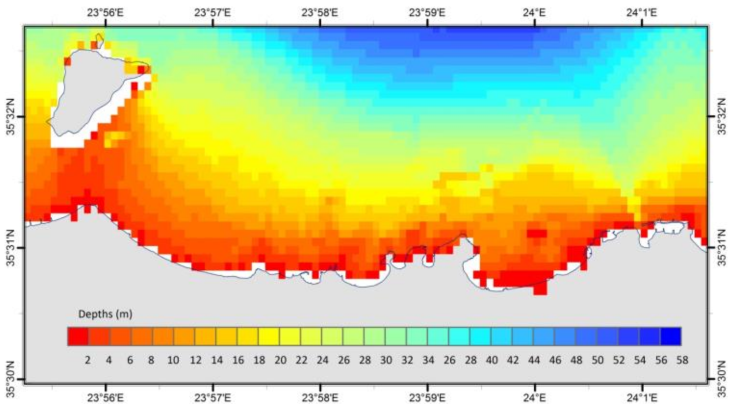

Figure 13. EMODnet Bathymetry DTM (~120m res)

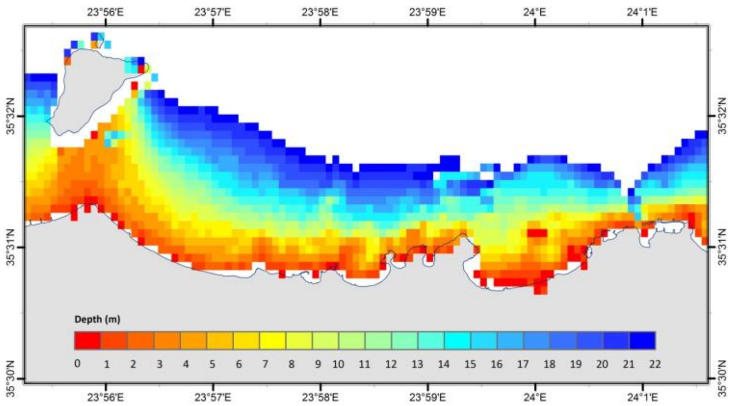

Figure 4.14. EMODnet Bathymetry 0-22m depths (~120m res)

4. The data sources of EMODnet DTM in the area of interest are the following:
   → a bathymetric dataset from multibeam survey provided by HCMR (https://www.emodnet-bathymetry.eu/v_cdi_v3/print_wfs.asp?edmo=269&identifier=GN36201500007_269_G74)
   → a bathymetric dataset from singlebeam survey provided by HCMR (https://www.emodnet-bathymetry.eu/v_cdi_v3/print_wfs.asp?edmo=269&identifier=GN36201409922_269_G74)
   → Satellite derived bathymetry, for the area of 0-17m depth provided by EOMAP (https://www.emodnet-bathymetry.eu/metadata-amp-data/composite-dtms-catalogue-service#/metadata/SDN_CPRD_4667_greece1001)
   → Data GEBCO, for the area of 17-50m depth (https://www.gebco.net/data_and_products/gebco_digital_atlas/)

   The coverage of each one is shown in Figure15 and the metadata of the is included as separate files.

Figure 4.15. EMODnet data sources (1: multibeam bathymetry, 2: singlebeam bathymetry , 3: satellite derived bathymetry and 4: GEBCO)

5. The EMODnet bathymetry dataset was reprojected and resampled (upsampled to 80m resolution) in order to be assigned the spatial resolution and the extend of the Sentinel results image. A few pixels of the sentinel-results image along the coastline are not assigned with the EMODnet ones, this happens because these pixel s are corresponded to pixels with no depth values in EMODnet DTM.
6. In terms of the existing reference bathymetry as shown in figure 15 and described previously, two datasets included to the EMODnet DTM have been provided by HCMR (no 1 & 2 - Figure15). These two datasets are referred to bathymetric acquisitions took place from January 2014 to May 2015 during various field campaigns by using both single and multi beam echo sounders. Swath bathymetry data and also single beam data, were acquired similarly as described in paragraph 2 "*Dedicated multi-beam bathymetry campaign over the northern coasts of Kos island*". As the resolution of the original datasets is much more higher of the one published in EMODnet DTM, the area covered by them, was rejected from the EMODnet resampled DTM. A new DTM in the same extent and resolution with the Sentinel-2 results, was produced using the sounding HCMR's data. Subsequently, this DTM was merged with the EMODnet DTM and covered the area previously rejected. The reference bathymetry (RDTM) is ready to be included in the assessment processing.
7. Sentinel 2 result image was converted to a point feature (vector) dataset. Each one of the elements of the point feature which was created, is positioned at the center of the corresponding raster pixel. In the points' attribute table, a field which contains the retrieved depth value of each pixel of the Sentinel-results image was also created.
8. Depth values from RDTM were also extracted and recorded in the attribute table of the point dataset created previously (step 7). The differences between the values of Sentinel 2 results and RDTM depths were calculated within the attribute table in a new field. Figure 16 shows the Sentinel-result image converted to points positioned at the centers of cells over the reference bathymetry - RDTM (same extend and spatial resolution). In Figure 17 is presented the spatial distribution of the absolute values of the above differences, in combination with depth zones defined by the isobath lines (5m interval) extracted from RDTM.

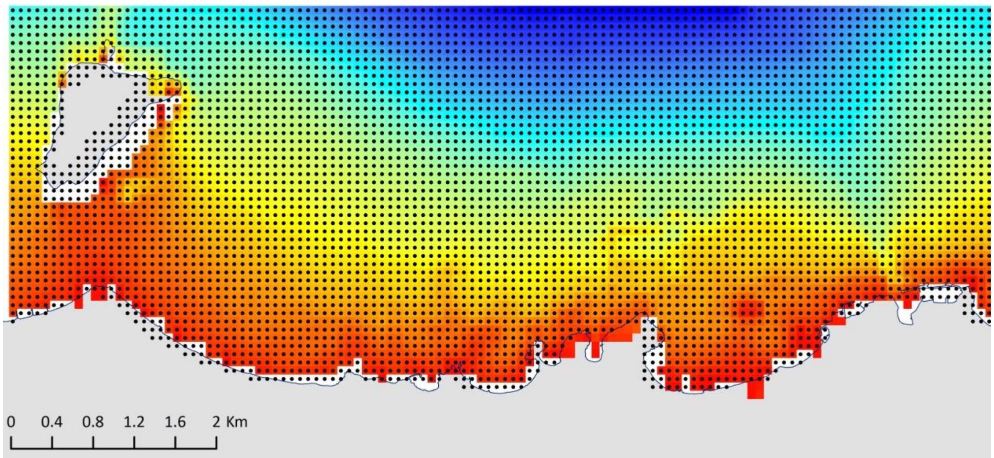

Figure 4.16. Sentinel-result image converted to points positioned at the centers of cells over the reference bathymetry - RDTM (same extend and spatial resolution)

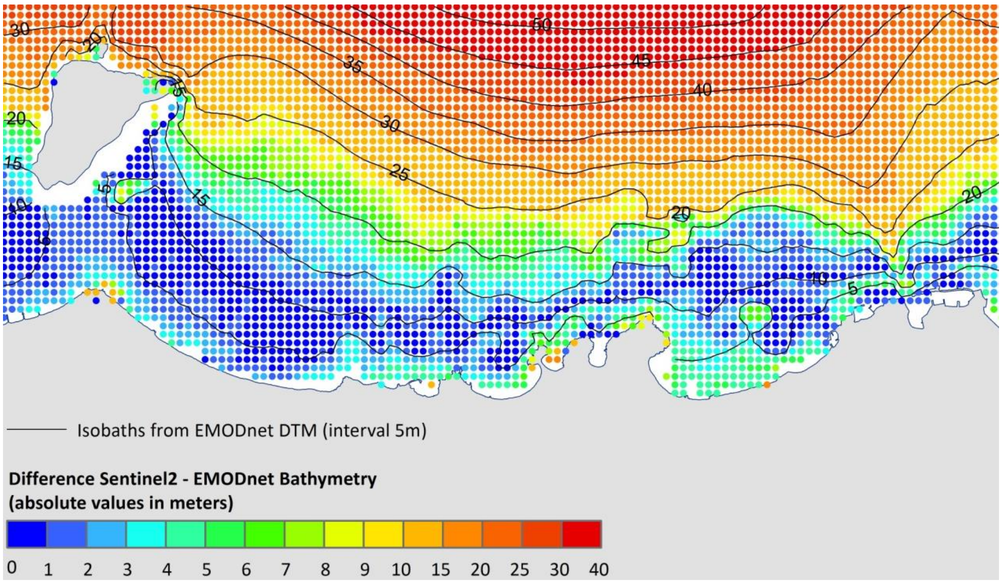

Figure 4.17. Absolute Differences (m) between Sentinel 2 results and reference bathymetry

9. The statistical evaluation was firstly applied to whole extend of the study area (depths 0 - 55m). Linear regression analysis shows a weak relationship (R2 = 0.458) between Sentinel 2 results and the RDTM (Figure 18). Taking into account the result image of the Absolute Differences (m) between Sentinel 2 results and reference bathymetry (Figure 17), linear regression was repeated over the zone of 0-30 m depth (Figure 19). A stronger correlation (R2 = 0.625) between the estimated and measured depths is shown as expected. Histogram of the frequencies of the absolute differences between the Sentinel 2 results and the depths from RDTM and the Bland-Altman plot, shows the difference between the Depths retrieved from Sentinel images and Measured depths vs Measured depths and the 95% confidence interval limits [mean±(1.96*st.dev)], applied at the extend of measured depths and also within the depth zones of [0 - 5], (5 - 10], (10 - 15], (15 - 20], (20 - 25] and (25 - 30] m. In Figures 20-23 are presented the above statistical plots. According to the statistical analysis it seems that the algorithm's results for depth extraction from Sentinel 2 images has the better response within the zone of 5 - 15m depth. where a percent of 75% of the assessment points, concerns differences lower than 2m. Finally, in Table 1 is presented the Root Mean Square Error (RMSE) and the Mean Absolute Error (MAE) for each one of the depth zones.

Table 4.1. Root Mean Square Error (RMSE) and the Mean Absolute Error (MAE) for each one of the depth zones

Depth zone	RMSE	MAE
0 - 5m	3.87	3.03
5 - 10m	1.84	1.32
10 - 15m	1.89	1.50
15 - 20m	4.34	4.06
20 - 25m	9.00	8.68
25 - 30m	14.07	13.76
30 - 35m	19.77	19.52
35 - 40m	23.14	23.08
40 - 45m	28.17	28.12
45 - 50m	33.32	33.27
50 - 55m	37.61	37.59

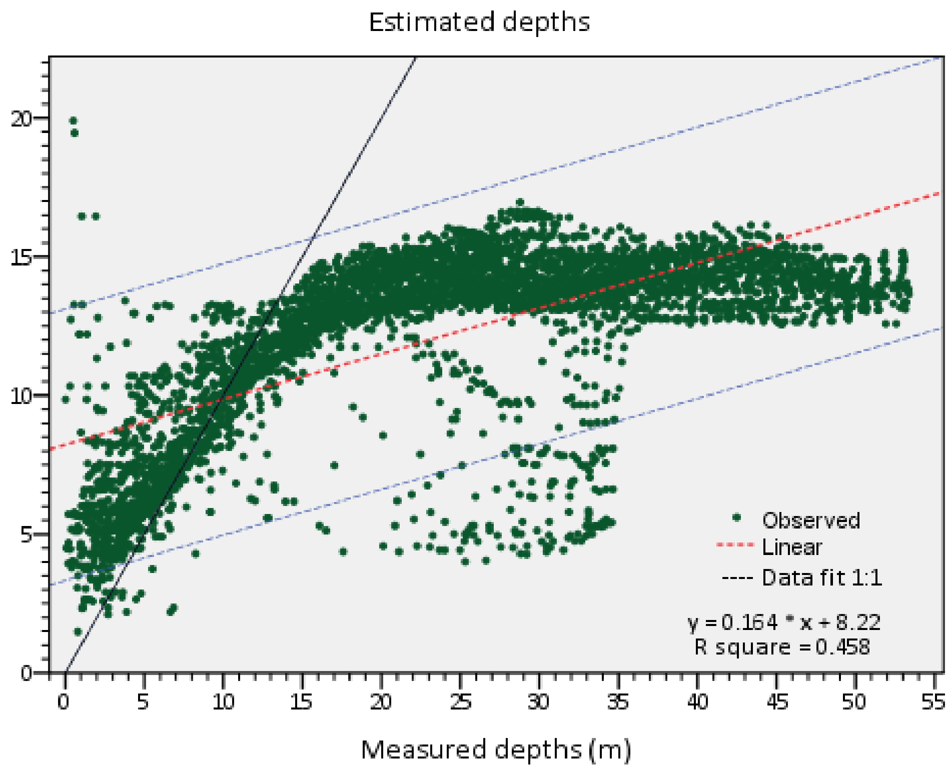

Figure 4.18. The relationship between the Sentinel 2 results and the measured depth values (0-55m depth).

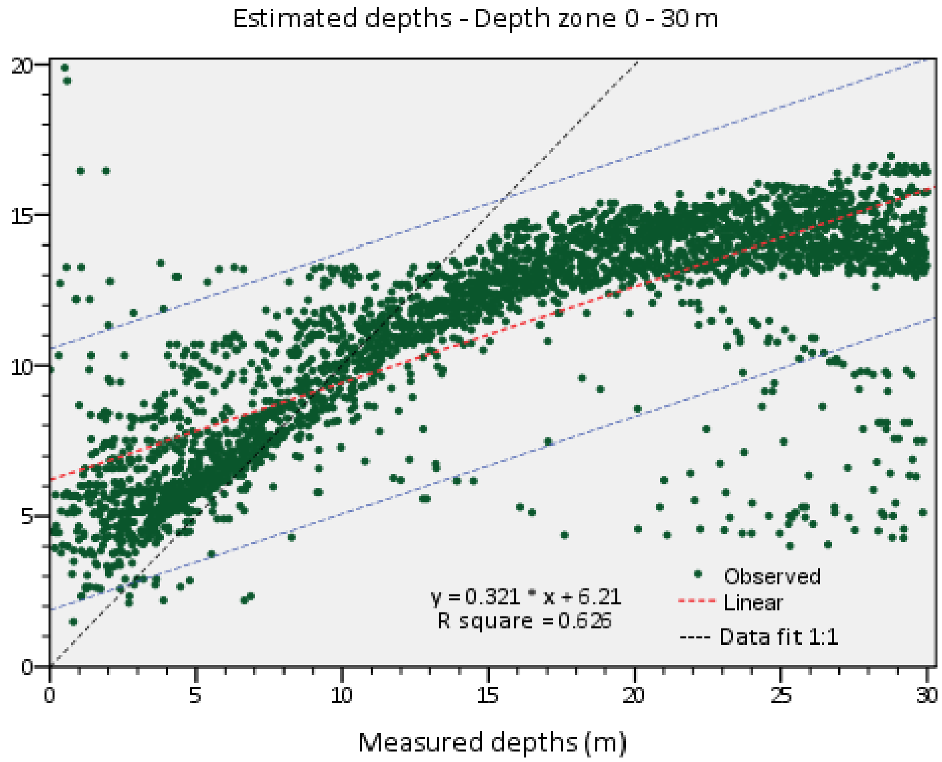

Figure 4.19. The relationship between the Sentinel 2 results and the measured depth values (0 - 30m).

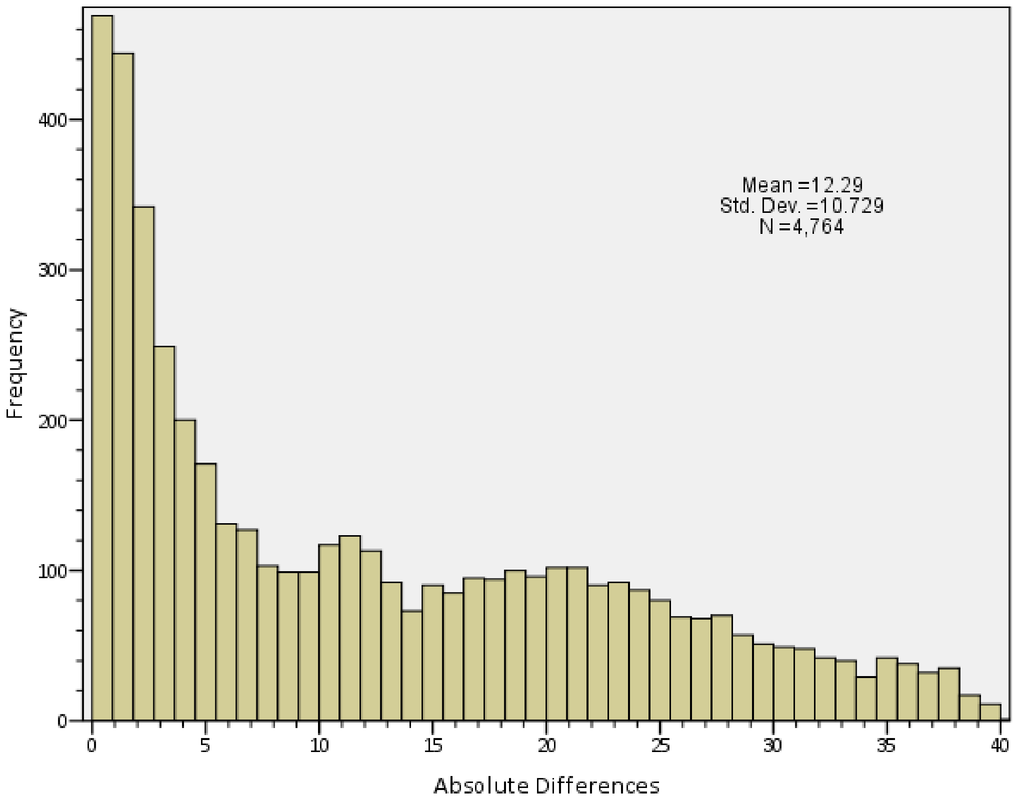

Figure 4.20. Histogram of the frequencies of the absolute differences between the Sentinel 2 results and the Measured depths (0-55 m depths)

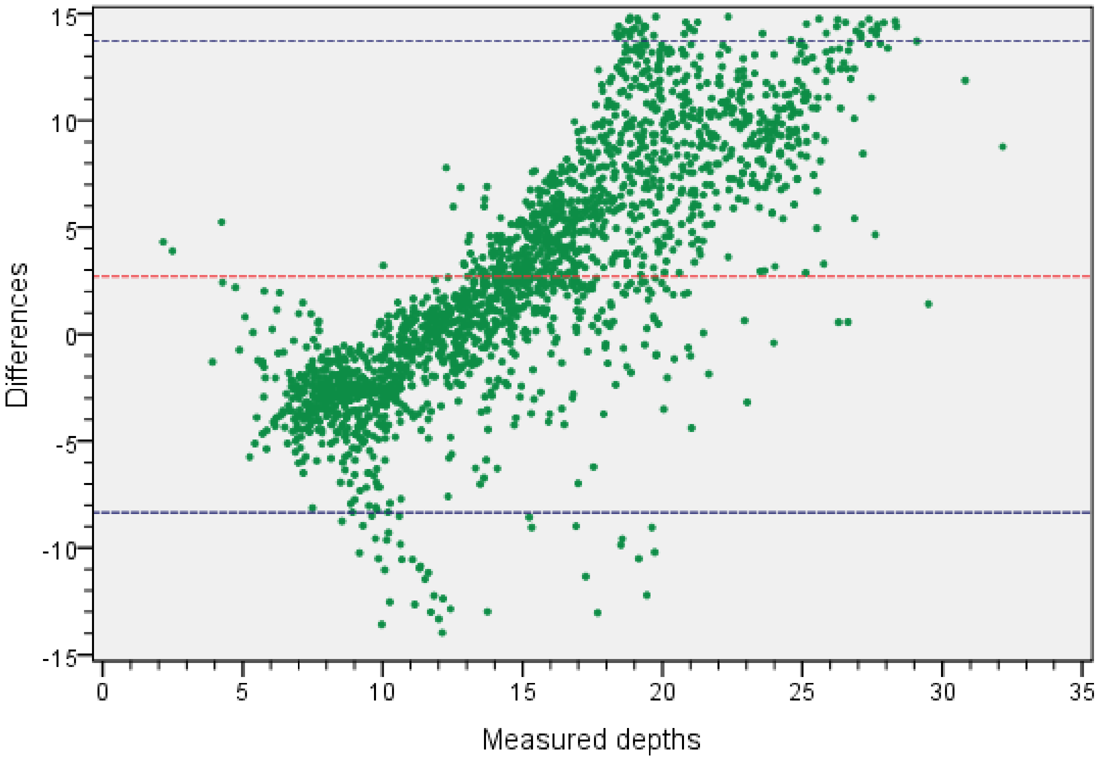

*Figure 4.21. The Bland-Altman plot, shows the difference between the Depths retrieved from Sentinel images and Measured depths vs Measured depths and the 95% confidence interval limits [mean±(1.96*st.dev)]*

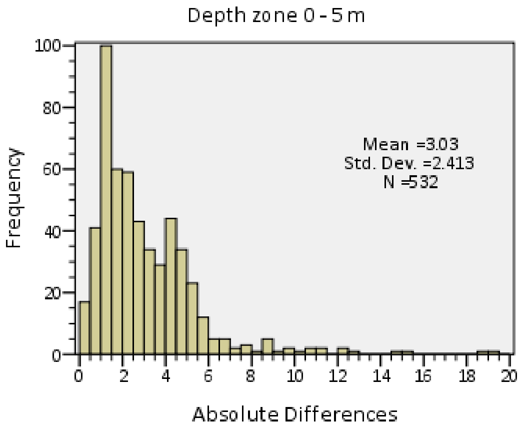

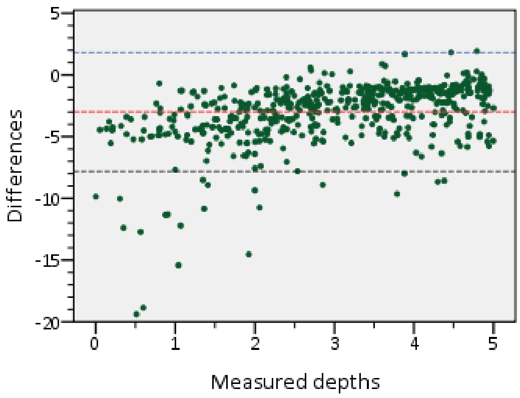

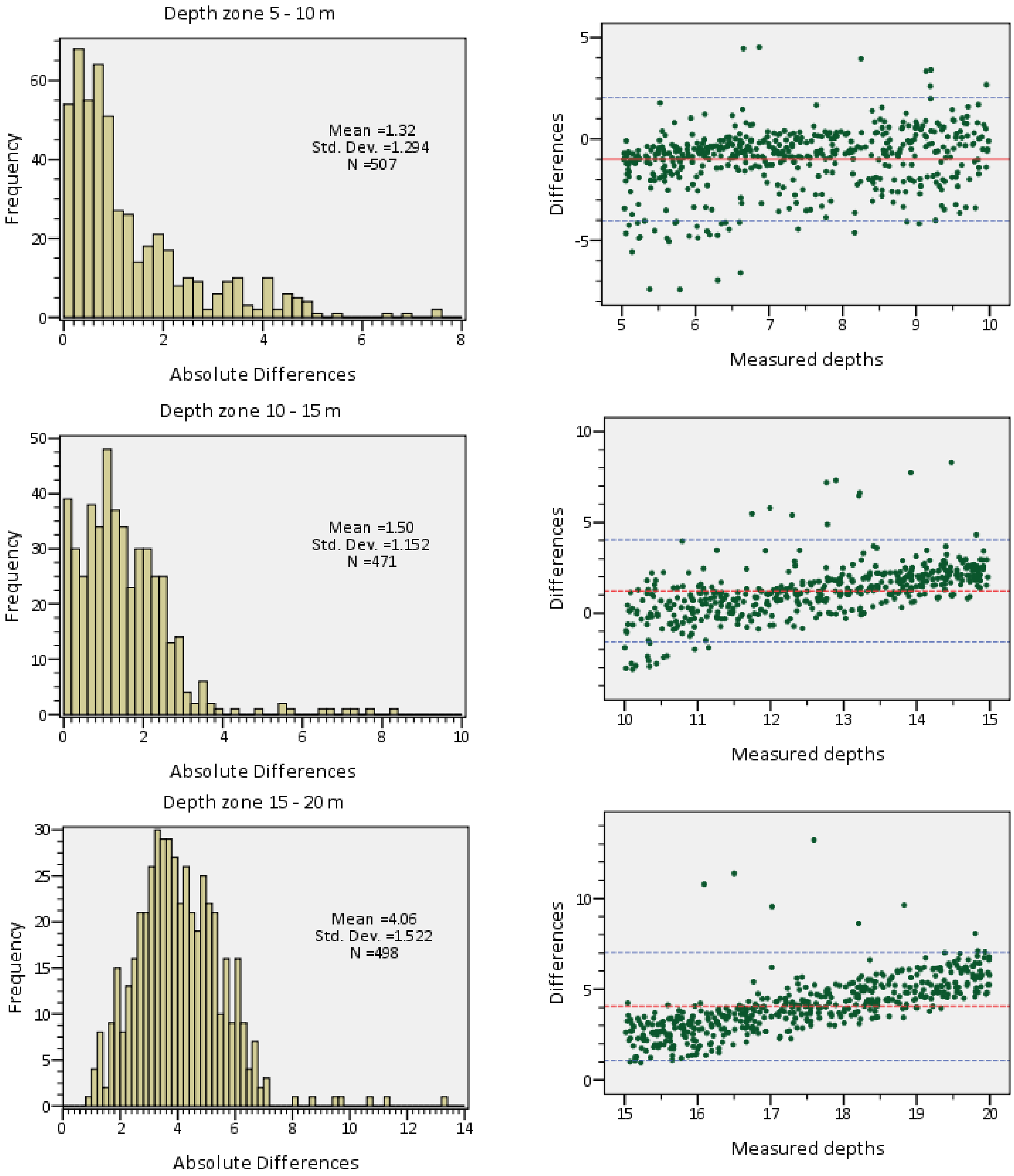

*Figure 4.22. Left: Histogram of the frequencies of the absolute differences between the Sentinel 2 results and the measured depth values for different depth zones. Right: The Bland-Altman plot, shows the difference between the Depths retrieved from Sentinel images and Measured depths vs Measured depths and the 95% confidence interval limits [mean±(1.96*st.dev)] for each depth zone.*

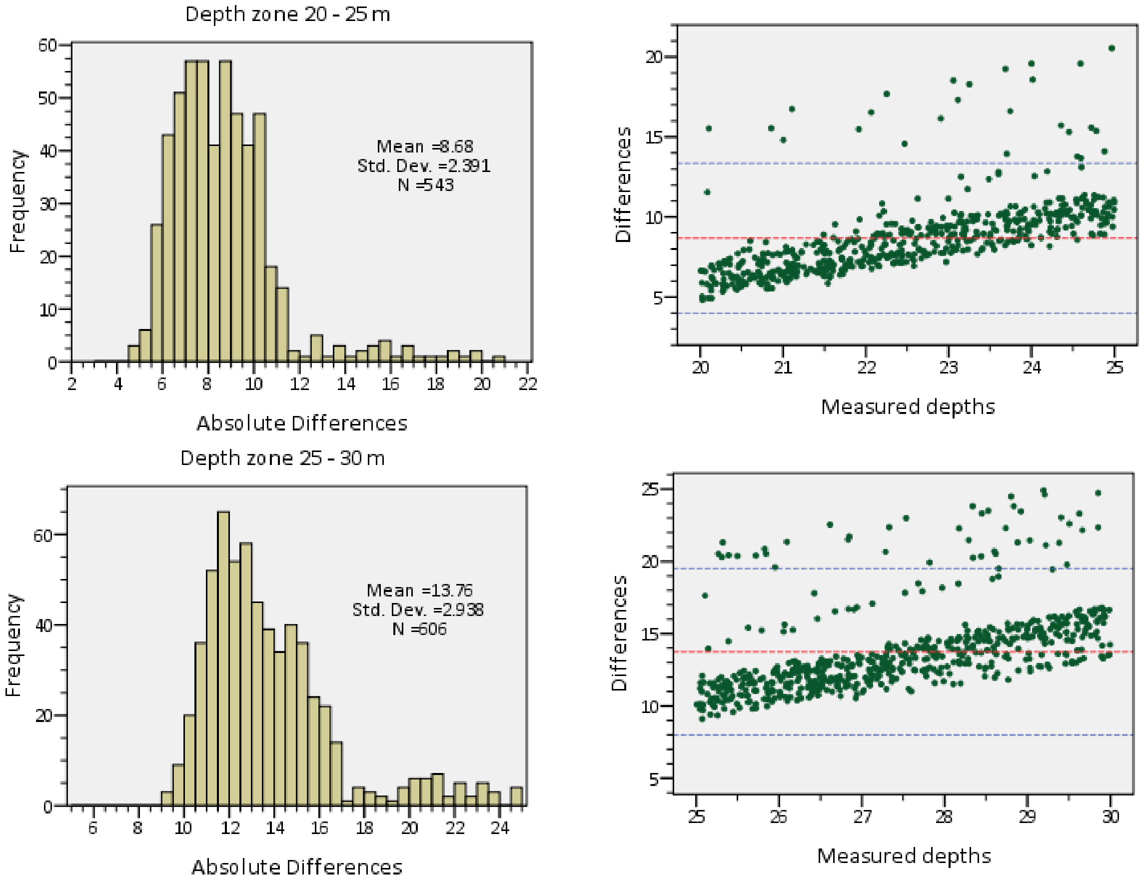

Figure 23. Left: Histogram of the frequencies of the absolute differences between the Sentinel 2 results and the measured depth values for different depth zones. Right: The Bland-Altman plot, shows the difference between the Depths retrieved from Sentinel images and Measured depths vs Measured depths and the 95% confidence interval limits [mean±(1.96*st.dev)] for each depth zone.

E. IV.3.3. Assessment of DP3 - Kos using the new survey bathymetry (Oct. 2019).

The third Data Package (DP3) provided by BGRM, was for the north coasts of Kos island. This dataset, as the previous ones, was provided in ENVI format georeferenced (UTM 35N), double precision coding, positive values towards deeper bathymetry and of 80m resolution (Figure 24). The assessment of the DP3 was taken place in relation of the new bathymetric data were acquired within the framework of the BathySent Project in October 2019.

Swath bathymetry (4-38m) and bathymetric data collected at very shallow waters (1-10 m) by the use of a single beam echo sounder were acquired onboard R/V Alcyon during a 4-day cruise realized in October 2019 (2 m res) are presented in Figure 25. The DP3 assessment process followed was the same as that used for the DP1 and DP2 but instead of the EMODnet DTM or RDTM the reference bathymetry was the new one from October campaign. Thus, the steps followed -preprocessing and statistical analysis-, are presented in the next Figures (Figure 4.26 – 4.32).

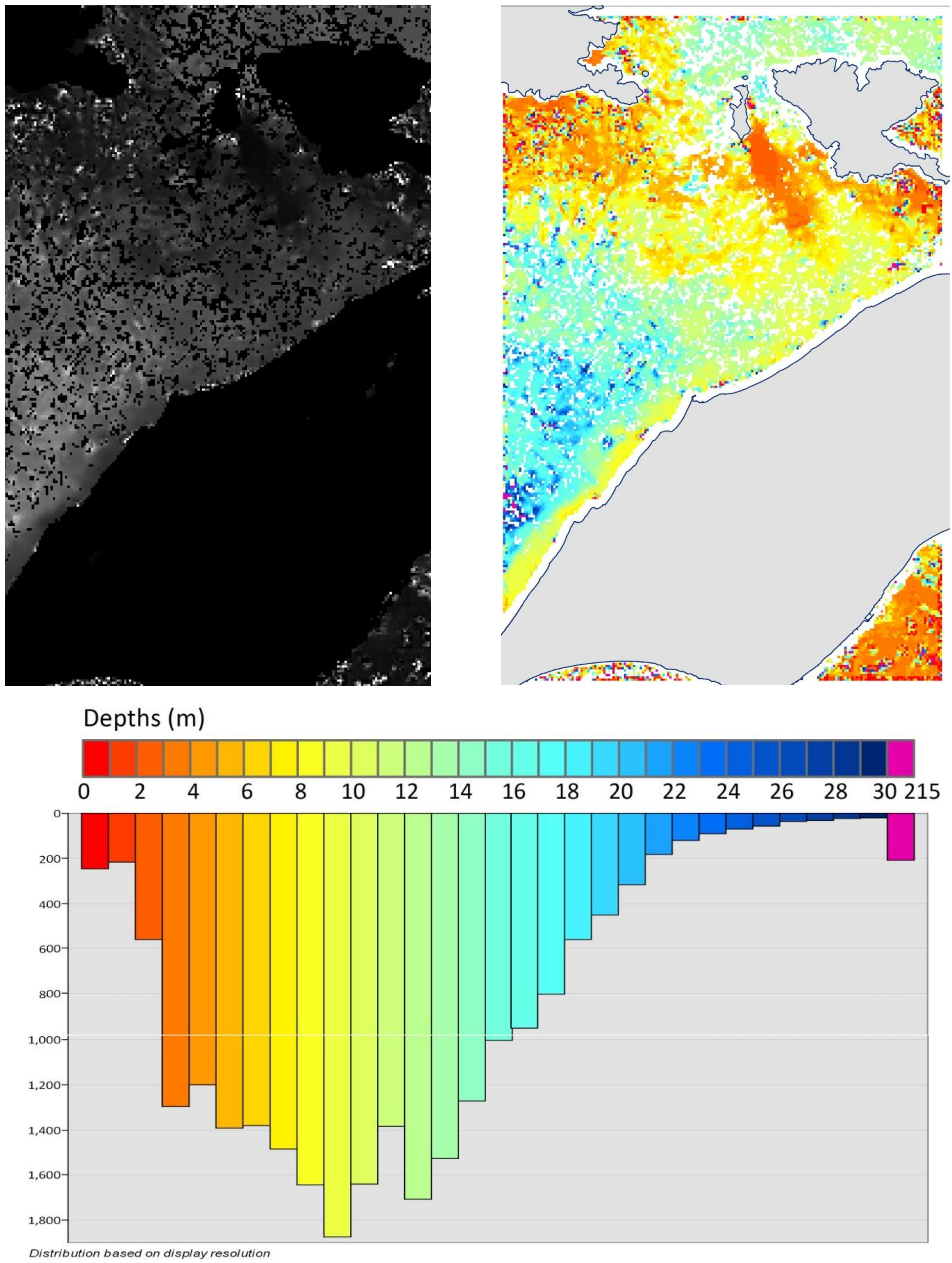

Figure 4.24. Top left - Sentinel 2 results (as delivered). Top Right - Sentinel 2 results. Bottom - Retrieved Depths distribution

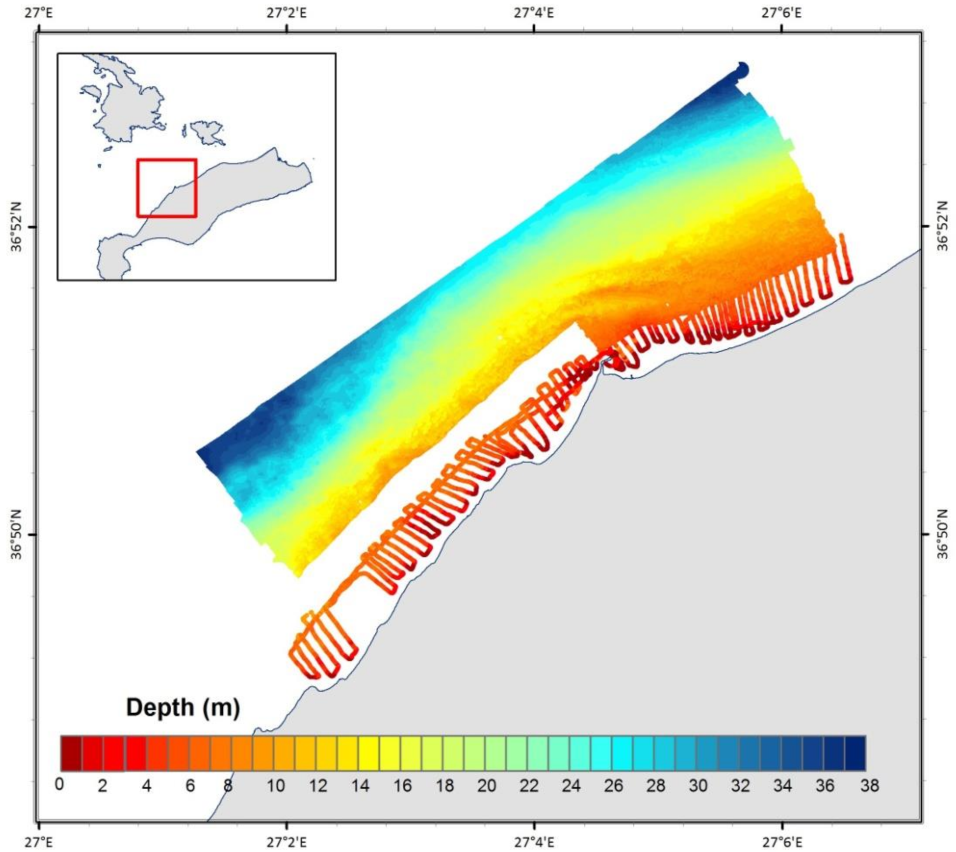

Figure 4.25. (up) Swath bathymetry (4-38m) and bathymetric data collected at very shallow waters (1-10 m) by the use of a single beam echo sounder were acquired onboard R/V Alcyon during a 4-day cruise realized in October 2019 (2 m res). Figure 27. (down) Sentinel-result image converted to points positioned at the centers of cells over the reference resampled DTM (80m res)

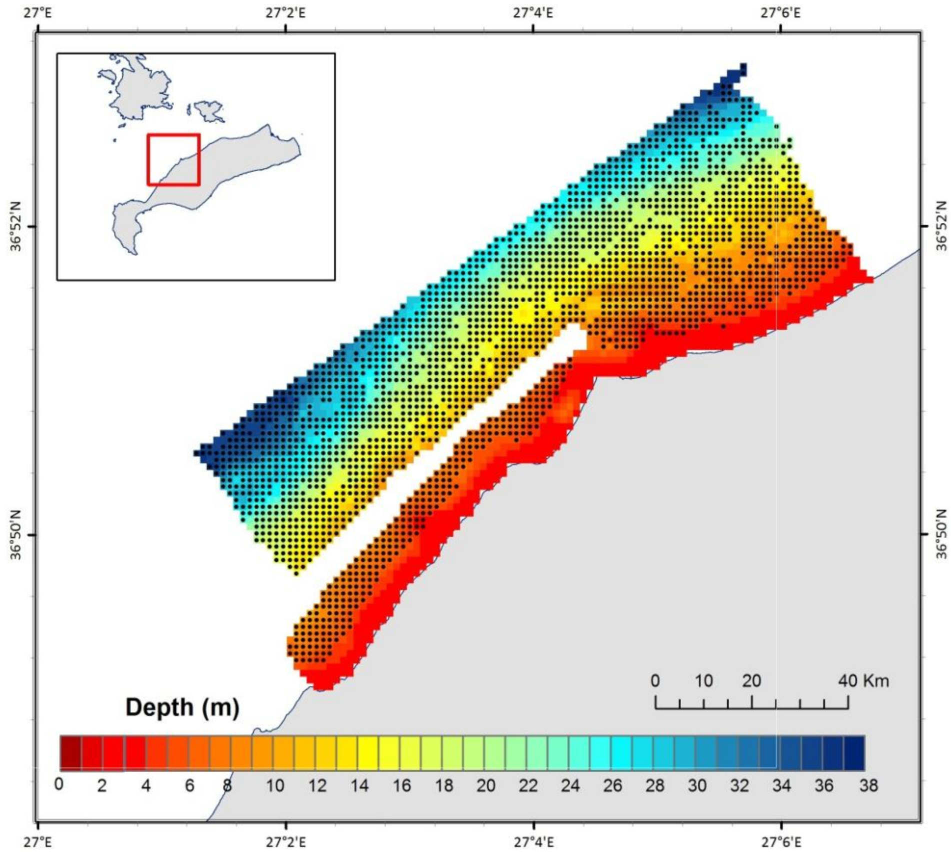
27°E
27°2'E
27°4'E
27°6'E
36°52'N
36°50'N
0 10 20 40 Km
Depth (m)
0 2 4 6 8 10 12 14 16 18 20 22 24 26 28 30 32 34 36 38

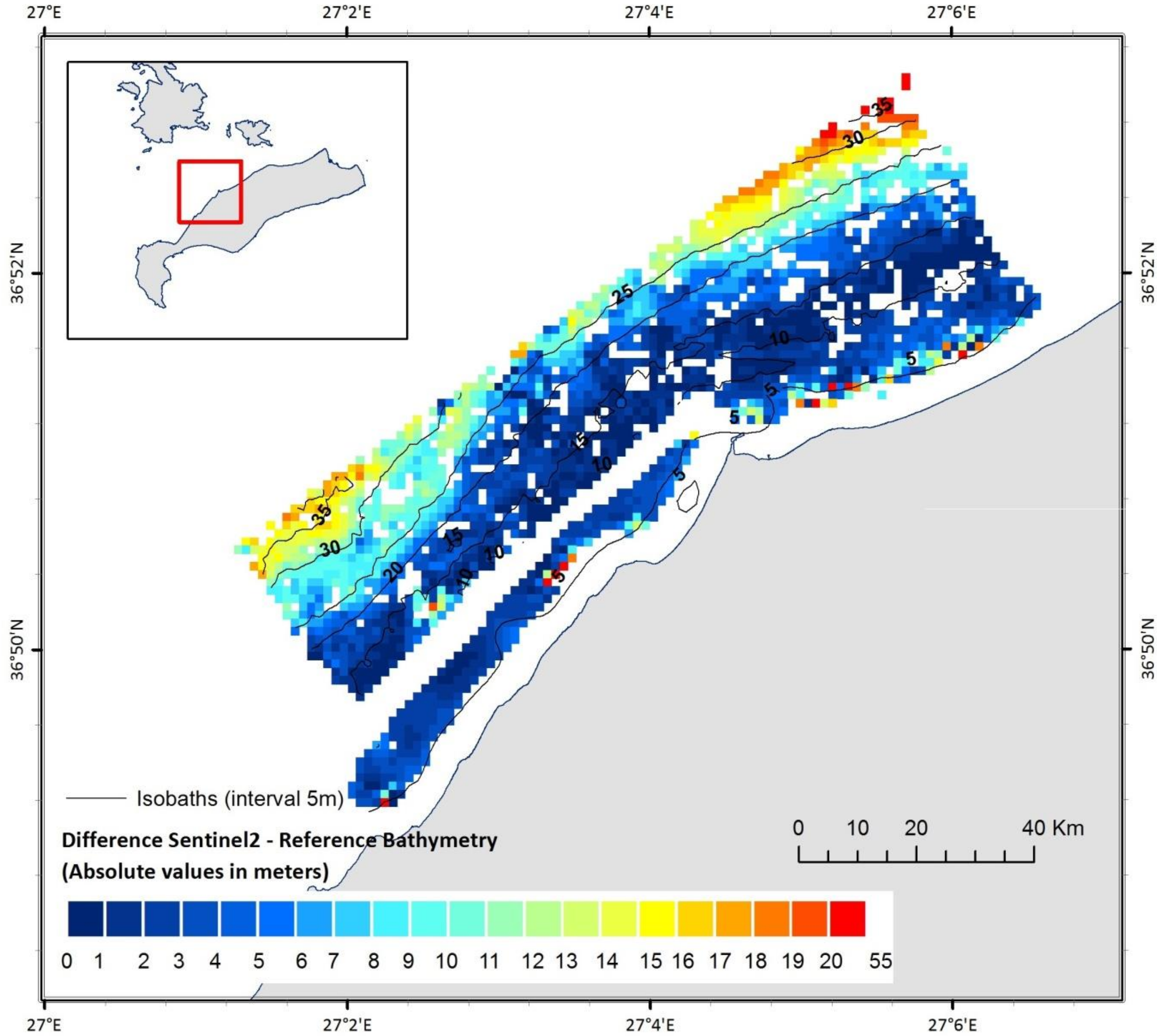

Figure 4.27. Absolute Differences (m) between Sentinel 2 results and reference Bathymetry

The statistical analysis performed, also the map of the absolute differences (MAE) between the BathySent derived bathymetry and the reference one, are shown that over the zone of 5 to 20 m depths the difference is around 3.5 m. in Table 2 is presented the Root Mean Square Error (RMSE) and the Mean Absolute Error (MAE) for each one of the depth zones. More specific, as in the histograms shown, 75% of the absolute differences of the assessed points corresponds to differences lower than 3.5, 1.9, 5 m for the zones of 5-10, 10-15 and 15-20 respectively. This indicates that that the BathySent algorithm retrieve sufficiently the depths of 5-20m zone. On the contrary, on the zone of 0 - 5 m depth, a percentage of 75% corresponds to differences of 6.5m depth which indicates that the algorithm doesn't retrieve sufficiently on 0-5m depth.

Table 4.2. Root Mean Square Error (RMSE) and the Mean Absolute Error (MAE) for each one of the depth zones

Depth zone	RMSE	MAE
0 - 5m	6.18	5.37
5 - 10m	3.58	2.99
10 - 15m	2.41	1.58
15 - 20m	4.14	3.74
20 - 25m	8.06	7.85
25 - 30m	10.54	10.22
30 - 40m	12.87	12.78

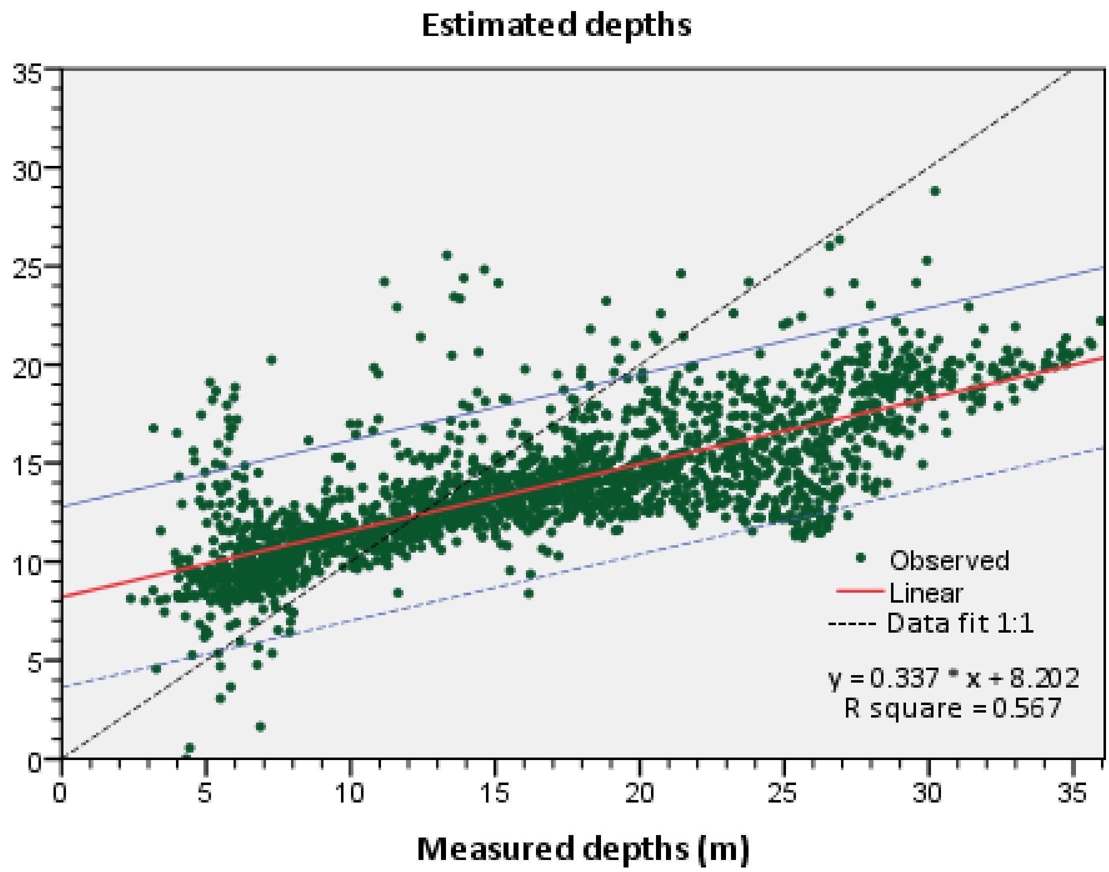

Figure 4.28. The relationship between the Sentinel 2 results and the measured depth values (applied at the extend of measured depths).

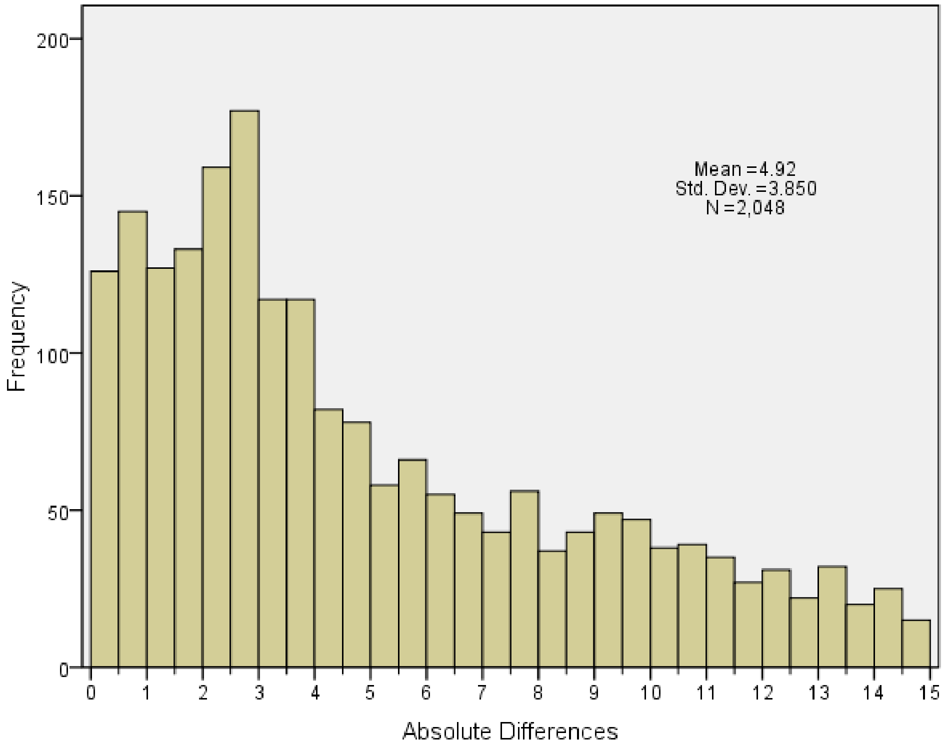

Figure 4.29. Histogram of the frequencies of the absolute differences between the Sentinel 2 results and the Measured depths (applied at the extend of measured depths).

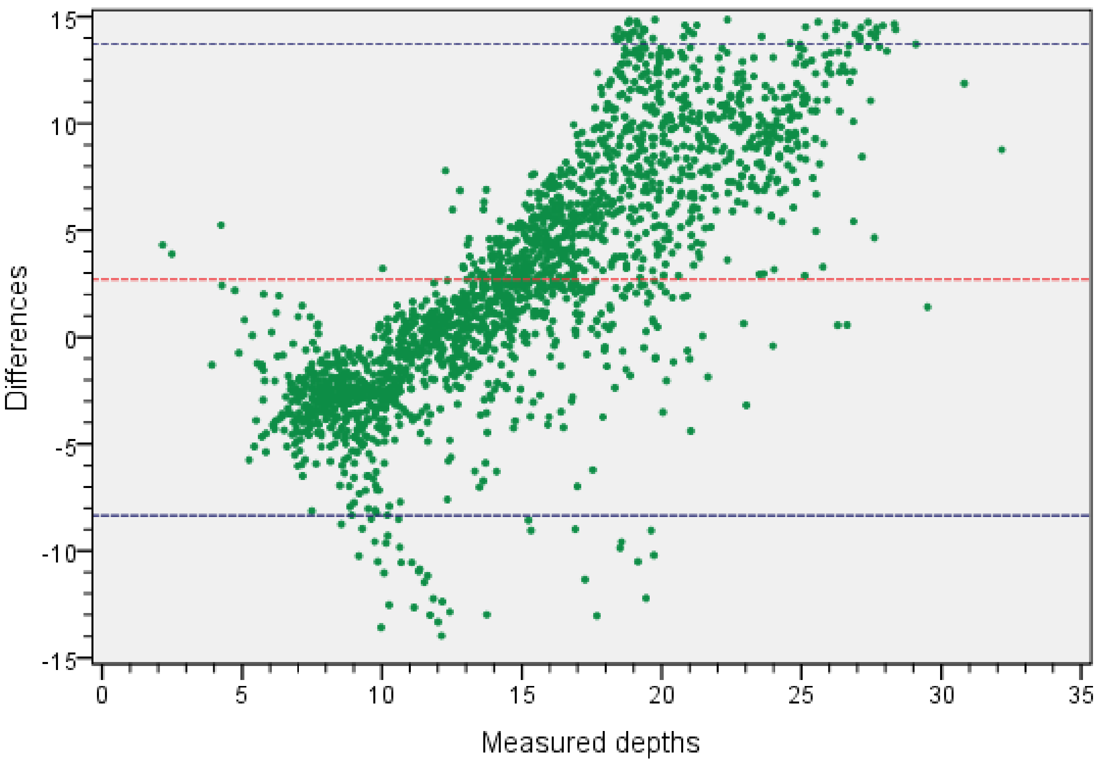

*Figure 4.30. The Bland-Altman plot, shows the difference between the Depths retrieved from Sentinel images and Measured depths vs Measured depths and the 95% confidence interval limits [mean±(1.96*st.dev)].*

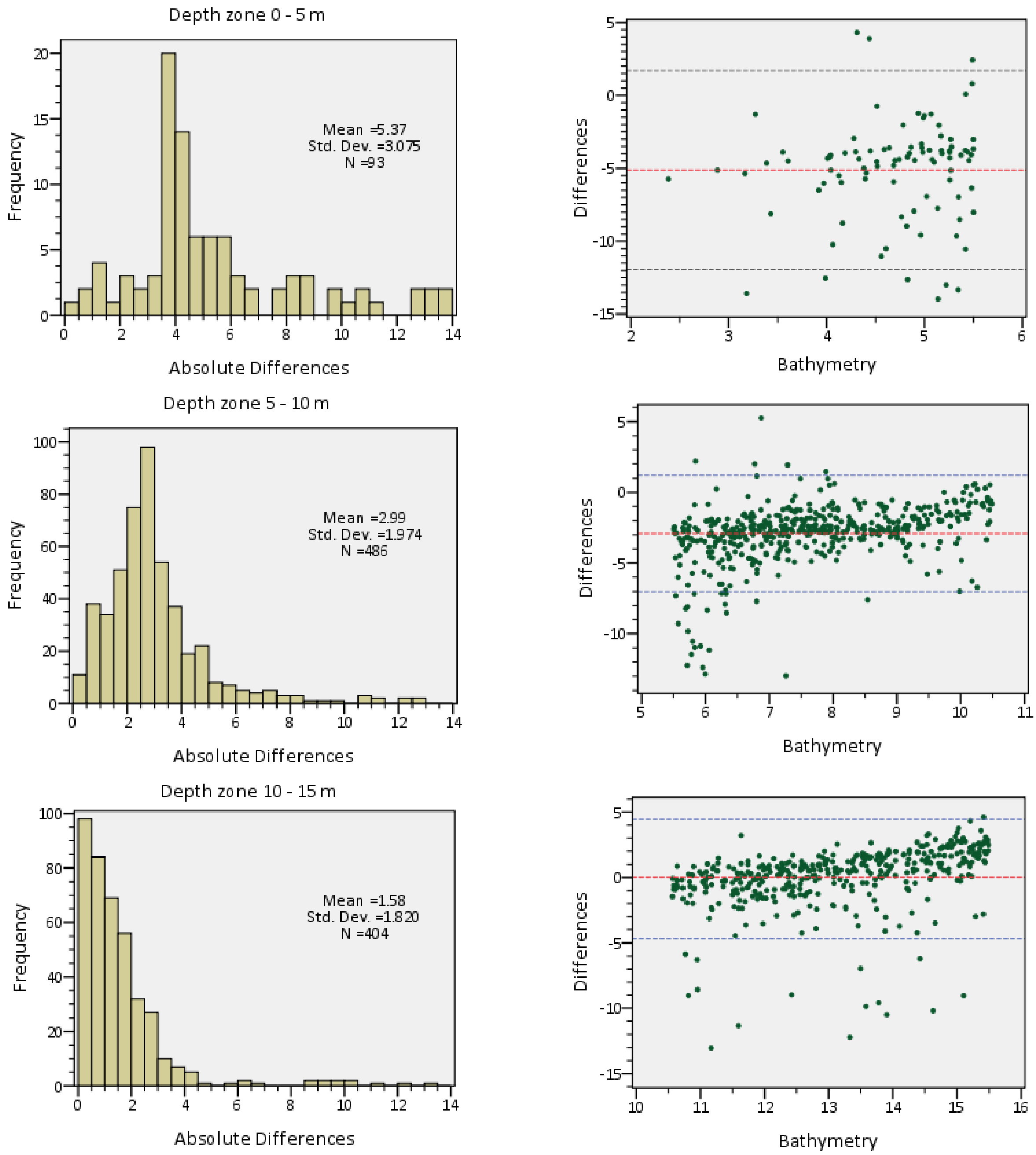

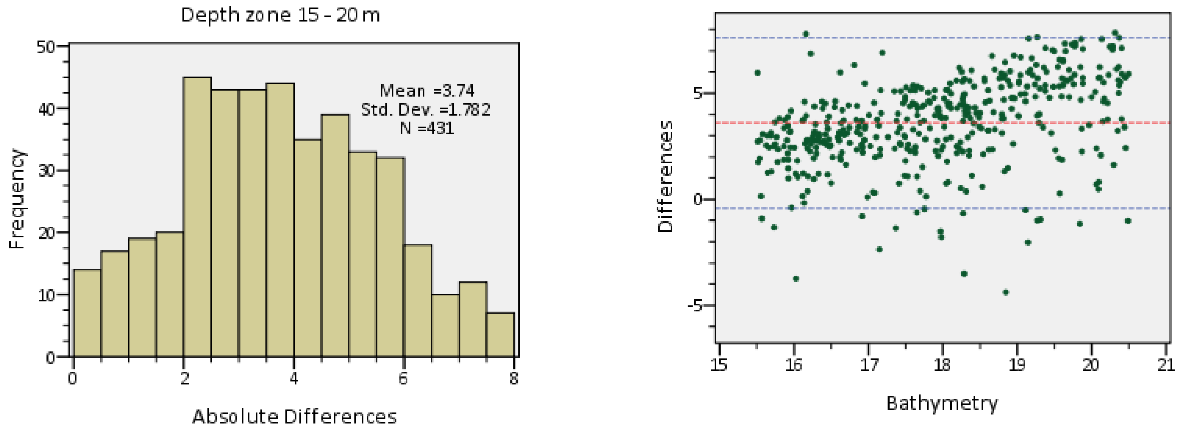

*Figure 4.31. Left: Histogram of the frequencies of the absolute differences between the Sentinel 2 results and the measured depth values for different depth zones). Right: The Bland-Altman plot, shows the difference between the Depths retrieved from Sentinel images and Measured depths vs Measured depths and the 95% confidence interval limits [mean±(1.96*st.dev)] for each depth zone.*

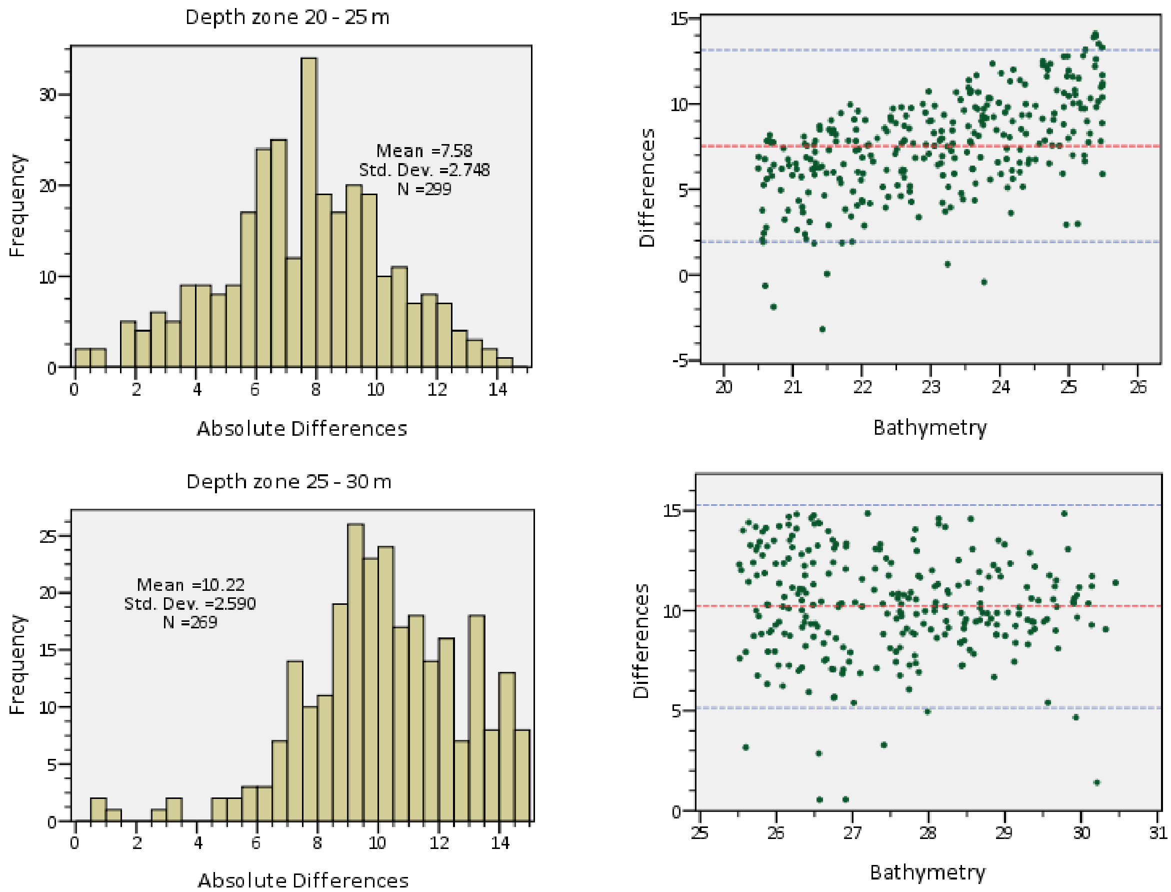

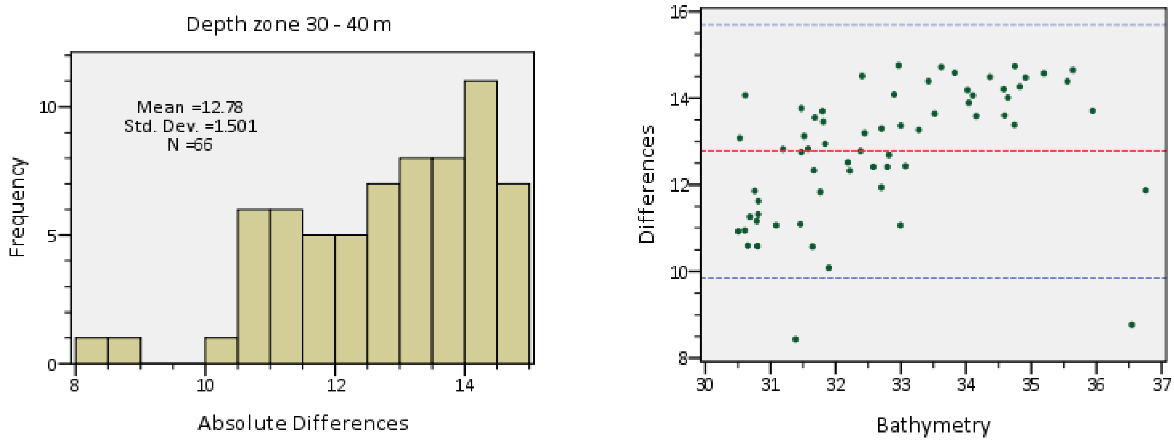

*Figure 4.32. Left: Histogram of the frequencies of the absolute differences between the Sentinel 2 results and the measured depth values for different depth zones). Right: The Bland-Altman plot, shows the difference between the Depths retrieved from Sentinel images and Measured depths vs Measured depths and the 95% confidence interval limits [mean±(1.96*st.dev)] for each depth zone.*

IV.4. Comparison between conventional EO-based bathymetry retrieval approaches and proposed innovative solution using Sentinel-2 data over pilot site.

In order to perform the comparison between conventional EO-based bathymetry retrieval approaches and the proposed innovative solution using Sentinel-2 data, the imagery of level-1C acquired by the satellite at 8:57:51.024Z on 30 September, 2019, were downloaded through Copernicus Open Access Hub.

Satellite image corrections was applied in terms of the adjacency effect (or nearby land areas), sea surface effects and atmospheric corrections using established methodologies. In order to eliminate all non-aquatic objects, a "water mask" have been created and applied to the image. Atmospheric correction refers to the process of removing the contributions by surface glint and atmospheric scattering from the measured total to obtain the water-leaving radiance.

For the atmospheric correction the darkest pixel technique and Sun Glint Correction have been applied. The darkest pixel technique assumes that there is a high probability that there are at least a few pixels in the image with very low reflectance values which area assumed to correspond to black surface with 0% reflectance. The lowest digital number (DN) in each band should in reality be zero and therefore its radiometric DN value represents the atmospheric additive effect (Chavez 1988). Therefore, the pixels from dark targets are indicators of the amount of upwelling path radiance and thus have to be removed.

Sun glint, the specular reflection of light from water surfaces, is a serious confounding factor for remote sensing of water column properties and benthos, limiting the quantity and accuracy of remotely sensed data. The method use data from the near-infrared (NIR) to give an indication of the amount of glint in the received signal. This is based on the assumption that the water-leaving radiance in this part of the spectrum is negligible and so any NIR signal remaining after atmospheric correction must be due to sun glint.

The deglinting methodology applied, which has been proposed by Hedley et al 2005, is based on the exploitation of the linear relationships between the NIR and the visible bands by using samples of image pixels displaying a range of sun glint. Therefore, image samples were carefully selected and for each visible band all the selected pixels were included in a linear regression of NIR brightness against the visible band brightness. All the image pixels were deglinted according to the following equation:

$$R'_i = R_i - b_i \left(R_{NIR} - \min_{NIR} \right)$$

where R'_i is the deglinted pixel in band i, R_i is the reflectance from visible band i, b_i is the regression slope, R_{NIR} is the NIR band value and the min_{NIR} the minimum NIR value of the sample.

Regarding the conventional EO-based bathymetry retrieval approaches the Linear Ratio Model was performed on the atmospherically corrected and deglinted image. The model developed by Stumpf et al apply the fundamental principle that every band has a different level of water body's absorption. The different level of absorption conceptually will generate the ratio between bands and this ratio will consistently change simultaneously when the depth changes. The ratio model is expressed by the following equation:

$$D = m_1 \frac{\ln\left(nR'_i\right)}{\ln\left(nR'_j\right)} - m_0$$

where D is the estimated depth, m_1 is a tunable constant defining the slope of the relationship between the ratio and depth, R'_i and R'_j are the bands i and j radiance of light reflected off the water surface, i, j are bands 1-4 ($i \neq j$), m_0 is the offset for zero depth, n is a constant chosen to assure both that the logarithm will be positive under any condition and that the ratio will produce a linear response with depth.

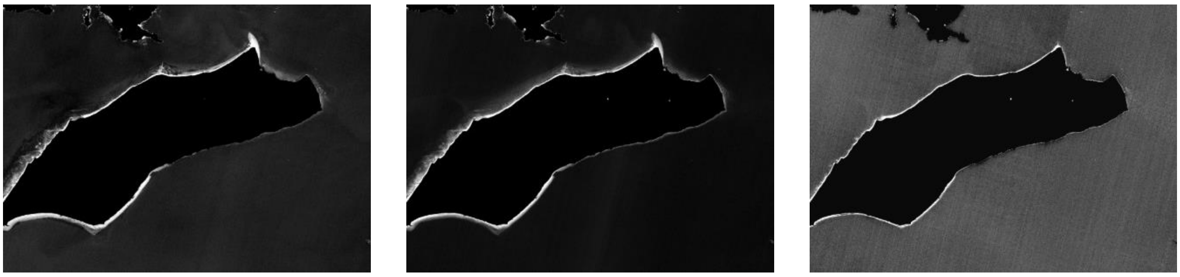

Figure 4.33. Atmospherically corrected and deglinted Sentinel Bands. Left: Band 2 -Blue, center: Band 3 - Green , right: Band 4 – Red

The above equation actually represents a linear regression between depths as dependent variable and the ratio (relative depths) as independent variable. The ratio was applied for the B-G band. In order to define the constant, that mean the coefficient of regression and model solving, known depths from field measurements are also required. The first test regarding the depth zone that the ratio model will be applied was the zone of 0-40m depths. A set of 120 control points from the reference bathymetry within the depths zone of 0-40m, were used in order to define the value of the constant; results is presented in Table 4.3.

Table 4.3. Model Summary			
R	R Square	Adjusted R Square	Std. Error of the Estimate
.781	.610	.608	4.796
The independent variable is the ratioBG			

$$D = -508,302 \frac{\ln\left(1000R'_2\right)}{\ln\left(1000R'_3\right)} + 549,108 \qquad (4.1)$$

Then, another set of 120 control points from the reference bathymetry within the depths zone of 0-20m, were randomly selected in order to define the value of the constant (table below). Results is presented in Table 4.4.

Table 4.4. Model Summary			
R	R Square	Adjusted R Square	Std. Error of the Estimate
.912	.831	.830	2.313
The independent variable is the ratioBG			

According the results of the previous linear regressions, the depth zone that the ratio model was decided to be applied was the zone of 0-20m depths. The equation to retrieve the bathymetry was:

$$D = -231,543 \frac{\ln\left(1000R'_2\right)}{\ln\left(1000R'_3\right)} + 244,338 \qquad (4.2)$$

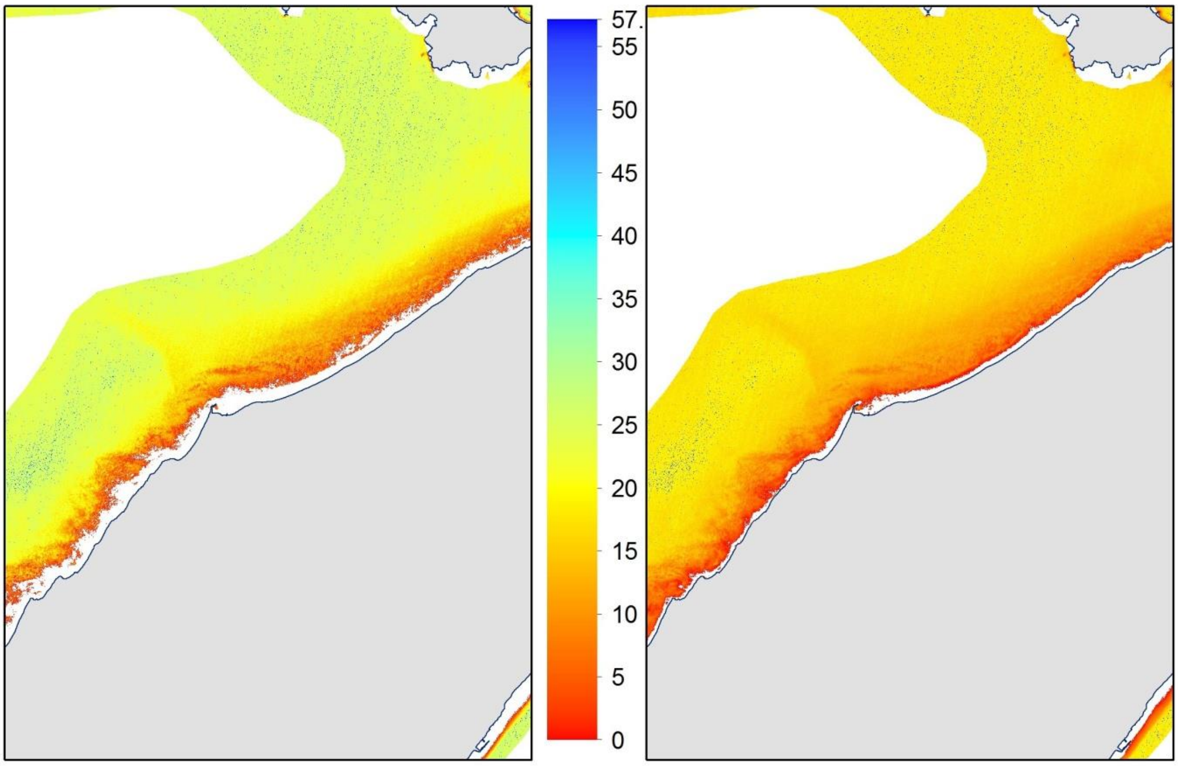

Figure 4.34. Ratio model derived bathymetries. Left: depth zone 0-40m equation 4.1, Right: depth zone 0-20m equation 4.2

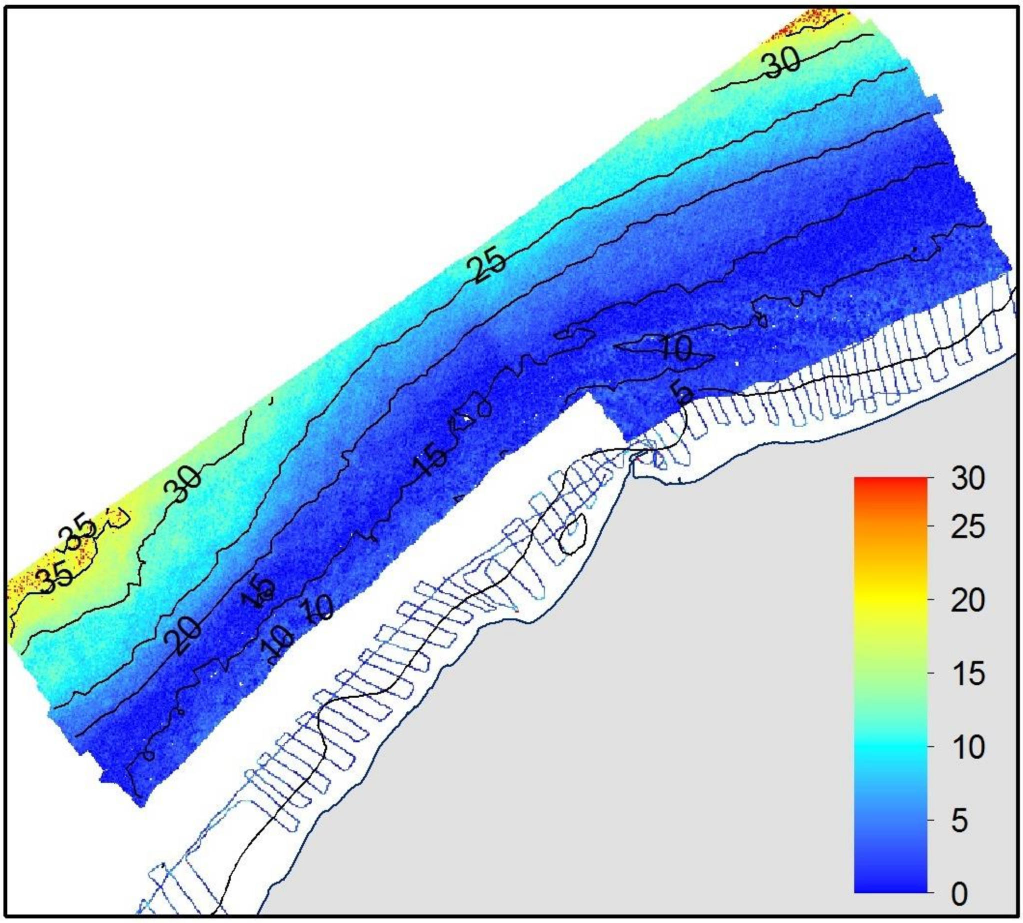

Figure 4.35. Absolute Differences (m) between Ratio model results (0-20m) and reference Bathymetry

The ratio derived depth applied on the zone of 0-20 m (as the linear regression was better fitted -R^2 = 0.831 - to the training depths) were tested and evaluated by using a number of points of known depth. A set of 995 control points with known depth from the "pool" of the soundings were randomly selected. The soundings which were used for the calibration of the models have been excluded from the "pool" when the random sampling for the control ones were performed.

The assessment of the ratio model's retrieved bathymetry was carried out by a similar processing activities as the one applied for the BathySent results. However, the reference bathymetry used both for the training and for the evaluation process, was re-gridded to 10m to be assigned the spatial resolution and the extend of the Sentinel image/ratio depths. The statistical analysis performed to evaluate the results of the ratio model is shown in Figure - diagrams 36-39. The estimated and measured depths are linear correlated with R2=0.710 that means that the 71% of the estimated depths values can be explained by the applied ratio equation. A number of approximately 30 points lies outside the zone of confidence interval, of which the half of them are referred to points of known depth lower 5 m (0-5m). A percent of about 80% of the points, concerns differences lower than 3m while the differences below

2m consist the 60% and differences below 1m the 30% . The MAE of the differences of the estimated vs measured depths is 1.92 with a standard deviation of 1.31m.

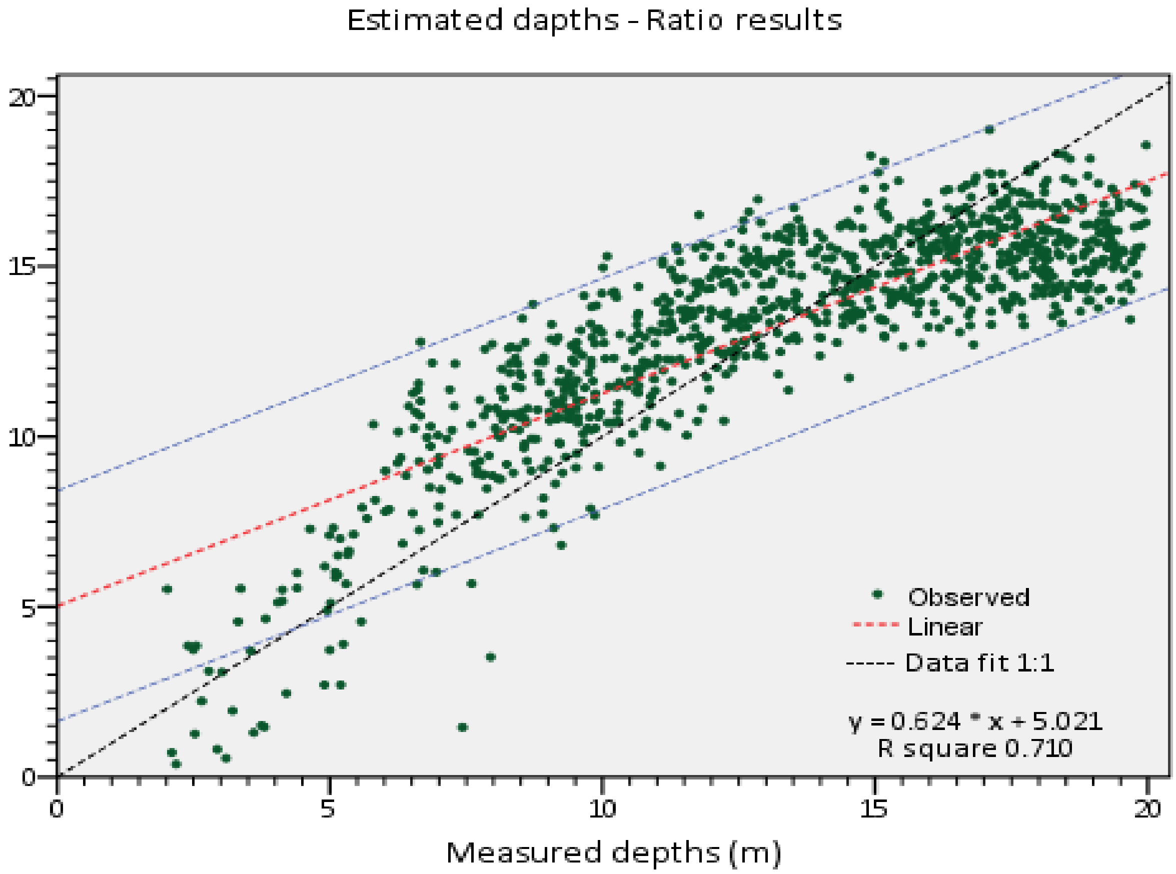

Figure 4.36. The relationship between the Ratio model results and the measured depth values.

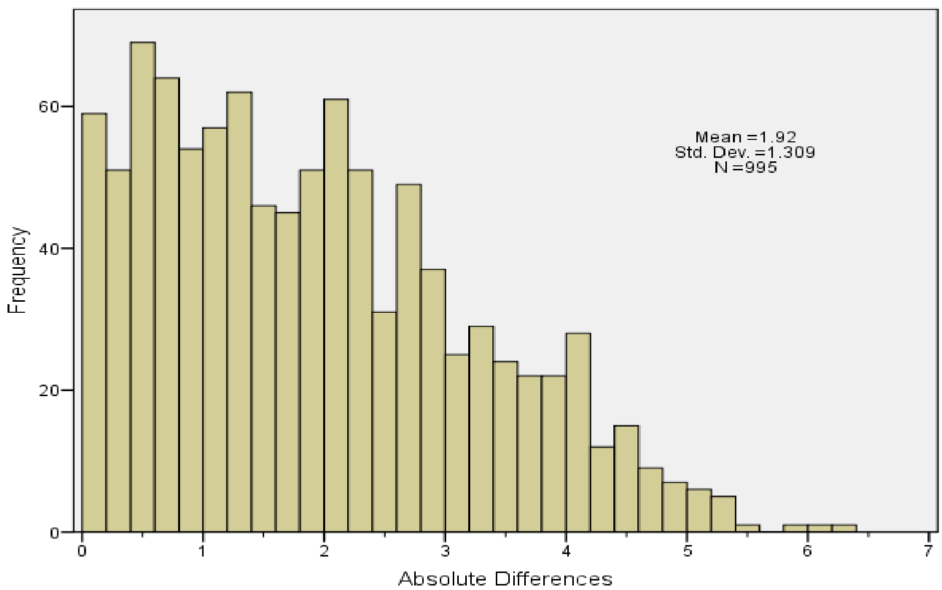

Figure 4.37. Histogram of the frequencies of the absolute differences between the Ratio model results and the Measured depths.

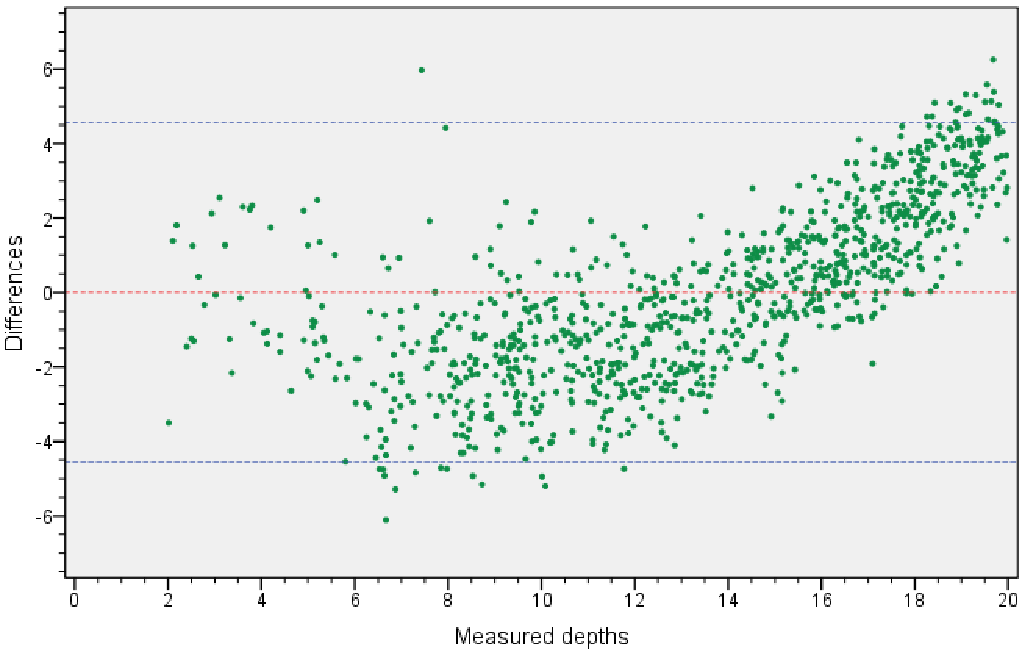

*Figure 4.38. The Bland-Altman plot, shows the difference between the Depths retrieved from Ratio model and Measured depths vs Measured depths and the 95% confidence interval limits [mean±(1.96*st.dev)]*

Table 4.5. Root Mean Square Error (RMSE) and the Mean Absolute Error (MAE) of ratio results

Root Mean Square Error (RMSE)		**Mean Absolute Error (MAE)**	
zone 0 - 5m	1.681688	zone 0 - 5m	1.48402
zone 5 - 10m	2.587831	zone 5 - 10m	2.231125
zone 10 - 15m	1.854709	zone 10 - 15m	1.504368
zone 15 - 20m	2.545428	zone 15 - 20m	2.124298
total	2.326078	total	1.923376

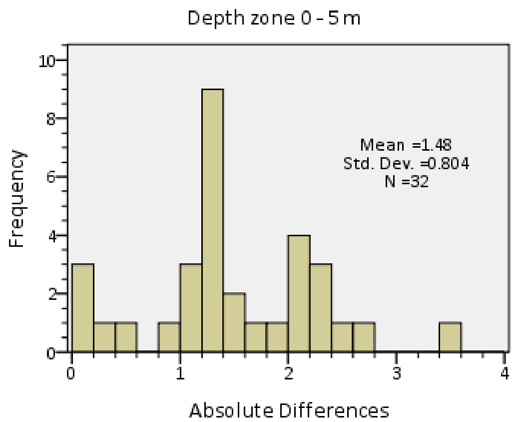

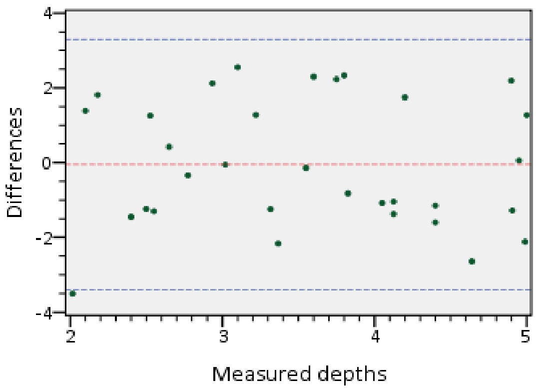

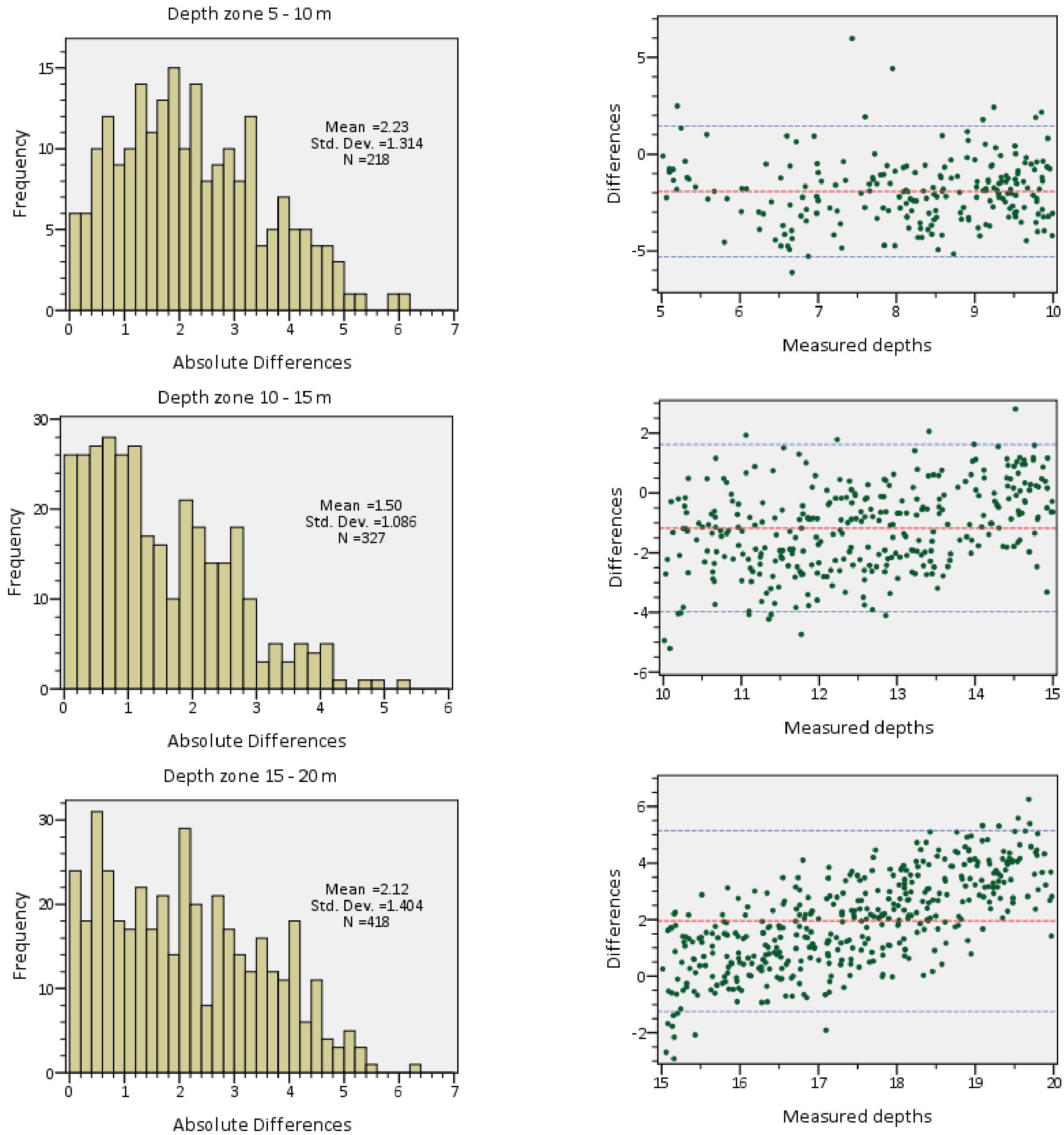

*Figure 4.39. Left: Histogram of the frequencies of the absolute differences between the Ratio model results and the measured depth values for different depth zones). Right: The Bland-Altman plot, shows the difference between the Depths retrieved from Ratio model and Measured depths vs Measured depths and the 95% confidence interval limits [mean±(1.96*st.dev)] for each depth zone.*

Finally, in order to compare the retrieved bathymetry from extracted from both algorithms the ratio bathymetry was resampled to 80m in order to be assigned the spatial resolution and the extend of the Sentinel. The differences were shown in Figure 4.40. The area defined by the red rectangle is the area that the reference bathymetry exists. Within this area, the absolute differences between of conventional EO-based bathymetry retrieval approaches (linear ratio model) and the proposed innovative solution using Sentinel-2 data, are mainly lower than 2m. According to the outcomes of the evaluation analysis of the two models, both models were considered to give more reliable results. Within the depth zone of 5-25m depth, both provides good response, however the ratio one provides better fit. The ratio model has the advantage of the spatial resolution that can be achieved (10m) against the bathysent where the resolution achieved is 80m. On the other hand Bathysent model does not need training depths, to be demonstrated on an area and also in wide scale.

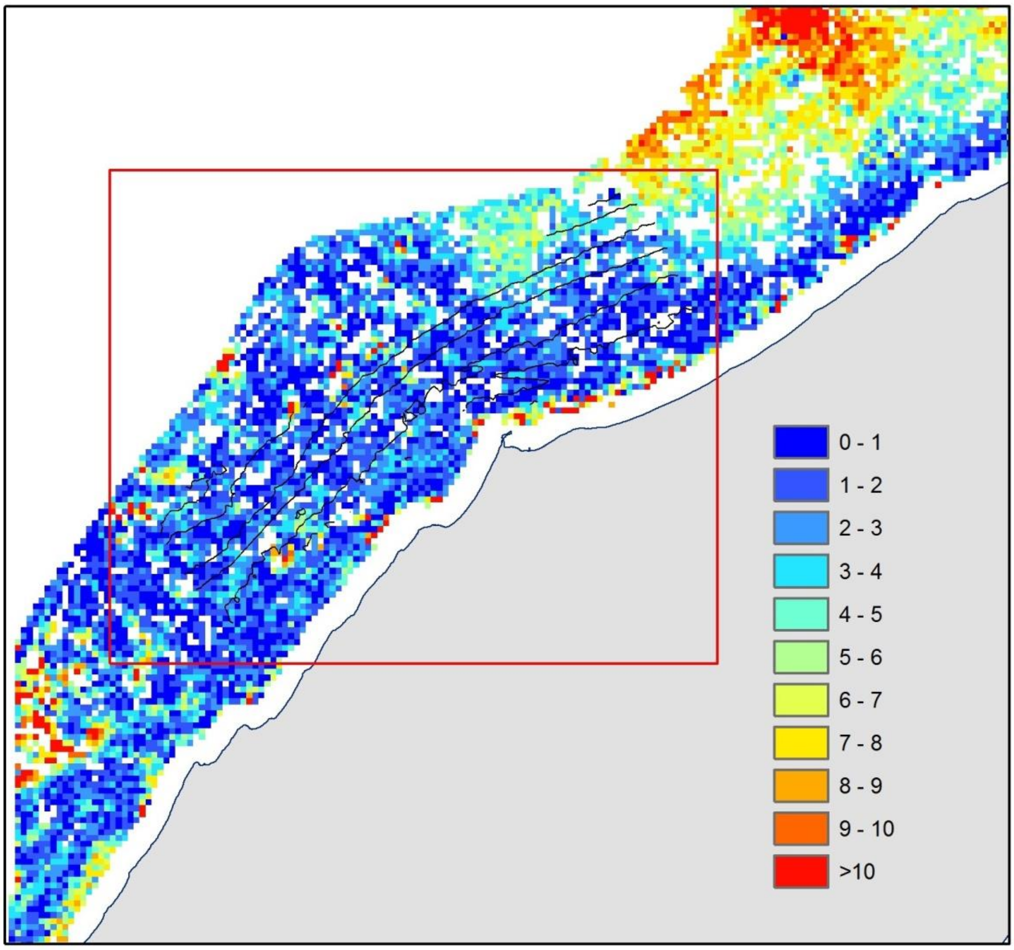

Figure 4.40. Absolute differences between conventional EO-based bathymetry retrieval approaches (linear ratio model) and the proposed innovative solution using Sentinel-2 data over the pilot area.

IV. 5 References

Stumpf, R. P., K. Holderied, and M. Sinclair 2003. Determination of water depth with high-resolution satellite imagery over variable bottom types. Limnol. Oceanogr., 48(1, part 2), pp. 547-556.

Chavez P., 1988. An improved Dark Object Subtraction technique for atmospheric scattering correction of multispectral data. Remote Sensing of Environment 24:459-479.

Hedley, J.D., Harborne A.R. and Mumby, P.J., 2005. Simple and robust removal of sun glint for mapping shallow-water benthos. Int. Journal of Remote Sensing, 26(10) pp. 2107-2112.

EMODnet Bathymetry Consortium (2018): EMODnet Digital Bathymetry (DTM). http://doi.org/10.12770/18ff0d48-b203-4a65-94a9-5fd8b0ec35f6

https://www.emodnet-bathymetry.eu/v_cdi_v3/print_wfs.asp?edmo=269&identifier=GN36201500007_269_G74

https://www.emodnet-bathymetry.eu/v_cdi_v3/print_wfs.asp?edmo=269&identifier=GN36201409922_269_G74

https://www.emodnet-bathymetry.eu/metadata-amp-data/composite-dtms-catalogue-service#/metadata/SDN_CPRD_4667_greece1001

https://www.emodnet-bathymetry.eu/metadata-amp-data/composite-dtms-catalogue-service#/metadata/SDN_CPRD_4667_greece1007

https://www.gebco.net/data_and_products/gebco_digital_atlas/

Chapter V : Wide Area Processing, technical data package (DP-2) description

This chapter aims at:

demonstrate the capacity of the proposed innovative retrieval approach to derive bathymetric measurements over wide areas using Sentinel-2 data.

Description of the PROCESSING

We chose to process five Sentinel 2 full frames over the South-Western coast of Portugal. It represents ~900 km of coast. This area of Europe is hit by ocean swell regularly, therefore it represent a potential favorable test for retrieving bathymetry deeper than 14 meters.

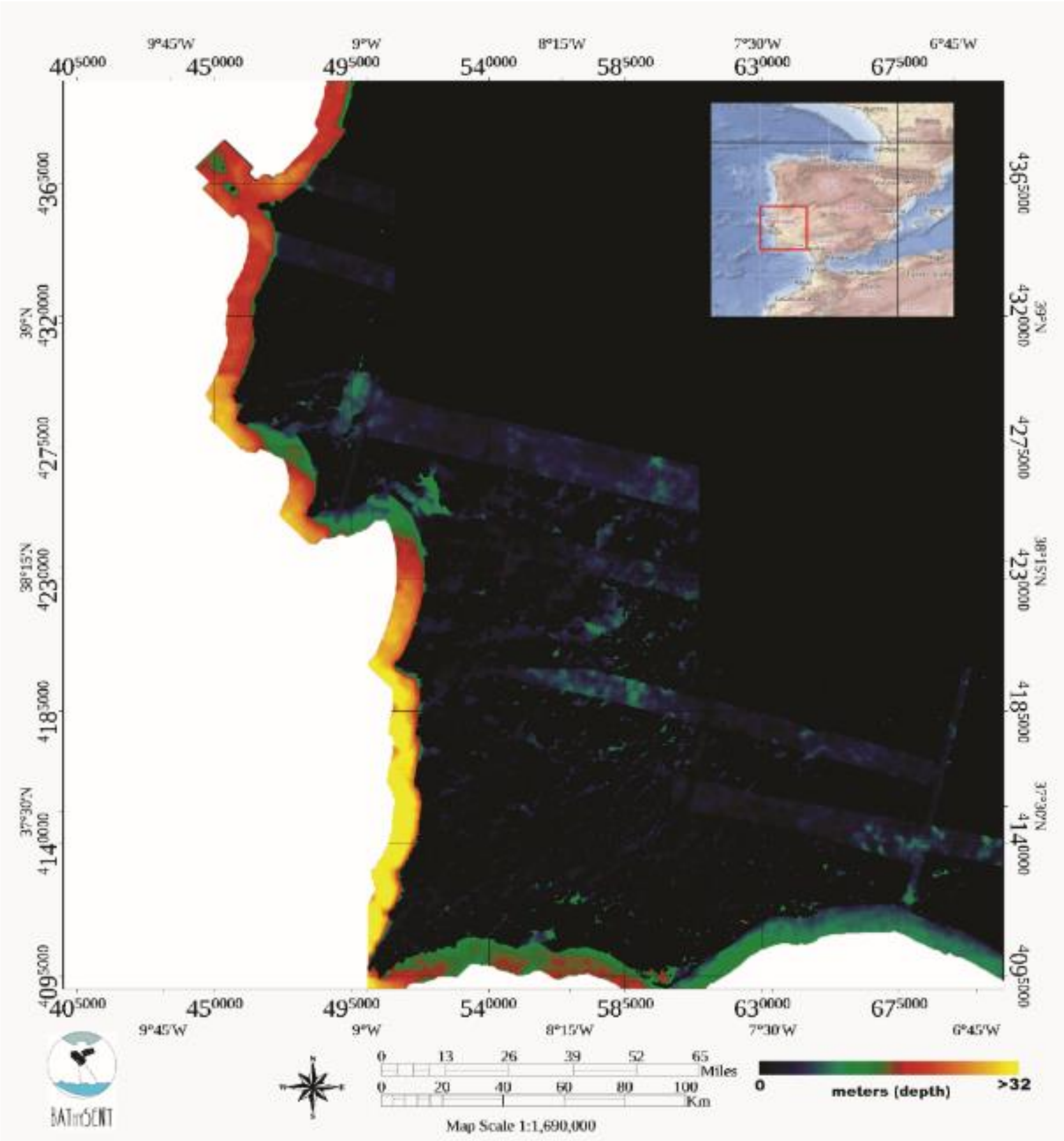

Figure 5.1. Bathymetry of the wide area, processed with BathySent.

The BathySent Python code ran on the Creodias cloud computing facilities. For each of the Sentinel 2 frames, we processed all the available archived data between 2018 and 2019. Depending on the frame, this number varies between 50 and 180 acquisitions per frame. No pre-processing is performed. Post-processing is needed, along with visual selection of each bathymetric results, in order to adjust the final processing parameters and filtering of spurious contribution to the final bathymetric map.

Given a list of Sentinel 2 dataset, the first step of the code generates land and cloud masks for each Sentinel 2 frames. We also mask the sea/ocean if it is further than 10 km from the land. The second steps generates a command line containing processing parameters for each Sentinel 2 frame. The third step generates bathymetric maps for each Sentinel 2 frame given step 1 and 2 as inputs.

For the initial test, we chose a Virtual Machine with 4 cores and 8 Gb of RAM. In this configuration, a full processing on a single Sentinel 2 frame takes about 25 minutes, including the manual selection of the Area of Interest on the Sentinel 2 archive and data list generation). An average of 140 frames are processed in ~60 hours. An interaction with the user is needed, still, to launch the processing, avoid undesired firewall logout, debugging and checking of the results in case of unwanted solutions.

As parameters, we chose to calculate bathymetry with a 64 pixels window, every 16 pixels. This yields a final map at a spatial resolution of 160 meters.

Once all the Bathymetries are calculated (one for each Sentinel 2 acquisition), we proceed with stacking of the results into one single map per Sentinel 2 frame. Our stacking procedure, tailored for BathySent, takes the maximum value over a temporal moving window and then takes the median of the calculated maxima.

Then, all the stacks are assembled into a mosaic. The mosaic is filtered with a Non Local Mean Filter to reduce spatial noises. The result is then saved as **Geotiff**.

Chapter VI: executive summary, conclusions and some recommendations for future developements

Objectives of the project

We have proposed to develop an automated method for mapping coastal bathymetry (water depths) based on Copernicus Sentinel-2 mission and assess its performances. The interest of using Sentinel-2 data lies on the capacity to cover large areas (National and European scale targeted), while benefiting from the short repeat cycle (5 days) of the mission. The systematic acquisition plan of Sentinel-2 is of major interest for studying and monitoring coastal morphodynamics. The proposed methodology avoids limitation of exiting techniques in terms of dependency on water turbidity and requirement for field calibration.

Algorithm development

In this project, we propose to extract bathymetry from a single Sentinel-2 dataset, exploiting the time lag that exists between two bands on the focal plane of the Sentinel-2 sensor. To tackle the issue of estimating bathymetry using two Sentinel-2 bands acquired quasi simultaneously, we developed a method based on cross-correlation analysis that exploits the spatial and temporal characteristics of the Sentinel-2 dataset to jointly extract both ocean swell celerity (c) and wavelengths λ.

We wrote the code in Python (V3) in reason of its portability and for facilitating the implementation on platforms.

Synthetic test

To estimate the quality of our method, we proceed on a simulated dataset where we control all the waves' parameters. We use a model able to simulate each individual wave on complex bathymetries and consider complex morphological site, from 0 to 14 meters depth. The model is based on known bathymetries. Results are in good agreement with the initial bathymetry (de Michele et al., in review, 2020). This test made us confident about the outcome of the Python code and its application to Sentinel-2 data.

Implemetation on CREODIAS

Assisted by Cloudferro, we accessed the CREODIAS platform www.creodias.eu. There, we could find the whole offer for Computing&Cloud and EO collection database. They provide cloud computing (virtual machines, operating systems) and storage (standard HDD and fast – SSD) services. Our Python code is now implemented there, in an encrypted environment. It runs close to the Sentinel archive. We used this configuration for the wide area processing. So, there is potential to upscale in the future.

Validation and Performance assessment

The main objective of the validation activity is to specify the uncertainty of the derived coastal bathymetry results as extracted by the proposed novel approach using the Sentinel-2 mission. We produced data packages on Kos Island, Kasos island and Crete island, Greece. Ultra-resolution swath bathymetry data were acquired by HCMR onboard R/V Alcyon (HCMR) during a 4-day cruise realized from 8th to 12th of October 2019, in the frame of BathySent project. In addition, bathymetric data were collected at very shallow waters (1-10 m) by the use of a single-beam echo sounder. A comparison with the « linear ratio model » multispectral method is also performed here.

The absolute differences between conventional EO-based bathymetry retrieval approaches (linear ratio model) and the proposed innovative solution using Sentinel-2 data are mainly lower than 2m. According to the outcomes of the evaluation analysis, both models were considered to give results that are more reliable within the depth zone of 5-25m.

Wide area processing

The code is successfully run on the South Western coast of Portugal, on 4 Sentinel 2 frames with more than 80 images per frame. We found depth up to 40 meters.

Conclusions

Today an operator can extract shallow bathymetries in selected areas exploiting the short revisit time and the full S2 archive. A supervisor need to check/filter the results. We calculated bathymetric values using a window of 64x64 pixels (640x640 meters), every 16 pixels (160 meters). Therefore, BathySent can produce Bathymetric maps with 160 meters grid, but the real spatial resolution need to be assessed.

Synthetic tests showed that BathySent could restitute bathymetry in the range 5-14 meters depth, with 2 meters standard deviation with respect to « sonar based » bathymetry. Validation in the Mediterranean shows that results are very good, in the range 5-25 meters depth: precision decreases with depth (as expected) ranging from 10% to 30% from 5 to 25 meters depth. The wide area processing, in the ocean coasts of Portugal, showed that BathySent could measure deeper bathymetry, at least up to 40 m depth. Precision and accuracy need to be assessed on the Wide Area dataset, in a future step.

The method based on “ratio model” saturates around 25 meters depth and need ground calibration. The bathysent method provides bathymetry at lower spatial resolution with respect to the “ratio model” but :

1) Bathysent does not need « in situ » calibration
2) Bathysent can go deeper than 25 meters

The access to the full archive of S2 is a key aspect for a successful retrieval: there is the <u>need</u> to combine multiple S2 acquisitions.

Cloud processing is as fast as 25 minutes per S2 frame, using a virtual machine with 4 cores and 8 Gb of RAM. Wide area processing on large dataset can be performed in reasonable time (few days). Human driven post processing is still needed (filtering, selecting the best results).

The strict condition for the method to work is the presence of ocean/sea swell. Although global retrieval of shallow bathymetry is feasible, the estimation at higher depths depends actually on local conditions.

Recommendations for future developments

Wind generated waves or currents can hamper the correct bathymetric estimation with BathySent. Therefore, work on pre-post processing is needed: algorithm development on how to automatically select the « good » bathymetries.

The spatial resolution of the results needs to be improved as the FFT window approaches the shallower bathymetries. Therefore, we highlight the need to improve the algorithm to address this issue e.g. by adaptive window sizes in a proper iteration scheme.

To improve the precision of the bathymetric retrieval, we might need to combine multiple sensors, multiple pixel resolutions, and multiple swell regimes e.g. combination of Landsat 8, Planet Labs and Sentinel-2.

We could add the post-processing functions to the Python code on CREODIAS; on what would be the evolution of the code already implemented. The processing can be further automated: a « user guide » can be developed.

Bathysent could be used to calibrate the conventional « ratio techniques », especially where there cannot be in-situ measurements.

There is the will to contribute to current developments implementing such services on cloud resources.

The Bathysent consortium could contribute to the pole of research institutes dealing with bathymetry from space, in France (pole ODATIS, led by CNES).

This document can lead to the preparation of a White Paper on requirements for bathymetry retrieval from EO and future missions.

BRGM is interested in an agreement for further exploitation of the code, together with CloudFerro on CREODIAS platform, after BathySent project.

BRGM will continue the methodological developments and will search for additional partial funding.

Annexe I: BathySent Algorithm Description (Pseudo code)

INPUTS:

- Technical Note TN-2 – BathySent Scientific & Technical Development Report

OUTPUTS:

- Technical Note TN-4 – BathySent Algorithm Description (Pseudo code)

PSEUDO CODE: Detailed Bathysent procedure

A. Inputs' extraction :

1 : Input of the bands B2,B4,B8 (adapted to the Sentinel 2 image format) and their geographic information

2 : time lags associated to the bands (respect to band 2)

3 : area of interest (defined by user)

4 : processing parameters. Default : processing windows size = 64 (640m), window overlap=0.75

B. inputs reformating :

1 : Resizing all bands to 10m. updating of geographic information

2 : extract data on the area of interest

3 : produce a sea/land mask based on Band B8 threholding (empirical threshold value : 750)

C. Processing procedures :

1 : Definition of masks for circular rings sampling the Fourrier domain (for the given processing window size) with wavelengths bin corresponding to twice the data size. We limit the wavelengths range to [20m-250m]

2 : Depth estimation

2.1 : start scanning the excerpts of Band B2 and B4 (excluding land areas detected on sea/land mask) with window size and overlap defined in A4 . For each scanning window position : estimation of fast Fourier transforms of B2 and B4

2.2 : based on the two FFT : computation of a spectrum defined as /** récupérerer formule sur l'autre rapport */

2.3 : estimation of periods and associated wavelenghts based on /** récupérer formuler autre rapport */. Amplitude of the spectrum is extracted as quality indicator in the further steps.

2.4 : fill wavelenghts rings' mask with periods and amplitudes. The period/amplitudes values affected to the wavelenghts' interval are estimated:

-Amplitude : average of the amplitudes associated to wavelenghts associated to the same wavelength sample

-Period : average of the periods associated to wavelenghts associated to the same wavelength sample but weighted by their associated amplitudes. As the wavelength « ring » covers all the direction, the aim been to favorise for a given waveleght's ring the more significant (in terms of actual waves) waves' direction.

2.5: for each ring of the wavelengths sampling mask : estimation of a depth based on the wavelength/period pair (based on the linear dispersion relation). Added to the wavelengths sampling mask.

2.6 : average of the depth associated to each wavelength sample weighted by the corresponding amplitude (to favourise the more significant wavelenghts in the [20m – 250m] interval). The unique depth value obtained will be associated to the position of the center of the window.

2.7 : updating scanning window position.

D. result export :

1 : computation of the geographic information of the product based on the initial geographic information of the B2 excerpt, the processing window size and the overlap value

2 : conversion of the depths' grid in a geotiff including geographic information